COMPOSITION AND STRATIGRAPHY OF LATE QUATERNARY SEDIMENTS FROM THE NORTHERN END OF JUAN DE FUCA RIDGE

RAYMOND ARNOLD COOK

B.Sc., The University of Alberta, 1973

A THESIS SUBMITTED IN PARTIAL FULFILMENT OF

THE REQUIREMENTS FOR THE DEGREE OF

MASTER OF SCIENCE

in

THE DEPARTMENT OF GEOLOGY

We accept this thesis as conforming to the

required standard

THE UNIVERSITY OF BRITISH COLUMBIA

May 1981

In presenting this thesis in partial fulfilment of the requirements for an advanced degree at the University of British Columbia, I agree that the Library shall make it freely available for reference and study. I further agree that permission for extensive copying of this thesis for scholarly purposes may be granted by the head of my department or by his or her representatives. It is understood that copying or publication of this thesis for financial gain shall not be allowed without my written permission.

Department of Geological Sciences

The University of British Columbia
2075 Wesbrook Place
Vancouver, Canada
V6T 1W5

Date April 29, 1981

DE-6 (2/79)

ABSTRACT

Sediments from the northern end of Juan de Fuca Ridge are Late Quaternary in age and contain widely correlatable cycles of turbidity current and hemipelagic sedimentation. Sediments from the Ridge were examined for their mineralogy, structure, components of the sand fraction, rates of sedimentation and grain size distribution to establish processes of sedimentation, stratigraphy, correlation and local hydrothermal relationships. Ten gravity and Phleger core sites along two profiles of the Ridge were examined in detail, one section was perpendicular to West Valley, the main spreading centre, and one section was within and parallel to West Valley. Sediment from Cascadia Basin was compared to the results of the Ridge study.

Changes in sedimentation defined by core X-radiograph structure, components of the sand fraction and grain size distribution, indicated cycles of relatively coarse sediment overlain by finer bioturbated sediment with a repeated stratigraphic relationship in all but one Juan de Fuca Ridge core. Changes in sediment composition are attributed to brief, episodic, continent derived turbidity current deposition followed by lengthy periods of hemipelagic sedimentation for each cycle. Differences in composition exist between sediment of ridges and valleys, with a greater winnowed foraminiferal-hemipelagic and a lesser turbidity current influence in the former area.

Radiocarbon dated foraminiferal-rich intervals from ridge sediments were exclusively Late Pleistocene with Middle Ridge sediment having an inferred 9000-9500 B.P. Late Pleistocene-Holocene boundary. Similar sedimentation cycles between Middle Ridge and valley localities enabled correlation of ridge and valley stratigraphy and the Late Pleistocene-Holocene boundary. A stratigraphic relationship based on the episodic deposition of continent derived turbidites

exists between the northern end of Juan de Fuca Ridge and the continental Pacific Northwest. Pulses of turbidity current sedimentation coincide with initial interglacial warming trends during the Late Pleistocene. Holocene sedimentation for Juan de Fuca Ridge is of hemipelagic origin with rare local turbidity current deposition. Hydrothermal minerals were not detected.

TABLE OF CONTENTS

LIST OF ILLUSTRATIONS

FIGURE

FIGURE

ACKNOWLEDGMENTS

This thesis was initiated under the joint supervision of Drs. R. L. Chase and J. W. Murray to both of whom the author is greatly indebted.

Thanks for assistance on the cruise go to G. Béland, J. Kennedy, R. MacDonald, D. Runkle and S. Thorn. The co-operation and assistance of the captain, officers and crew of the research vessel, C. F. A. V. Endeavour was greatly appreciated.

Invaluable technical assistance and access to the Sedigraph units at Pacific Environmental Institute were made to the author by Dr. C. Pharo and his technician Ms. V. Chamberlain. Similar aid and discussion of pertinent hydrographic and oceanographic factors were readily supplied throughout this study by Dr. E. V. Grill, Department of Oceanography, U. B. C.. Mr. A. Hay, Department of Oceanography, U. B. C., generously supplied substantial assistance on the grain size studies and generated the necessary computer programming to treat the study area grain size values. To all the above people the author is extremely indebted.

Additional thanks go to Dr. A. E. Burgess, Department of Radiology, U. B. C., for the X-raying of the study area cores and to E. Montgomery for his necessary and often timely assistance during this thesis preparation.

Finally to my wife Harriet, son Matthew and to all members of my family we are at the beginning.

Financial support for this study came from grants to, Drs. R. L. Chase, E. V. Grill and J. W. Murray from, the National Science and Engineering Council of Canada, Energy, Mines and Resources Canada, the British Columbia Ministry of Energy, Mines and Petroleum Resources, Cominco Ltd, Placer Development Ltd, and the University of British Columbia.

PLATE

Chapter I

INTRODUCTION

INTRODUCTION

Three consecutive years of deep-sea cruises were inititated by the University of British Columbia (U.B.C.) in 1977, to determine the presence and extent of hydrothermal deposits on the Juan de Fuca and Explorer Ridges. Sediment chemistry from the initial cruise indicated no obvious hydrothermal concentrations. The relationship of chemistry and sediment composition was unknown, requiring a detailed examination. This study examined the structure, composition, and stratigraphy of surface sediment recovered in cores from the northern end of Juan de Fuca Ridge. The study area which lies between latitudes 48°10' and 48°50' north, and longitudes 128°15' and 129°10' west is 40 km north-south by 60 km east-west (Fig.1).

Deep-sea sedimentation and mineralogy have been investigated since the famous Challenger Expedition (1872-1876). Local investigations on the interaction of marine processes and sedimentation have been largely confined to coastal areas, which typically have large fluvial sediment budgets and hydrographic processes which strongly interact, a relationship that can confuse or reinforce subtle yet significant stratigraphic changes in sedimentation and sediment mineralogy.

With acceptance of the theory of plate tectonics, deep-sea geological research has shifted to encompass the examination of the interacting plate boundaries. Scientific interest in noneconomic sediments coincident with plate boundaries has been secondary to interest in mantle-derived hydrothermal products. The understanding of sedimentation at divergent margins must be preceded by an understanding of local parameters affecting sedimentation and sediment mineralogy.

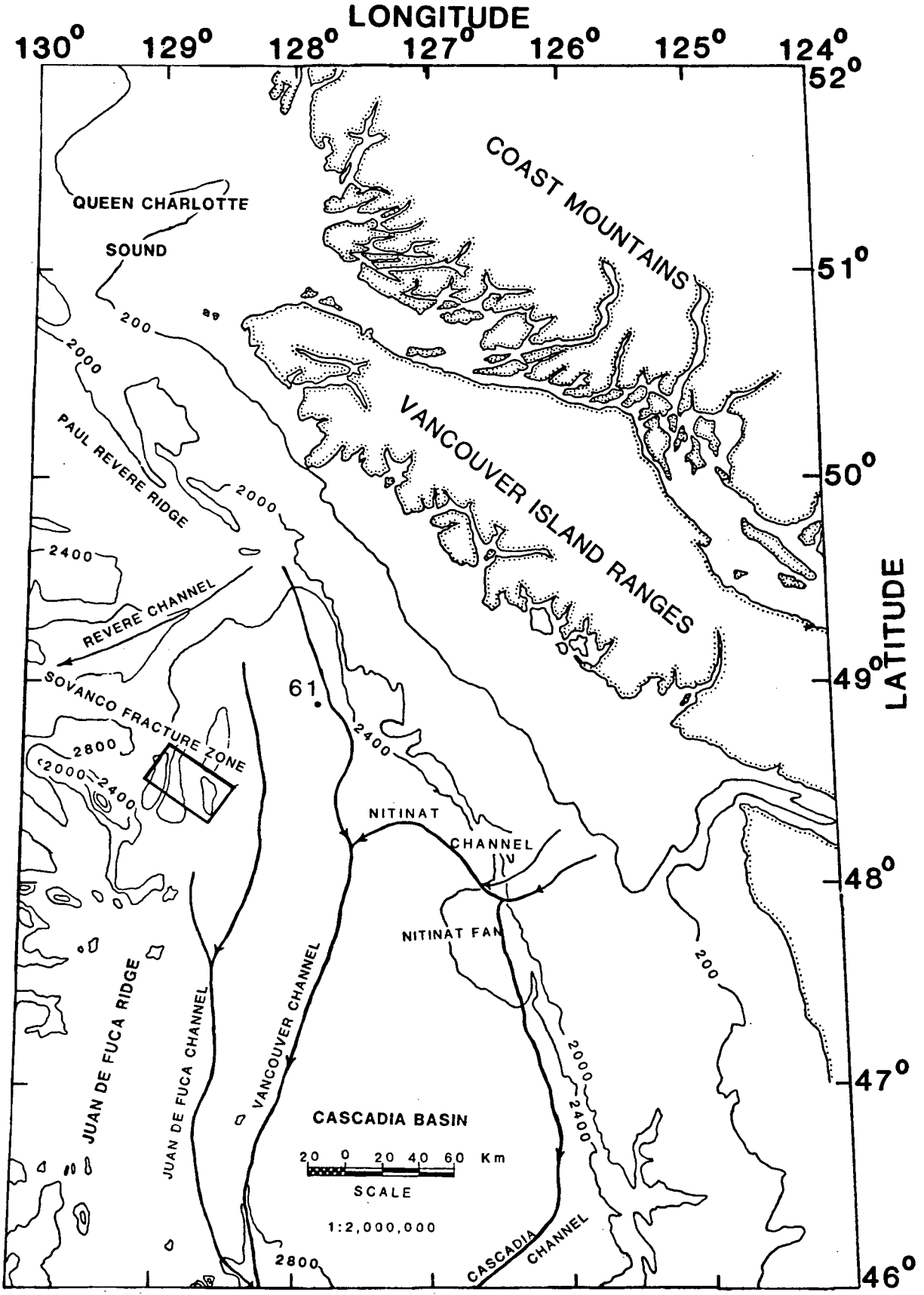

FIGURE 1. Bathymetric contour map of the Western Canadian continental margin and seafloor adapted from the Juan de Fuca Plate Relief Map (1978) compiled by the Earth Physics Branch, Canada. The Juan de Fuca Ridge study area is outlined, Cascadia Basin core 77-14-61 and the major geographic features and deep-sea channels (Carson, 1971) are located.

Deep-sea sediment budgets far from continental influence are small and primarily of hemipelagic, pelagic and hydrogenous sedimentation, these components are dominated by different hydrographic factors than those of the continental terrace. Localities that express synchronous changes in patterns of both deep-sea and continental terrace sediments are rare and difficult to correlate due to variable geography and hydrography.

In the northeast Pacific the dominant deep-sea topographic features are ridges, offsetting fracture zones, troughs and seamounts. The Explorer, Juan de Fuca and Gorda Ridges are all near the North American continental margin. The northern end of each ridge is closest to the continental margin and exhibits the greatest relief (Barr, 1972; McManus, et al, 1972).

Major changes in the rate and style of sedimentation in the northeast Pacific during the Late Pleistocene and Holocene epochs are well documented from studies of the continental terrace and adjacent abyssal plains (Duncan and Kulm, 1970; Duncan, Kulm and Griggs, 1970; Griggs and Kulm, 1970; Horn et al, 1971; Nelson and Kulm, 1973; Windom, 1976). Studies on the correlatable synchronous patterns of deep-sea sedimentation are few and inconclusive (Carson and McManus, 1971; Phipps, 1977). The proximity of the northern ends of the northeast Pacific ridges to the continental margin, combined with ridge topography, creates localities where sedimentary regimes of the deep-sea and continental terraces intermingle.

TECTONIC SETTING

The Juan de Fuca Ridge, a spreading ridge segment between the Pacific and Juan de Fuca plates, strikes north northeast. In east-west cross-section the broad ridge has superimposed parallel elongate hills and valleys of subdued relief, but lacks an obvious median valley (Barr, 1972; Barr and Chase, 1973; Wakeham, 1977). The ridge is characterized by asymmetric

spreading with a half spreading rate of 2.9 cm/yr (Atwater, 1970; Wakeham, 1977). Geophysical studies have described relatively aseismic volcanic basement with high intensity magnetization (Lucas, 1972; Barr, 1972; Wakeham, 1977). High heat flow has been measured at numerous points on the ridge, with the highest values occurring near the northern end of the Juan de Fuca Ridge and its contact with the Sovanco Fracture Zone (Davis and Lister, 1977b).

At its northern end the Juan de Fuca Ridge has three parallel grabens: West Valley, Middle Valley and East Valley, separated by three parallel horsts: West Ridge, Middle Ridge and East Ridge (Fig.2) (Barr, 1972; Davis and Lister, 1977a), formed by tilted, rotated fault blocks. These ridges

PREVIOUS WORK

Prior studies of the northeast Pacific including the Juan de Fuca Ridge were initially directed at bathymetry and mapping (Barr, 1972, McManus, et al, 1972). Regional bathymetric descriptions were published by McManus; Mammerickx and Taylor; Chase, Menard and Mammerickx; and Barr (Barr, 1972). Detailed bathymetry of the northern end of Juan de Fuca Ridge, which includes the study area, was published by Barr (1972) and Davis and Lister (1977a).

Research on deep-sea sedimentation in the northeast Pacific was largely the result of regional reconnaissance. Studies concentrated on ice-rafted material, turbidites, and deep-sea channels of the Cascadia Basin and neighbouring abyssal plains (Griggs and Kulm, 1970;Horn, Ewing and Ewing, 1971; Horn et al, 1971; Kent et al, 1971; Listizin, 1972; Nelson and Kulm, 1973; Stewart, 1976; vonHuene et al, 1976). Sediment of the continental terrace and Cascadia Abyssal Plain off Washington and Oregon were analyzed for Late Quaternary changes in sediment mineralogy. Chronostratigraphy was dependent on radiocarbon dates, biogenic and volcanogenic stratigraphic

markers (Nelson et al, 1968; Duncan et al, 1970; Duncan, Kulm and Griggs, 1970; White, 1970; Kulm et al, 1975; Karlin, 1980). The regional applicability of biogenic stratigraphic markers was, however, locally limited because they are time-transgressive on a regional scale (Barnard and McManus, 1973; Phipps, 1977). Mineralogical studies of the surface sediments include Rateev et al, (1969), Windom (1969), Lisitzin (1972), Kido (1974), Windom (1976). Studies on the stratigraphy of deep-sea sediments to basement are contained in the DSDP reports (Kulm et al, 1973). Gross correlations for the Late Quaternary have been made on the basis of nonradiocarbon stratigraphic marker horizons including Mazama Ash (Nelson et al, 1968), radiolaria to foraminiferal ratio (Duncan, Fowler and Kulm, 1970; Barnard and McManus, 1973) and pulses of glacial detritus (vonHuene, et al, 1976).

Sediments at the northern end of Juan de Fuca Ridge, although influenced by similar mineralogic and sedimentation controls documented elsewhere from the northeast Pacific, had not been examined prior to this study. Previous investigations of the present study area have been tectonic, and involved only superficial examination of sediments (Lucas, 1972; Barr, 1972; McManus et al, 1972: Barr and Chase, 1973; Davis and Lister, 1977a; Davis and Lister, 1977b). Using continuous seismic-reflection profiles (CSP), (McManus et al, 1972) divided the sediments into two units, A and B. Unit A was described as a sequence of turbidites that overlay the ridge basement. Near the end of unit A deposition (0.7 million years B.P.), block faulting, uplift and tilting formed the ridges. Unit B, which unconformably overlies the deformed sediments of unit A has little deformation, is confined to the valleys and was interpreted to be post-deformational (Barr, 1972; McManus et al, 1972). A detailed geophysical study augmented

by gravity coring was conducted by Davis and Lister (1977a). The cored sediment was primarily examined to aid in the interpretation of the acoustic reflective character of the sediment column. Davis and Lister (1977a and b) recognized, as did McManus et al (1972) and Barr (1972) the great thickness of sediment of Middle and East Valleys which contrast with very thin sediments of West Valley. The Sovanco Fracture Zone (a ridge and parallel trough) and its contact with West Ridge was proposed as a barrier which prevented sedimentation by turbidity currents on Juan de Fuca Abyssal Plain and West Valley (Barr, 1972; McManus et al, 1972; Davis and Lister, 1977 a and b).

Rates of sedimentation, computed from the age of the outer edge of the central Brunhes magnetic anomaly of the basement (0.69 my: Barr, 1972), range, for the total thickness of Middle Valley sediment, from 55 to 170 cm/1000yr (McManus et al, 1972) or 670 to 1000 cm/1000yr (Davis and Lister, 1977a) with negligible sedimentation from 10,000 yr B.P. to the present (Davis and Lister, 1977a).

HYDROGRAPHY

Limited data is available for the water column above the northern end of Juan de Fuca Ridge. In the most detailed study, Thomson (1973) discussed the variation and distribution of physical properties of seawater to depths of 1500 metres along Line P, which consisted of a number of hydrographic stations stretching from the mouth of the Strait of Juan de Fuca to ocean weather station P (latitude 50°00'N and longitude 145°00'W). Some of the hydrographic stations measured lie above the study area.

In conjunction with the U.B.C. study (1977) bottomwater measurements were made at several coring stations by Dr. E. V. Grill (U.B.C.). The results of Dr. Grill's work and that of Thomson (1973), will collectively be discussed in Chapter II in relation to the influence of hydrography on Juan de Fuca Ridge sedimentation.

Chapter II

SEDIMENT TEXTURE AND STRATIGRAPHY

INTRODUCTION

Research on sediments from oceanic ridges in the northeast Pacific has aided in the interpretation of the deep-sea stratigraphic record and helped unravel the complex interrelationship of biogenous, hydrogenous, halmyrolitic and terrigenous components (Selk, 1977; Phipps, 1977; Bȇland in prep.; Hanson in prep.; Price in prep.;).

The bathymetry for this study of Juan de Fuca Ridge was recorded by a 3.5 kHz echo sounding system along eight parallel northwest-southeast shiptracks (Fig.2). Continuous seismic-reflection profiles were recorded along some of the same shiptracks. The resultant bathymetry was used to select core sites in the various local sedimentary environments.

Cores selected for sedimentological analysis were sited on dominant physiographic features of Juan de Fuca Ridge. Cores along two lines were studied, one perpendicular to the ridge axis and the other parallel to West Valley, the active spreading rift (Figs.3 and 4).

METHODS

One hundred and twenty samples were analyzed from eight 6.5 cm diameter gravity and three 3.5 cm diameter Phleger cores (Appendix I). Seven of the cores were X-radiographed to illustrate structural features. The samples for sediment analysis were taken at five centimetre intervals in the Phleger cores and at ten to fifteen centimetres in the gravity cores. West Valley, West Ridge, Middle Valley, Middle Ridge, East Valley and Cascadia Basin cores yielded 64, 9, 7, 17, 15 and 7 samples respectively.

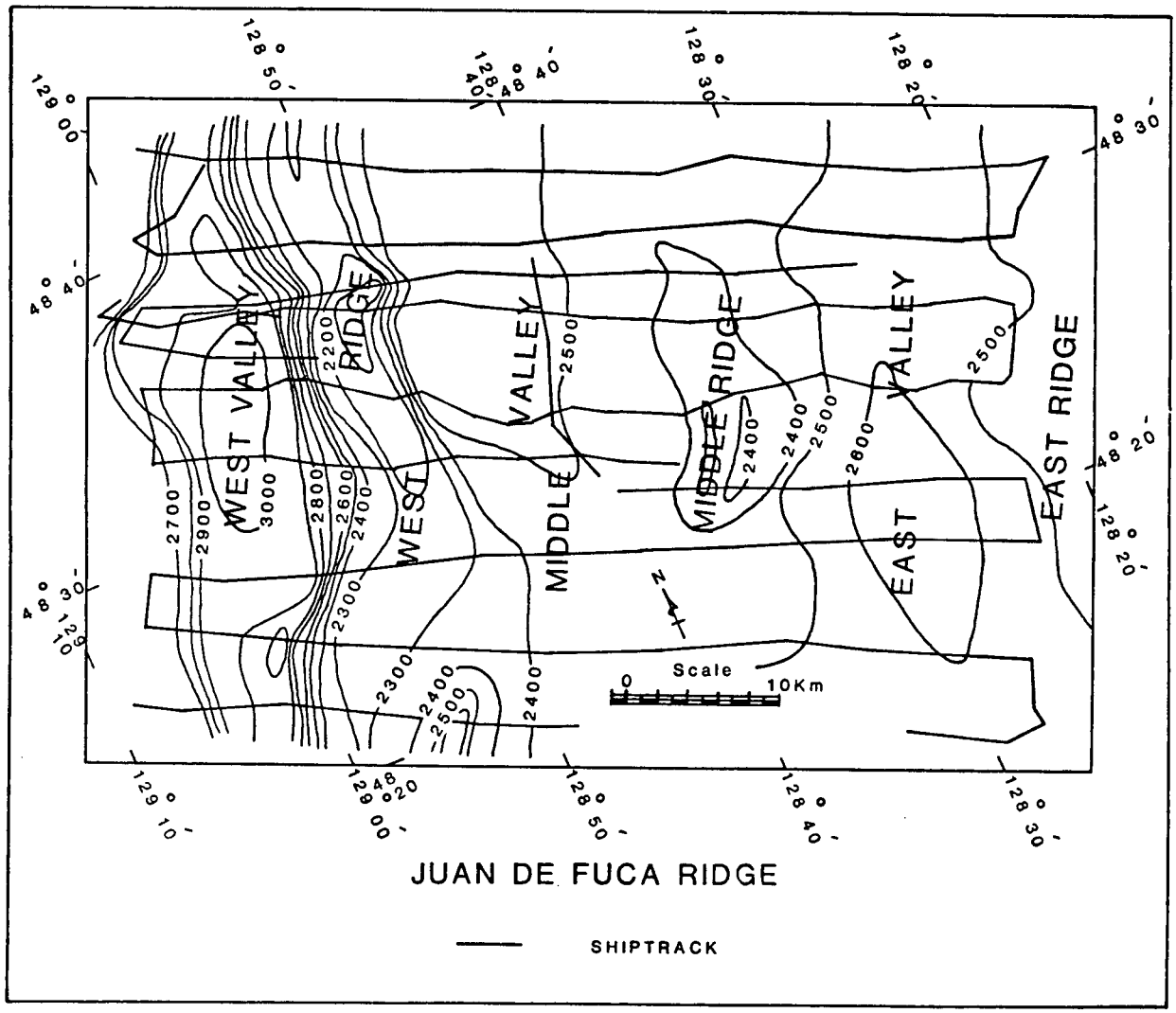

FIGURE 2. Bathymetric map (100 metre interval) and shiptrack of the northern end of Juan de Fuca Ridge. Navigation is by Loran A - C. F. A. V. Endeavour, 1977. Spreading axes are West Valley and possibly Middle Valley.

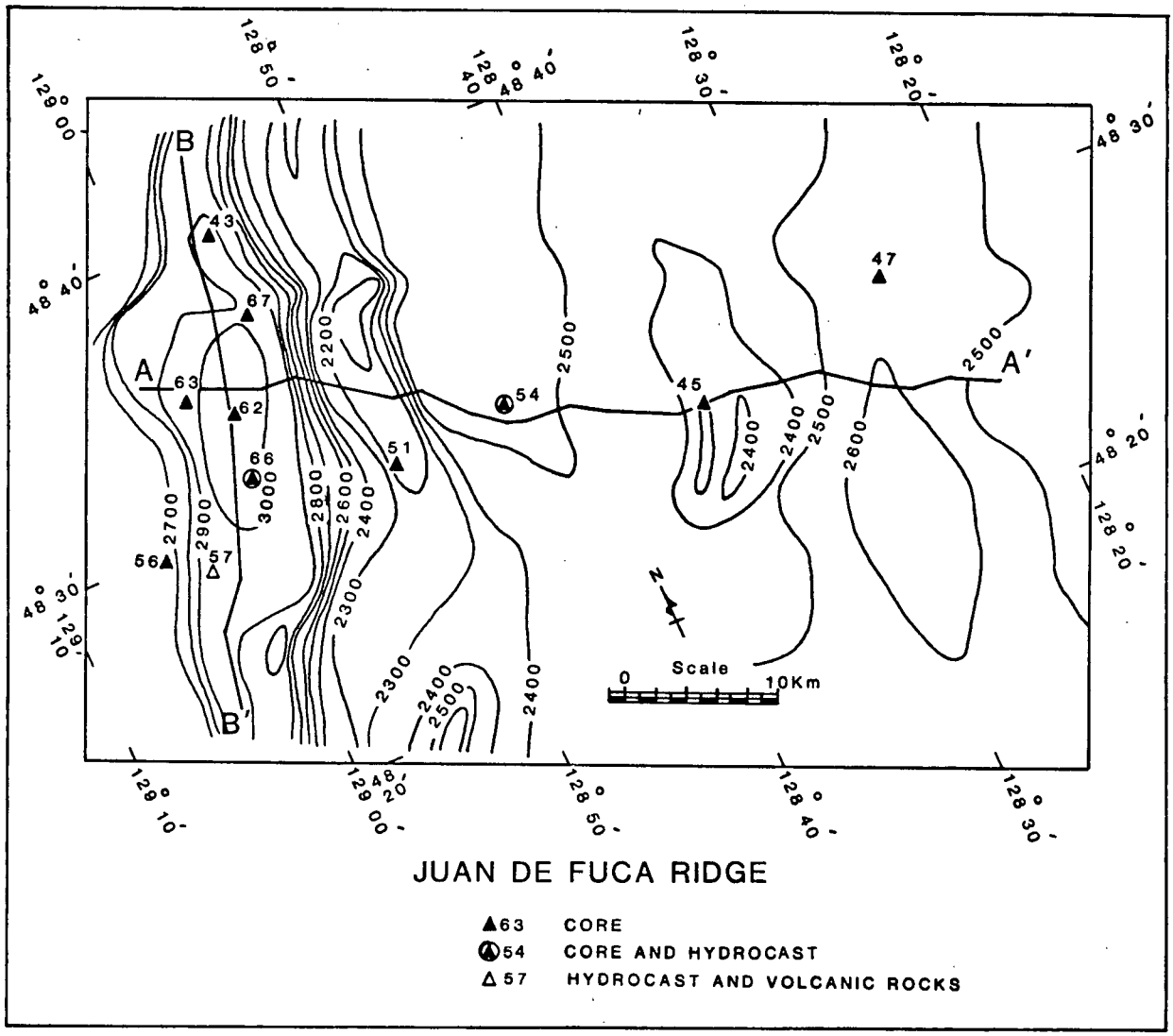

FIGURE 3. Bathymetric contour map (100 metre interval) of the northern end of Juan de Fuca Ridge showing cores and studied sections AA' and BB'.

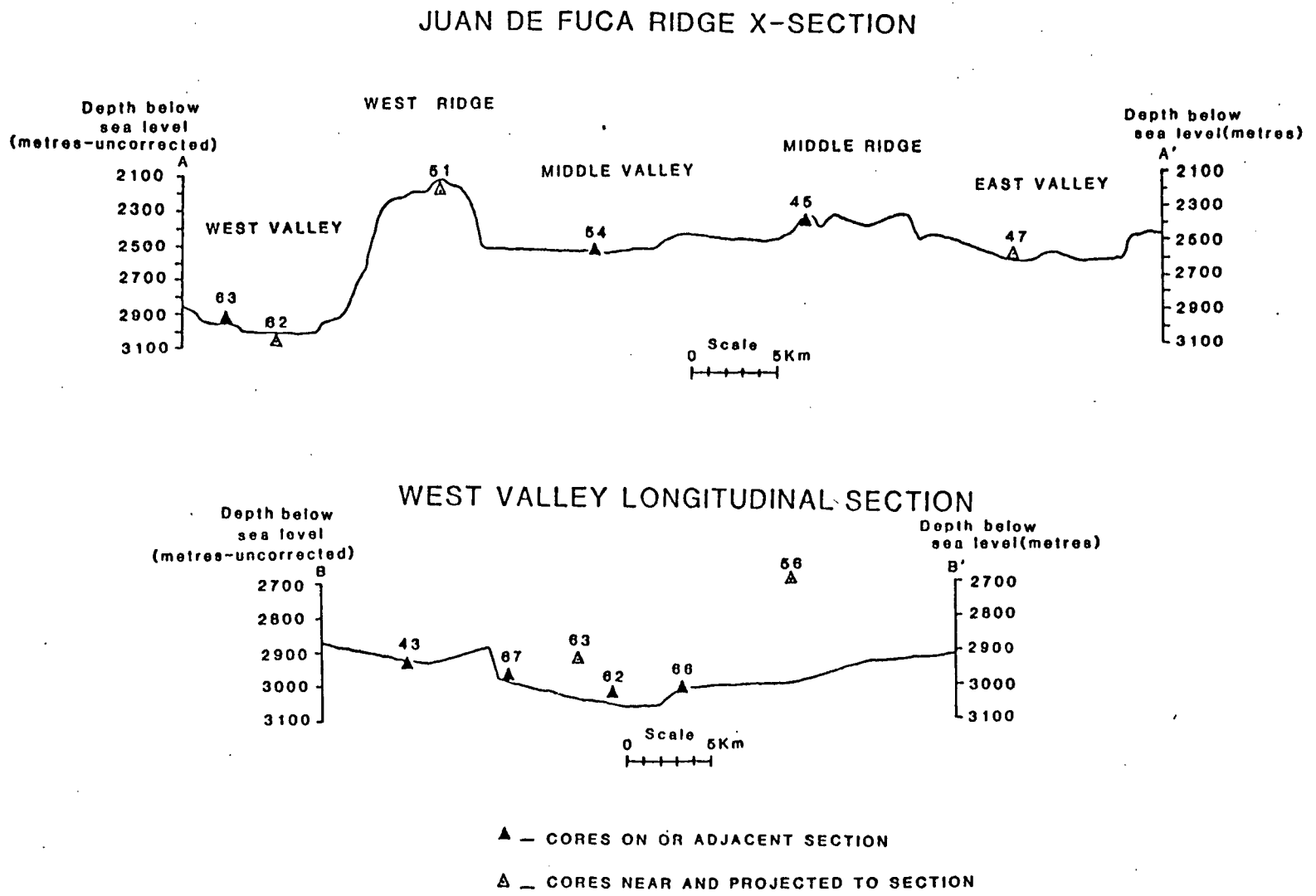

FIGURE 4. Bathymetric profile AA' from spreading axis (West Valley) southeastward showing studied core locations. Core site 51 is projected northeast along West Ridge, and site 47 is projected southwest along East Valley onto profile.

Bathymetric profile BB' is a northwest to southeast longitudinal section along West Valley showing studied core locations, cores 56 and 63 are projected northeast onto profile.

Examination of X-radiographs verified that repeated major structural features were sampled within each core.

Analyses of particle size distribution were performed on 1.25 gram sediment samples using both a Micromeritics Sedigraph 5000, and a 5000D Particle Size Analyzer (Micromeritics Instruction Manual, 1975). Each sample was prepared from a 2.5 gram aliquot of air-dried sediment. Carbonate was removed by reaction with dilute acetic acid on selected samples from cores 45 and 51. Other core samples, which contain less than 3% $CaCO_3$ as indicated by prior chemical analyses, were not so treated. Salt was removed from each sample, including those acidified, by repeated washing with distilled water as described below. Samples were wet-sieved with distilled water through a 63 μm mesh, then mixed and centrifuged for 1.5 hrs in 100 ml polyethylene test tubes with approximately 90 ml of distilled water at 2100 rpm using an I.E.C. centrifuge with a #240 head, a radius of 23 cm and distance of 8.5 cm from headcentre to the test tube opening. Samples were washed and centrifuged twice, the supernatant liquid was decanted off, and the remaining sediment mixed into a slurry with a 40 ml solution of 5 grams of Calgon per litre of distilled water. The slurry was homogenized using a magnetic stirrer and 20 ml was pipeted off and placed in 25 ml bottles for Sedigraph analysis. Garnet standards and a baseline solution of 5 gram/litre calgon were run prior to every ten samples analyzed. Triplicate runs of cumulative curves for the same sample plotted with $\pm$ 1.5% of the initial trace. Computer processing of data points at 1/4 ϕ intervals from the cumulative curve produced by the Sedigraph enabled the determination of size-distribution statistics and construction of bargraphs and arithmetic and logarithmic cumulative curves for each analyzed sample. The sand fraction was examined under the binocular

microscope at 60 to 80 times magnification to determine proportions of its components.

The sand sized fraction was divided into four major components: biogenic (radiolarian, foraminiferal, diatom and ostracod tests); detrital minerals; carbonaceous material (degraded terrigenous plant debris); and authigenic material (framboidal pyrite). The identities of detrital and authigenic components were determined by X-ray diffraction and scanning electron microscopy. Visual estimates, expressed as percentages were made of proportions of each component. The latter are only approximate, but are meaningful when combined with quantitative measurements to illustrate sedimentation patterns. A graphic depiction of proportions of radiolaria to foraminifera was used to indicate relative changes in planktics and illustrate which organism most strongly dominates the biogenic component.

Four radiocarbon dates were obtained from foraminiferal-rich ridge-top cores. X-radiographs of these cores show little disturbance of the sediment over dated intervals. Samples for radiocarbon dating were removed with a stainless steel spatula, the outer two millimetres of sediment being discarded. The sample was then washed onto a 63 μm brass sieve with distilled water, cleaned ultrasonically in glass beakers, sieved again, optically examined at 60 to 100 times magnification, picked clean of organic contaminants, packaged in aluminum foil and sent for analysis to Irene Stehli of Dicarb Radioisotope Laboratory, Chagrin Falls, Ohio, U.S.A.

RESULTS

Sedimentary Structures

X-radiographs of gravity cores from West Valley (Appendix II) each show numerous zones of closely spaced laminae, which overlie a distinct (scoured) surface. The laminae are overlain by sediment which appears

massive except for burrows, possibly of holothurians, and collectively forms a sequence of zones. The frequency of burrows generally decreases upsection within a sequence of zones. Large intervals exist that individually contain a distinct basal erosional contact, overlain by several closely spaced thin sequences of zoned laminated and massive sediment, overlain by a final sequence that consistently contains massive sediment more than 20 cm thick. These intervals are commonly repeated two to three times in each gravity core and appear cyclical. Sediment cycles that are structurally similar are found in four of the X-radiographed cores illustrated, cores 45, 62, 63 and 67 (Appendix II), three of which, 62, 63 and 67 are located within 7 kilometres of each other, at approximately the same depth in West Valley. The remaining core, 45, is from a much shallower depth on Middle Ridge, 28 kilometres southeast of the others, but clearly contains structural cycles strikingly similar to those in the West Valley cores.

Three other X-radiographs (56, 66 and 51) are illustrated to show structural variation. Core 66 is a 46 cm long Phleger core from West Valley, in which the single cycle observed may be the analogue of the shallowest cycle in cores 62, 63 and 67. Core 56, from the west scarp of West Valley, a potentially unstable area affected by local slumping and turbidity currents, has two main cycles, with thinner sequences that are more highly bioturbated than any other core. The most homogenous and massive of all X-radiographed cores is core 51 from West Ridge, which lacks the sediment sequences described above.

Grain Size Distribution

Except for the clay-silt boundary, the boundaries between sand, silt and clay used in this study are those of Folk and Ward (1957) and Folk (1974).

An inflection at approximately 9Ø, observed in all cumulative curves, prompted the use of 9Ø for the clay-silt boundary, rather than Folk's preferred 8Ø.

Statistical Variation

Due to the abundance of clay in the sediment, conclusive resolution of mean, standard deviation, skewness and kurtosis is difficult using conventional statistic methods (Folk and Ward, 1957; Folk, 1974). Projection of the slope of the graphic clay tail, obtaining 100% cumulative weight percent, results in conventionally unacceptable clay weight percentages and sizes finer than 18Ø for most samples. The graphic result was probably due to post-depositional reworking and experimental disaggregation of clay that initially deposited as aggregates such as fecal pellets, particulate matter and coatings on sand and silt grains.

Inherent difficulty exists for statistical interpretation of cumulative curve results on clay-rich sediments. Stokes law of settling is considered valid for clay to silt sized particles where sediment is assigned workable density values and spherical diameters. Sediments from the Juan de Fuca Ridge and Cascadia Basin are dominantly mud with at least 40 and commonly greater than 60 percent clay. Clay minerals are not spherical, but platy and irregular in shape, possess a positive lattice charge that may result in cohesion between clays, and have variable densities. All of these factors, and the small size of the particles, make measurement and statistical treatment based on Stokes law suspect (Blatt, Middleton, and Murray, 1972). Statistics based on an inferred normal distribution, which accurately relate experimental to natural relationships require selection of an experimental mean coincident with the natural mean. A clay tail on the probability curve that reflects the experimental and not

the natural composition will shift the experimental mean away from the natural mean. Standard deviation, skewness and kurtosis values used to deduce environment are then based on experimental mean value and therefore include the mean bias. Correction of the experimental mean to overlap with the natural mean, and statistical testing of this relationship, must precede a conventional statistical examination of sediment environment. No attempt to do this has been made for this study.

In describing changes in texture this study does not determine the experimental and natural statistical relationship but depends solely on grain size distribution boundaries that validly fall within Stokes law determination.

Variation Of Grain Size Distribution Between Ridges And Valleys

Three dominant grain size ranges include all the Juan de Fuca Ridge sediment; sandy silt to silt, mud and clay (Folk, 1974) (Fig.5). It is apparent from Figure 5, that the valleys contain sediment both finer and coarser than that found from the ridges. Cores from West Valley contained the largest proportion of coarse sediment, which could reflect either the sedimentation peculiar to the locality or simply a bias due to more detailed areal and depth sampling than that performed on the other physiographic regions. Middle Valley and East Valley contain the finest sediment in the area, and several samples are similar to or finer than sediment analyzed from the Cascadia Basin. West Ridge sediment tends to be massive with more sand, more clay and less silt than Middle Ridge and valley sediments. In conclusion, the grain size distribution of sediment throughout the area shows differences that suggest varying sedimentation processes(Appendix IV).

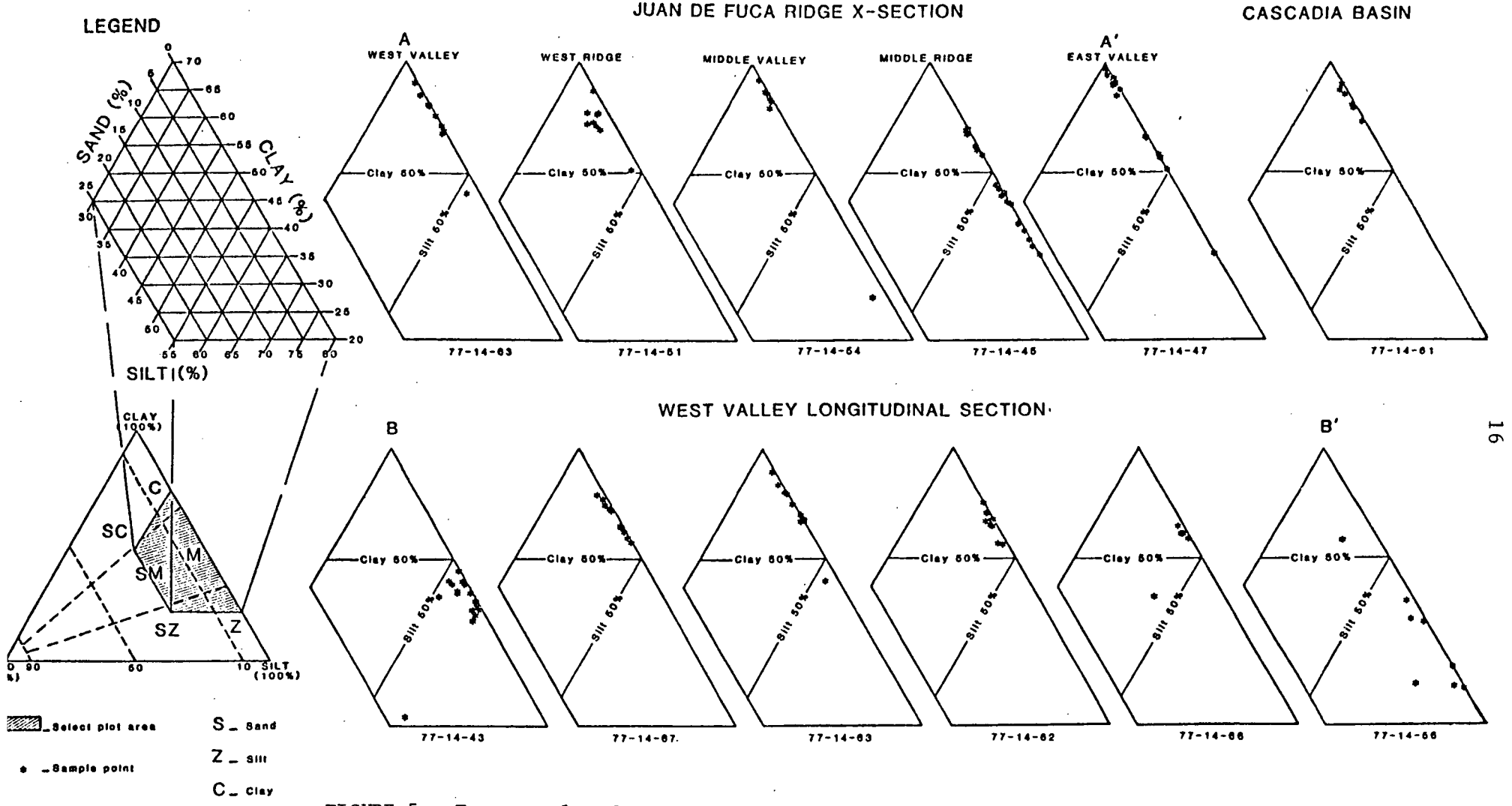

FIGURE 5. Ternary plot fractions illustrating grain size distribution by region along studied sections AA' and BB' from Juan de Fuca Ridge. Cascadia Basin core 77-14-61 is also illustrated as is Folk's (1974) classification nomenclature.

Changes Of Colour And Grain Size Downcore (Appendix II)

The colour of the Juan de Fuca Ridge muds varies widely from a dark to medium gray (N3, N4, N5) for the coarser grain sizes and dusky yellowgreen to light olivegray (5GY5/2 to 5Y5/2) for the finer sediments. Fluctuations in clay size parallel those structural changes described from the X-radiographs. Core 45 from Middle Ridge typically illustrates the trends (Fig.6). The sand component comprises less than one percent of each sample analyzed from core 45. Figure 6 shows that a textural change in clay is quantitatively and symmetrically reflected in the silt trace. The grain size analyses showed very little sand in any of the cores. One sample contains 22 weight percent sand, thirteen samples ranged between 3 and 11 weight percent sand and the remaining 106 samples each contain less than 3 weight percent sand. It is therefore considered valid to use clay fluctuations to illustrate changes in sediment within and between analyzed cores. An examination of the clay changes in core 45 show three gradational fining upward cycles. Changes from fine to coarse sediment are abrupt suggesting a rapid rather than gradational sedimentation process. Changes from coarse to fine sediment and from fine to coarse sediment appear to be cyclical in core 45 as with all the Juan de Fuca Ridge cores.

An obvious feature between valley and Middle Ridge cores is that valley cores show a decided drop in clay content with sediment depth while Middle Ridge sediment demonstrates an increase. This relationship based solely on grain size initially appears inversely related.

Sand Fraction

Optical examination of the fraction greater than 62.5 μm from each sample revealed four components based on composition and source: (1) A biogenic component that includes radiolarian, foraminifera, diatom

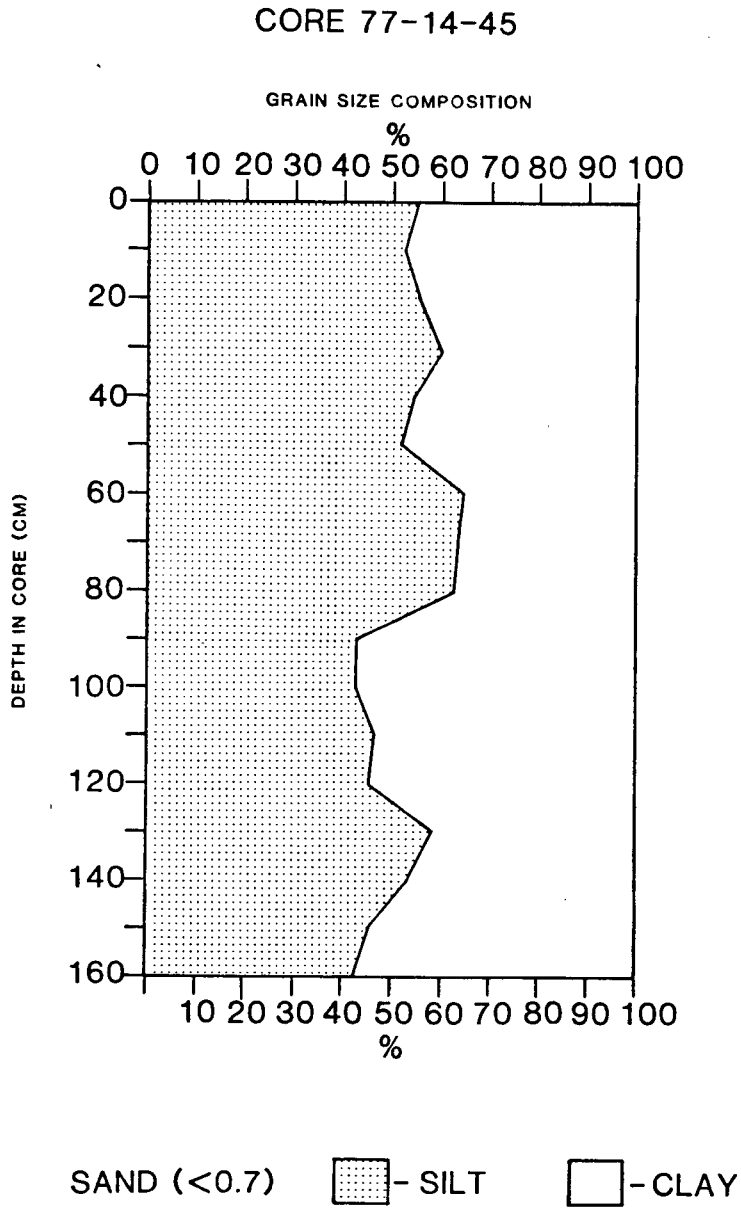

FIGURE 6. Grain size composition for percentage sand, silt and clay in core 77-14-45 from Middle Ridge. The small sand component results in an obvious symmetry for silt and clay.

and ostracod tests; (2) a detrital component that includes quartz, mica, basalt, plagioclase, obsidian and less common minerals; (3) carbonaceous and (4) authigenic components which include decayed terrigenous plant debris and framboidal pyrite respectively. Results are illustrated in Figures 7 and 8, which demonstrate the changes along West Valley and across Juan de Fuca Ridge. The relative abundances of radiolaria and foraminifera also shown, illustrate which organism dominated a given biogenic component (Duncan, Fowler and Kulm, 1970; Barnard and McManus, 1973; Phipps, 1977). Clearly the components are not as sensitive as grain size or structural changes in defining cyclical periods of sedimentation. Difficulty exists when one component is so relatively abundant that it masks the subtle changes in sedimentation reflected by the other components (Plates 1 and 2). This problem is most evident in cores that contained a high foraminiferal content although even here a major influx of detrital material is apparent. The gross changes in sand components roughly parallels the previously described sedimentation sequences noted from the X-radiographs and grain size analyses. An exception to this is West Valley core 62 which contains eroded and laminated horizons on the X-radiograph (Appendix II) that were not sampled. The resultant record of changes in grain size with structure changes is incomplete when compared to other more favourably sampled cores.

Composite proportions of the sand size components are plotted alongside the previously described sedimentation sequences in Figure 9. Sediments immediately overlying buried eroded surfaces have up to 80 to 90 percent as detrital component, with mica $>$ quartz $>$ plagioclase $\geq$ basalt $\pm$ obsidian. All nondetrital components are collectively reduced to 20 percent by dilution in such intervals of detrital dominated sediment.

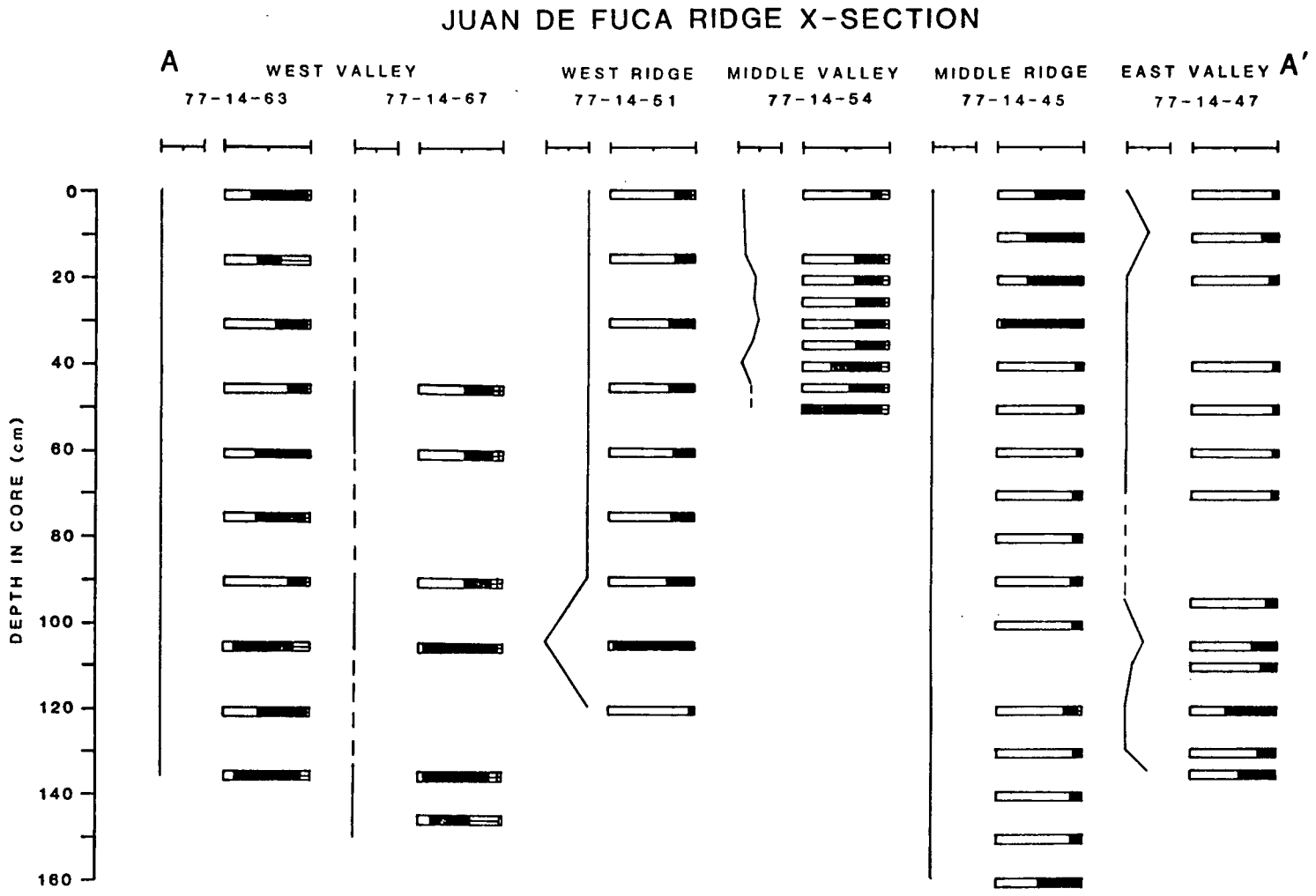

FIGURE 7. Components of the sand size fraction in relative percent are illustrated for cores of profile AA' from Figure 4. The symbols are described in Figure 8.

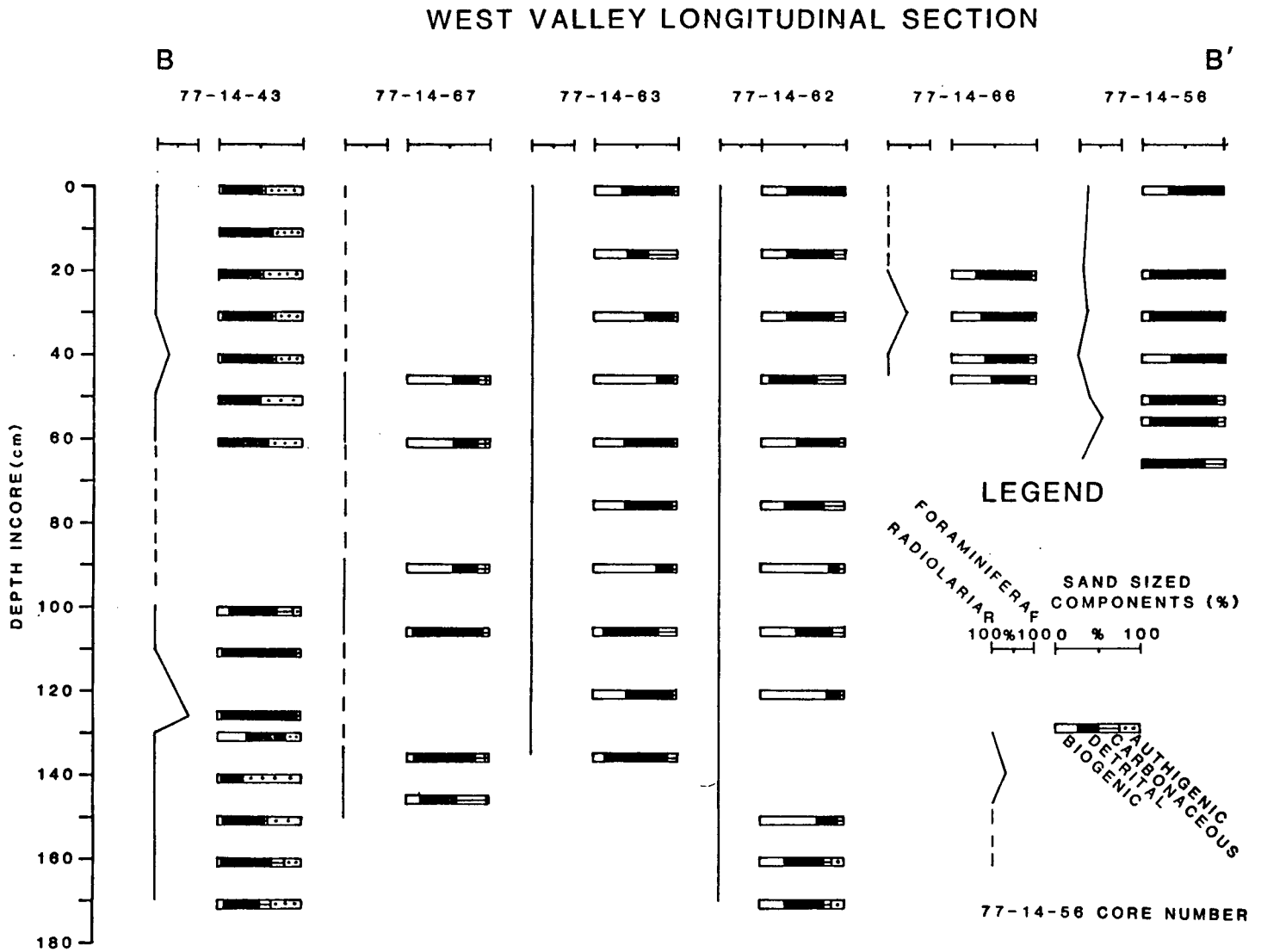

FIGURE 8. Components of the sand size fraction in relative percent are illustrated for cores of profile BB' from Figure 4.

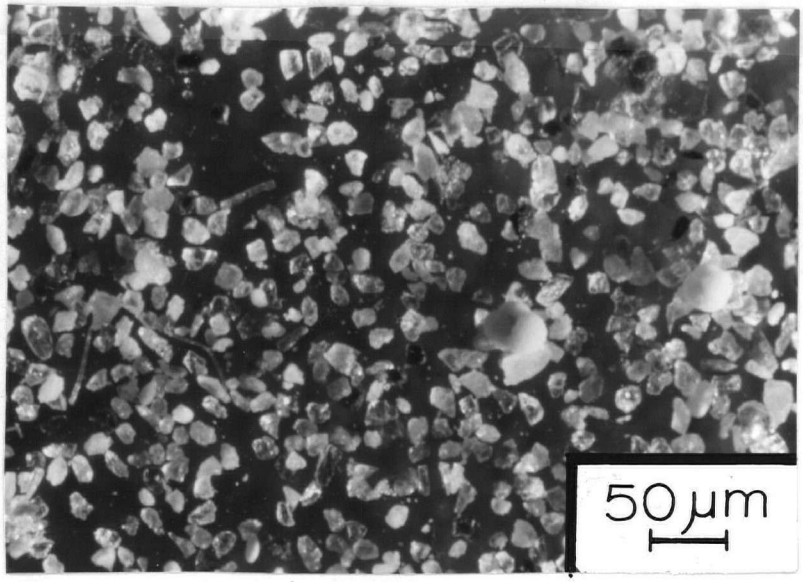

PLATE 1. Photomicrograph showing the sand component from the coarse basal sediment of a turbidite sequence (West Valley core 77-14-43)(Mag. 20x).

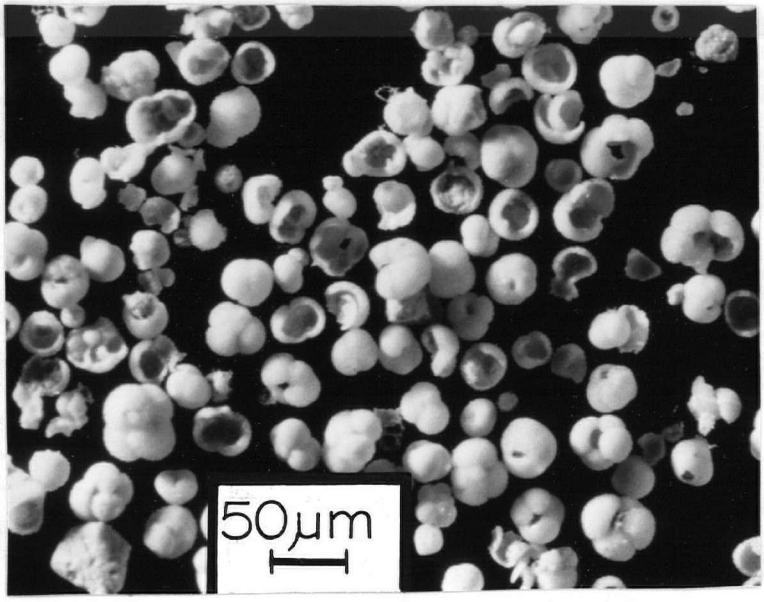

PLATE 2. Photomicrograph showing the sand component of a biogenic-rich and foraminiferal dominated sample typical of cored ridge sediment (Middle Ridge core 77-14-45)(Mag. 20x).

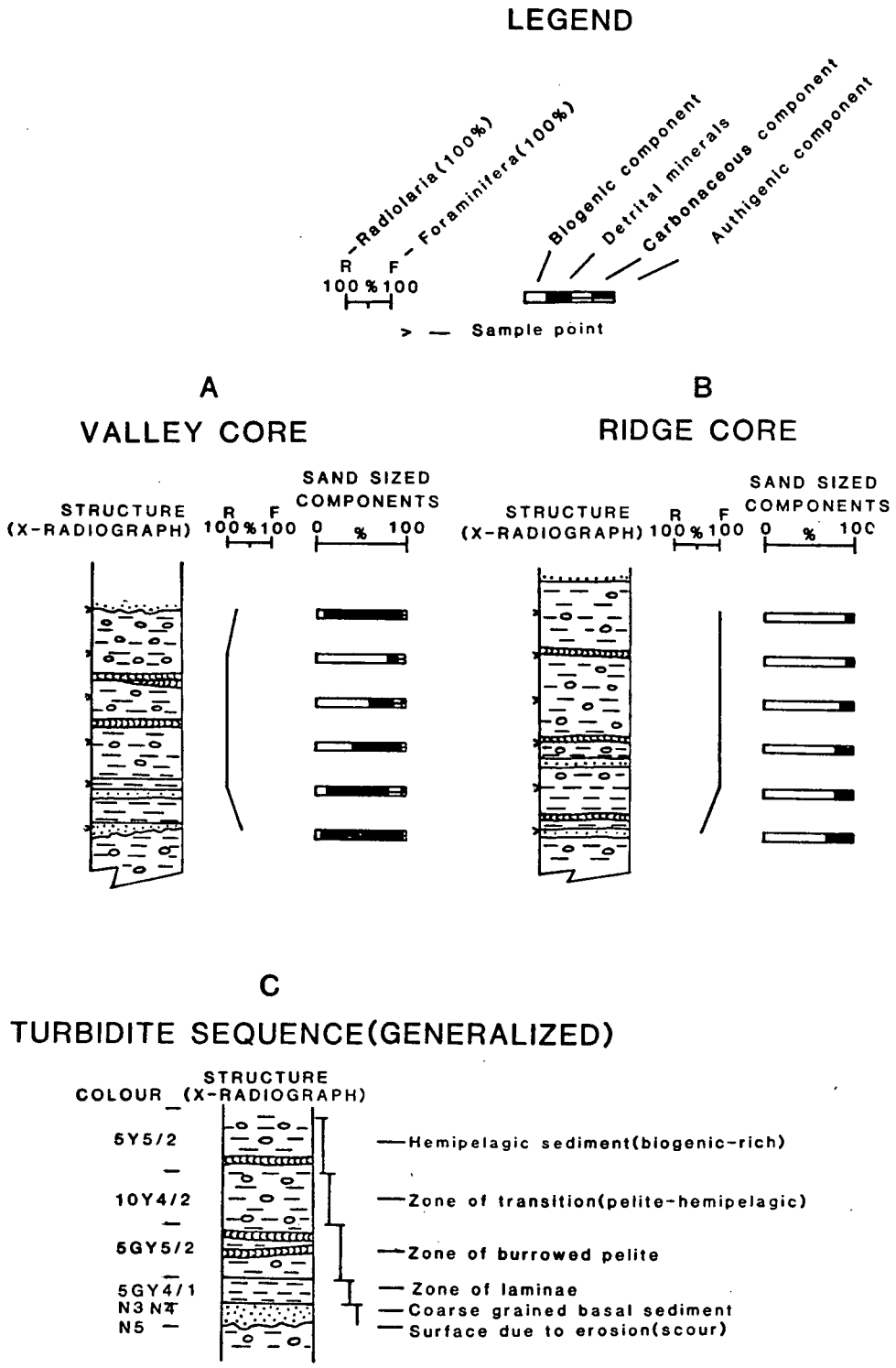

FIGURE 9. Generalized sequences from cores of the northern end of Juan de Fuca Ridge based on X-radiograph structure and sand size fraction components for A. Valley, B. Ridge and C. Idealized turbidite sequence overlain by hemipelagic sediment.

The biogenic component in detrital dominated sediment may exhibit a slight increase in foraminifera, a feature recognized elsewhere as an entrained turbidite fauna (Plate 1) (Griggs and Kulm, 1970). In the overlying laminated and massive sediments a gradational increase in the amount of biogenic and carbonaceous components at the expense of the detrital component takes place with fining of sediment. In all of the sequences the uppermost, finest grained sediment with reduced burrowing exhibits the largest biogenic component, with planktics much greater than benthics. The same fine grained sediment contains a much reduced detrital sand component and often lacks carbonaceous or authigenic components. Slight variation of the previously described sequence in each core can be attributed to local physiography and hydrography.

Biogenic materials in ridge cores differ from those in valley cores. West Valley sediments, the deepest in the study area, are dominated almost exclusively by radiolarian tests, except where foraminifera occur in the coarsest of samples. Frequently these samples contain more robust benthic forms than planktic forms. These foraminifera are believed to have been transported, from shallower regions. In Middle and East Valley also, the biogenic component is dominated by radiolaria. In sediments from West and Middle Ridges foraminifera dominate the biogenic component (Plate 2).

Occurrence of the authigenic component does not appear to be physiographically controlled. Framboidal pyrite occurs in both the ridge and West Valley sediments (Figs. 7 and 8). West Valley cores 62 and especially 43 contain significant proportions of authigenic pyrite in the sand size material. The ridge sediment also contains substantial authigenic pyrite although the abundant foraminiferal component diminishes its absolute percentage. The source of the pyrite is conjectural: Studies of

anaerobic sediments with high organic content suggest that anaerobic bacteria decomposing protoplasm provides significant quantities of sulphur which combines with dissolved iron to produce intermediate minerals that with alteration result in authigenic pyrite (Farrand, 1970; Siesser and Rogers, 1976). In the present study, optical examination of biogenic material revealed radiolarian tests, foraminiferal shells and worm tubes lined or infilled with abundant framboidal pyrite (Plate 3). Large irregular aggregates of framboidal pyrite were also observed with no apparent biological association (Plate 4). Identical occurrences in reduced sediments off the northwest coast of Africa were attributed to pyrite replacement of irregular masses of decomposed organic tissue in the sediment (Siesser and Rogers, 1976). Ridge sediment, relatively abundant in pyrite as discussed in later sections, exhibits reworking by bottom currents, a mechanism that apparently concentrates the mineral.

Radiocarbon Dates And Rates Of Sedimentation

Four radiocarbon dates were obtained from foraminifera picked from two ridge cores: Core 51 (West Ridge), sampled over the intervals of 0 to 12 centimetres and 79 to 87 centimetres, yielded dates of 19,000 B.P. plus 840 to minus 930 years and 23,660 B.P. plus 1350 to minus 1620 years respectively; Core 45 (Middle Ridge), sampled over the interval 33 to 54 centimetres and 85 to 109 centimetres, yielded dates of 10,170 B.P. plus 630 to minus 690 years and 14,970 plus 620 to minus 680 years respectively (Appendix III). The selection of radiocarbon sample intervals were dependent on sufficient biogenic ^{14}C to produce detectable ages from undisturbed sediment which, for Middle Ridge, preceded periods of turbidite deposition. Optical examination of the same intervals shows a ratio of planktic to benthic foraminifera greater than 100:1. Sedimentation rates

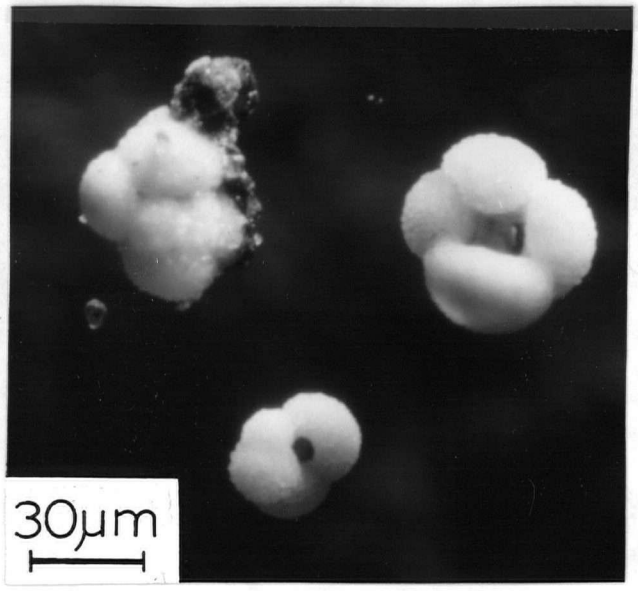

PLATE 3. Photomicrograph showing planktic foraminiferal shells from Middle Ridge core 77-14-45 with pyrite aggregates found in contact with the shell surface (upper left of photo) and within the shells (dark material lining the umbilical region)(Mag. 50x).

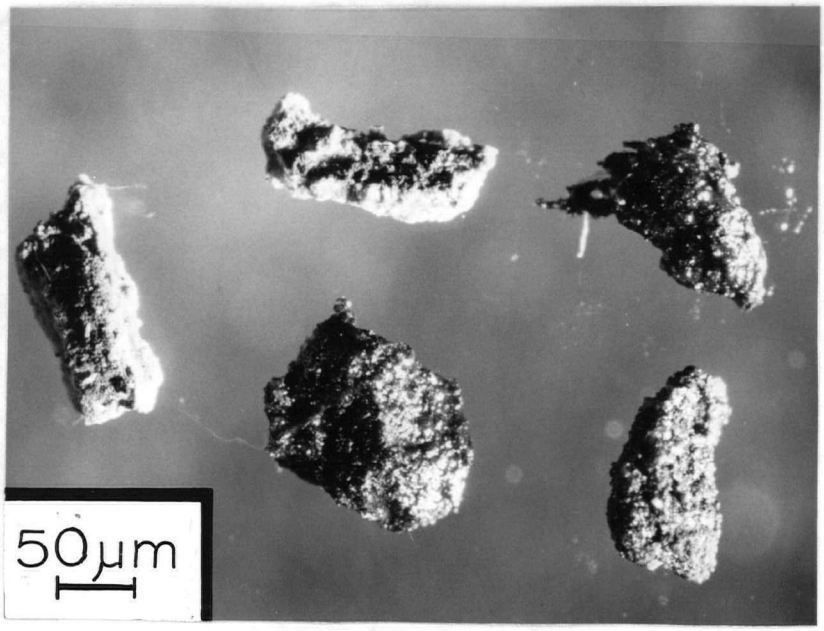

PLATE 4. Photomicrograph showing massive aggregates (lower centre and right of photo) of pyrite with no apparent biogenic association (West Valley core 77-14-43). Arenaceous worm (?) burrows (light coloured material) lined with dark coloured pyrite aggregates (upper left and upper centre of photo)(Mag. 20x).

based on sample interval midpoints and age differences are 11.1 cm/1000 years for core 45 and 16.5 cm/1000 years for core 51 (Turekian and Stuiver, 1964).

DISCUSSION

Variation In Structure And Size Distribution

Sediment structure and size distribution, although dependant on physiographic location, can show widespread cyclic changes. Griggs and Kulm (1970), Horn et al, (1971) and Nelson and Kulm (1973), in regional studies, recognized such cycles in cores from the northeast Pacific and from Cascadia Deep-sea Channel, and attributed them to turbidity current influxes, alternating with periods of hemipelagic sedimentation. The Juan de Fuca Ridge sediments correspond to the rapidly and slowly deposited distal turbidites of Horn et al, (1971), Bouma and Hollister (1973), Nelson and Kulm (1973) and Walker and Mutti (1973).

Generalized Turbidite Sequence

A turbidite, for the purpose of this study, is the deposit of a turbidity current (Walker and Mutti, 1973), a form of sediment gravity flow, in which the sediment is primarily supported by the upward component of fluid turbulence (Middleton and Hampton, 1973). The idealized sequence of a turbidite was subdivided into five divisions called A, B, C, D, and E by Bouma (1962). A generalized turbidite sequence characterizing the cored sediment from Juan de Fuca Ridge begins with a scoured contact overlain by parallel laminae, followed by massive mud (Fig.10). The sequence fines upward from sandy silt to silty clay. The laminae are distinct, and the laminated sediment ranges in thickness from 0.1 to 1.0 centimetres. The colour (wet) ranges from dark gray (N3) for the coarsest sections to dark greenish-gray (5GY4/1) for the finer laminae. A massive highly bioturbated

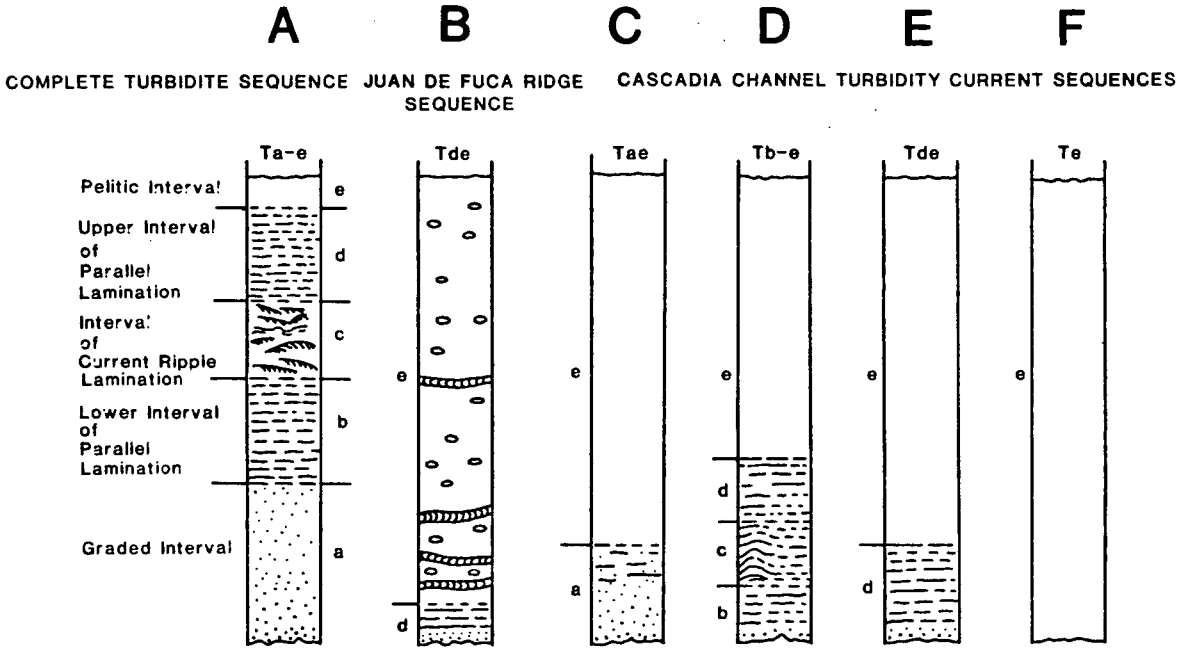

FIGURE 10. A. Complete turbidite sequence of Bouma (1962).
B. Typical sequence, Juan de Fuca Ridge.
C-F. Turbidite sequences of Cascadia Channel (Griggs and Kulm, 1970).

layer of mud a few to several tens of centimetres thick overlies the laminated sediment, is usually dusky yellow-green (5GY5/2) to grayish olive (10Y4/2) and fines upward. The Juan de Fuca Ridge turbidite sequence resembles the upper division of parallel lamination (D) and pelitic division (E) of Bouma (1962) (Fig.16). The top is a zone of biogenic-rich, light olive-gray (5Y5/2), clay dominated mud which commonly caps the sequence, appears hemipelagic in origin and may be absent due to scour by the next turbidity current.

Turbidite Correlation

Three cycles (I, II, III) containing potentially correlatable turbidites are found in West Valley sediment (Fig.15). The cycles are best seen in X-radiograph structures. Each cycle is composed of one or more closely spaced turbidites with intervening massive sediment. Cycles are generally located at depths between 0 and 25cm (I), 25 and 85cm(II) and 80 and 120cm(III). A consistent 50 to 60 cm of massive (turbidite and hemipelagic) sediment separates laminated sequences of cycle I from II, and 20 to 30 cm separates laminated sequences of cycle II from III. Grain size distribution values parallel the structural changes.

Superimposed on the West Valley turbidite cycles are changes in sediment characteristics above and below an approximate 40 to 50 cm sediment depth. Sediment below 40 to 50 cm contains stronger scouring, thicker laminae, more coarse and less fine sediment and more entrained foraminifera in the turbidites. The massive sediment below 40 to 50 cm also contains more coarse and less fine sediment, as much or more carbonaceous and authigenic material, and more foraminifera than sediment above the 40 to 50 cm level. Although X-radiograph profiles are lacking for East Valley core 47, all of the other sediment changes described downcore

in West Valley occur in East Valley. Middle Valley sediment was not sampled deep enough to determine cycles II and III. The change in valley sediment characteristics below and above 40 to 50 cm for Juan de Fuca Ridge was observed for the sediment in and adjacent to the Cascadia Deep-Sea Channel by Griggs and Kulm (1970) for the Late Pleistocene and Holocene respectively.

Hemipelagic Sediment

Hemipelagic sedimentation was widespread and continuous throughout the area but was modified by processes dependent upon local physiography. Typically the resultant sediment (1) is composed of silty clay, but, when winnowed, clayey silt, (2) has a high biogenic component with radiolaria dominant in the valleys and foraminifera dominant on the ridges, (3) contains minor authigenic pyrite which, when reworked may be concentrated, (4) contains few holothurian burrows and (5) has a colour (wet) ranging from grayish-olive (10Y4/2) to light olive-gray (5Y5/2). Difficulty exists in distinguishing hemipelagic sediment from the fine turbidite sediment of pelitic division (E) of Bouma (1962), produced from the "dilute cloud" of the turbidity current described by Middleton and Hampton (1973). Generally a greater terrigenous component distinguishes a turbidite "cloud" pelitic sediment from hemipelagic sediment. Massive sediment directly above the laminated (D) turbidite sequence, containing dominantly silt to silty mud, more abundant carbonaceous material (terrigenous plant debris), frequent bioturbation, and a moderate biogenic and authigenic component is pelitic turbidite. A transition exists in most massive sequences between turbidite pelite and hemipelagic sediment (Fig.11).

Few compositional differences exist at a core site for hemipelagic

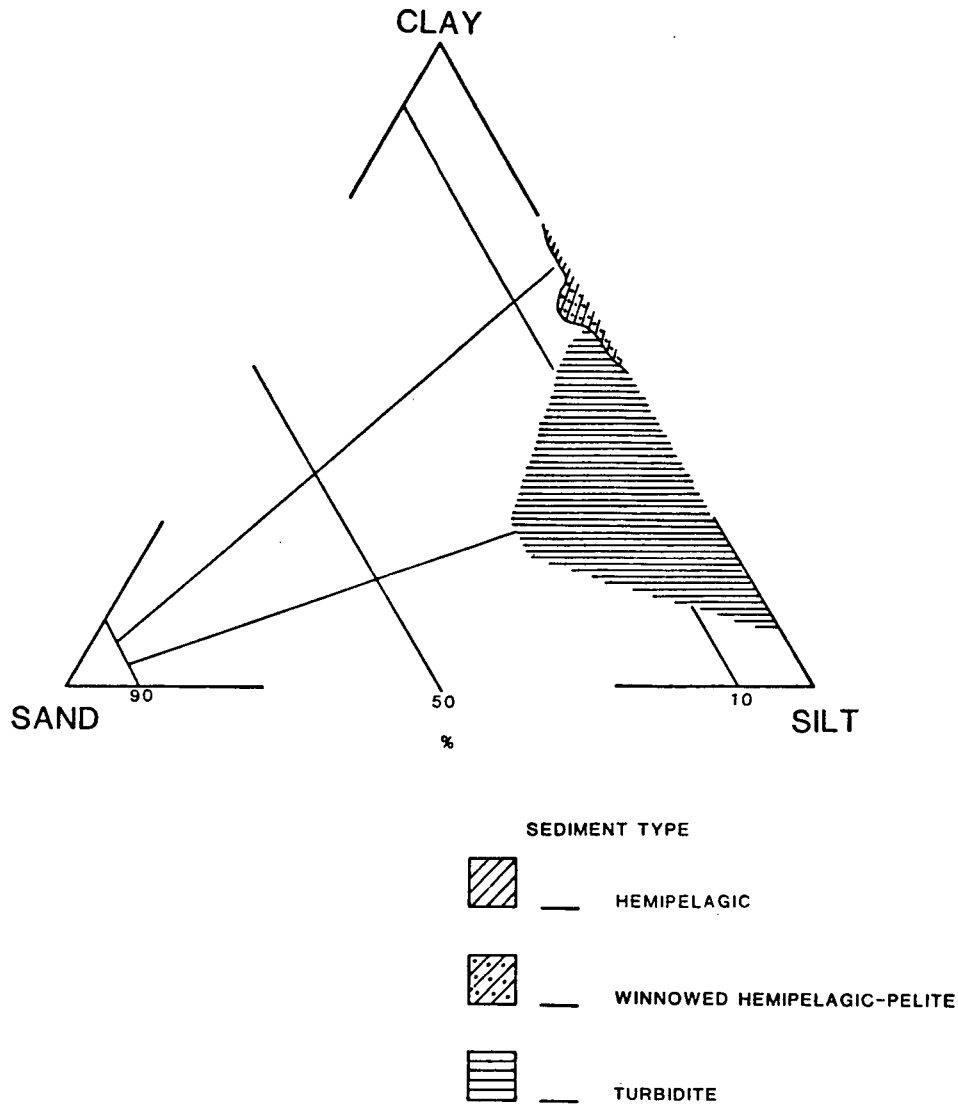

FIGURE 11. Generalized styles of sedimentation for the northern end of Juan de Fuca Ridge. Nomenclature zones after Folk (1974) as in Figure 5.

sediment between turbidite cycles. In the valleys, the massive sediment below 40 to 50 cm possess a larger turbidite pelite component than massive sediment above this interval.

Winnowed Sediment

The ridges are dominated by hemipelagic-pelite sediment which differs from that in the valleys. The postulate that the difference is partly due to winnowing is discussed below.

Reworking of sediment by currents that move sediment (Lisitzin, 1972; Bouma and Hollister, 1973), is not confined to ridges although it is well developed there. West and Middle Ridges are the shallowest bathymetric features of the study area, being much higher than the adjacent valley floors. West Ridge contains massive foraminiferal-rich sediment that is dominated by sand and clay, with low silt. The sediment, based on radiocarbon dates, is Late Pleistocene. The sand is dominated by planktic foraminifera and ice-rafted detritus. Authigenic pyrite is abundant when compared to most valley sediment. In the mineralogy chapter, the concentration of well crystallized coarse clay and the absence of poorly crystalline fine clay from the ridges is pointed out. Middle Ridge sediments are compositionally similar to those of West Ridge except that the lower elevation has resulted in a more substantial contribution of sediment from the "dilute cloud" of valley turbidity currents. The grain size composition, distribution and abundance of clay minerals and concentration of authigenic pyrite in West and Middle Ridge sediments all suggest sediment reworking. Prell (1977) described reworked (winnowed) sediment from the Colombia Basin, Caribbean Sea, based on relationships that appear similar to West and Middle Ridges. Winnowed Colombia Basin sediment was identified by bottom photography and comparison of proportions

of foraminiferal, coccolith and clay components and concentration of the foraminiferal and sand components. Bottom photographs of tranquil and current-smoothed seafloor sediments, led Prell (1977) to postulate that localities such as ridges, major escarpments and other seafloor obstacles lead to streamlining and acceleration of watermasses with an associated selective erosion of fines. West and Middle Ridges possess sediment characteristics and physiographic relationships similar to those described by Prell (1977) for winnowed sediment.

Stratigraphy

The stratigraphic relationships in sediment from the Juan de Fuca Ridge were based on radiocarbon dates and sedimentation cycles in cores from Middle and West Ridge. Correlation between ridge and valley stratigraphy is based solely on parallel changes in sedimentation patterns and characteristics. Chronologic datum levels within marine sediments are commonly defined by index fossils or radiocarbon dates, all of which are dependent on preserved biogenic material. Factors affecting the biogenic component in dateable sediment must be understood prior to the establishment of such datum levels for correlation.

Changes in the position and chemistry of ocean watermasses with time can significantly vary both the productivity of a shelly organism in surface water and the preserved fauna in the sediment (Peterson, 1966; Berger, 1967, 1971, 1976). Conversely, marked changes in the preserved faunal record through a core may suggest temporal shifts and changes in watermasses.

Hydrography

Documentation of periodically repeated hydrographic measurements were initiated in the northeast Pacific at station P in 1952 and along Line P in 1959 (Thomson, 1973). Additional hydrographic data was added from stations located 1.5° of latitude north and south of Line P in 1972 (Fig.12). Observations at the stations included salinity-temperature-depth (STD) profiles and temperature-depth profiles measured with expendable bathythermographs. The results of the study demonstrate a northeast-trending zone of mixing watermasses that divides the oceanic from the coastal domain (Fig.12). Seaward of the zone a rapid decrease in parameter variation and statistical variance occurs while coastward the opposite is evident. The zone of transition or mixed water is best centered between latitudes 48° to 50°N and longitudes 128° to 129°W. The transition zone coincides most directly with station 5 of Line P, (latitudes 48°45'N, longitude 128°40'W) which lies in the area of the present study (Figs.12 and 13). Station 5 is interpreted as central to the area of transition or mixed water between the northward flowing coastal current and the eastward flowing West Wind Drift (Thomson, 1973).

Near-bottomwater hydrographic measurements were made at several stations in conjunction with this study by Dr. E. V. Grill (U.B.C.) (Fig.13). Measurements were made 20 and 50 metres off bottom with one 500 metres off bottom. The hydrocasts ranged in depth from 1816 to 2980 metres based on thermometric measurements. Temperature values ranged from 1.71 to 2.03°C, and decreased with depth. Oxygen and salinity values increased with depth. Oxygen values ranged from 1.75 ml/l at 2945 m depth. Salinity values ranged from 34.588°/oo at 1816 m to 34.647°/oo at 2758 m (deeper values were within 0.002 of 34.645°/oo).

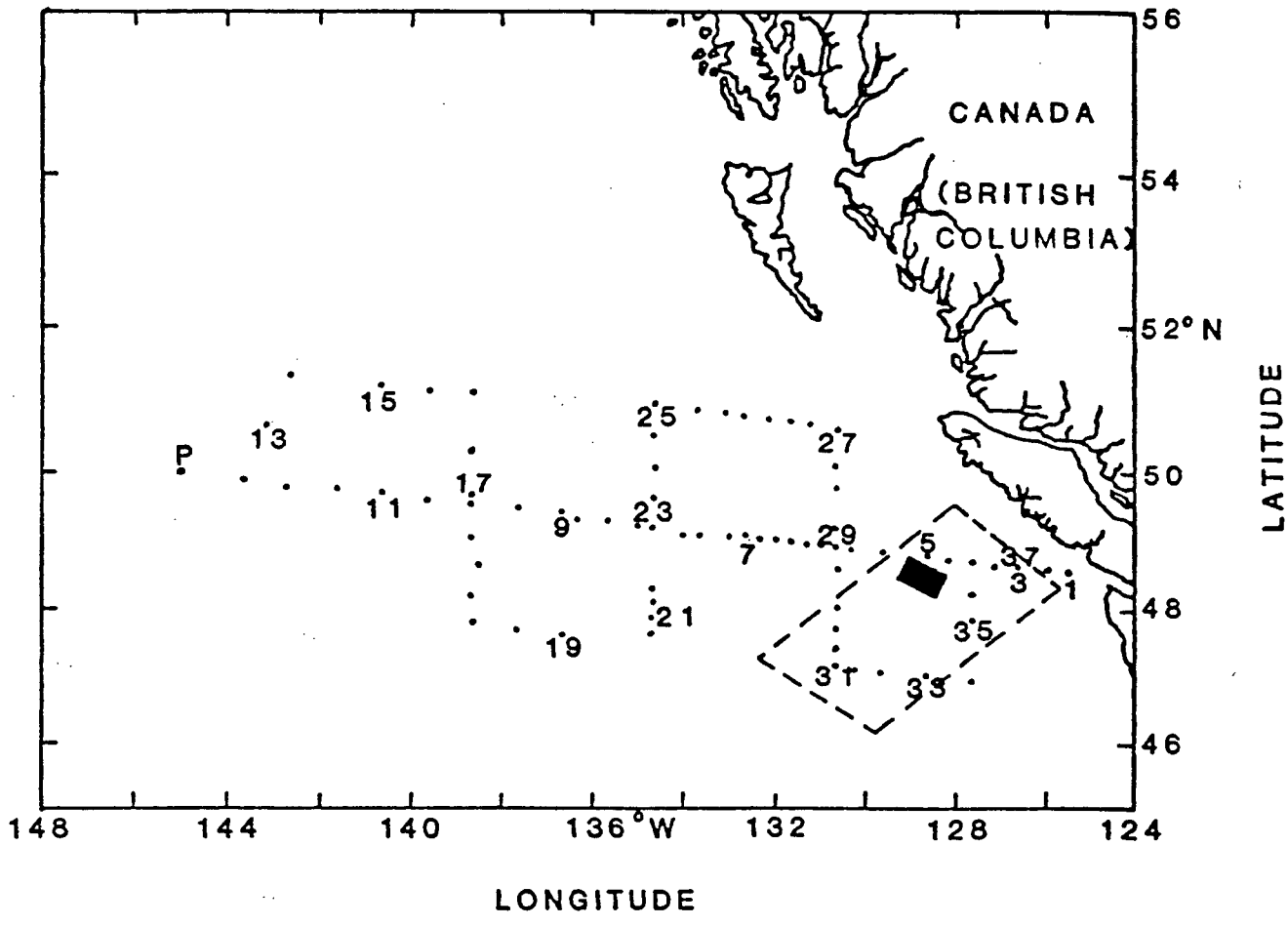

FIGURE 12. Location map of hydrographic survey adapted from Thomson (1973) showing: Line P with odd numbered stations, zone of lateral mixing between oceanic and coastal domain waters (dashed line), and Juan de Fuca Ridge study area (solid colour).

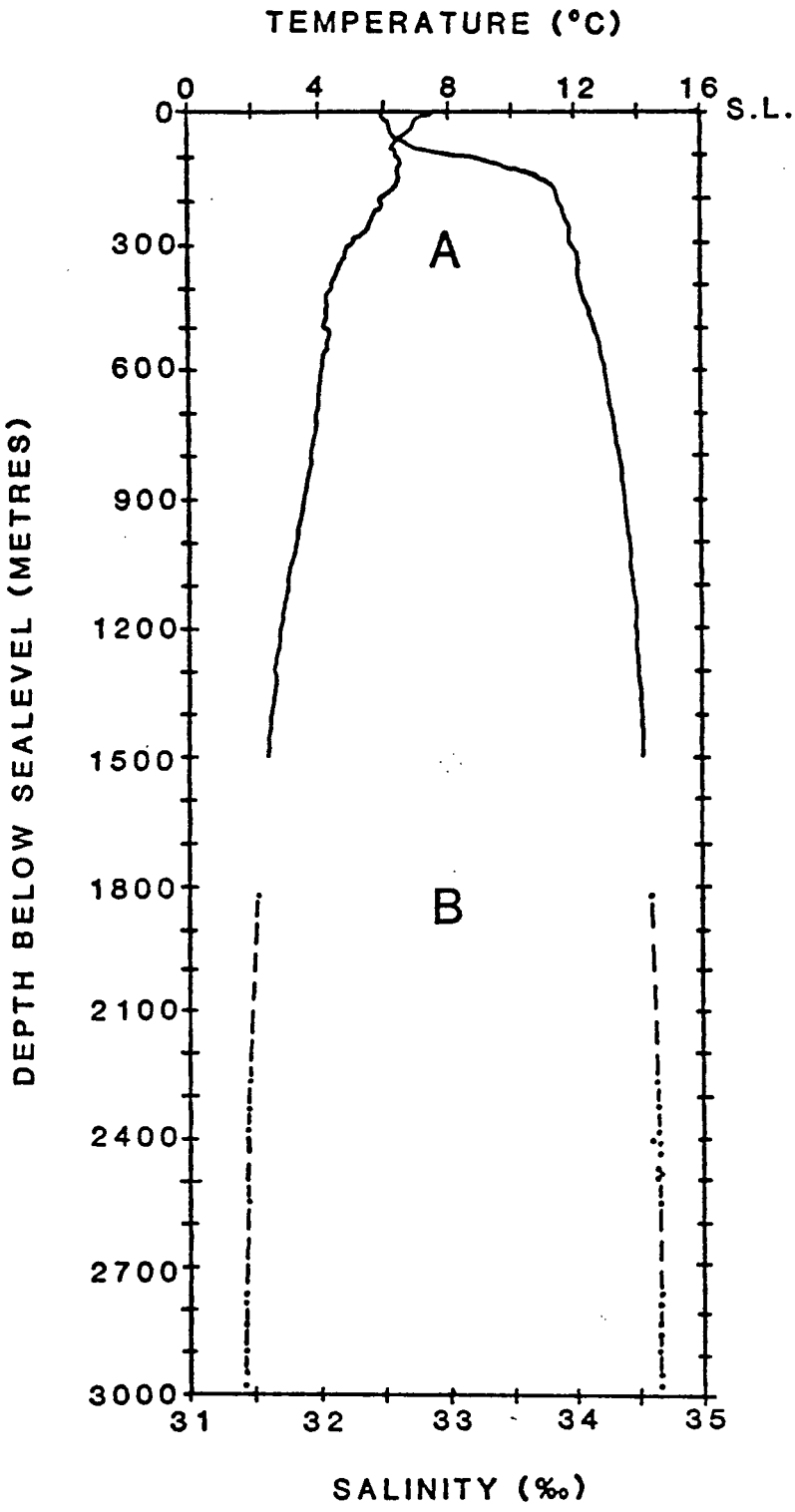

FIGURE 13. Hydrographic profile above the northern end of Juan de Fuca Ridge. Profile A, is based on hydrographic station 5 (Thomson, 1973), and profile B, is the result of hydrographic measurements from directly above the seafloor (E.V.Grill,U.B.C.,1977).

The lowest temperature and the highest salinity and oxygen content occurred in the deepest part of West Valley, highest temperatures and lowest salinity and oxygen contents occurred above Middle Ridge (measurements were not made above West Ridge). Hydrographic measurements within Middle and East Valleys had intermediate values.

Circulation Patterns Affecting The Juan de Fuca Ridge

Based on the areal distribution of the bottomwater hydrographic parameters it appears that the flow of colder, more saline and thus denser watermass which contains the highest oxygen content, is affected by bottom topography. Streamlining of bottom watermasses although undetected by hydrographic measurements, may have been widespread due to the effects of basement relief on ocean water movement (Thomson, 1973). The water column above the study area was described earlier as a zone of lateral mixing of the West Wind Drift and the northern continental current. The lateral mixing, especially of surface waters, may affect the distribution of pelagic and planktic components in the underlying sediments.

Relationship Of Faunal Preservation And Hydrography On Stratigraphy

The interrelationship of microfaunal productivity and preservation, and watermass chemistry has been used by many workers in the interpretation of marine stratigraphy (Frerichs, 1968; Duncan, Fowler and Kulm, 1970; Berger and Winterer, 1974; Berger and Killingsley, 1977). Zooplankton with carbonate tests show large fertility and species fluctuations dependent on small changes in watermass chemistry or temperature (Berger, 1971; Emiliani, 1971; Imbrie and Kipp, 1971).

Change in the ratio of foraminifera to radiolaria in sediments has been widely used as an indicator of Late Quaternary climatic and

oceanographic changes in the northeast Pacific (Duncan, Fowler and Kulm, 1970; Nelson and Kulm, 1973; Phipps, 1977). This change was later described as time-transgressive for regional studies but of local merit (Barnard and McManus, 1973; Phipps, 1977). A similar change has been found in this study. The relief in the study area is 800 metres and the abundance of foraminiferal shells decreases with depth (Figs.7 and 8). In cores from West Valley, radiolaria dominate the biogenic component, except when foraminifera have been introduced by turbidity currents. Sediments of West and Middle Ridges, are in contrast, dominated by planktic foraminifera to the relative exclusion of radiolaria. Sediments cored from intermediate depths suggest a transition of foraminiferal abundance between the bathymetric extremes.

The West and Middle Ridge sediments are dominantly hemipelagic and show evidence of winnowing with a moderate dilution of Middle Ridge plankton by turbidite fines. Turbidity current "dilute cloud" sedimentation on Middle Ridge is apparent during three separate cycles by turbidite deposition (Fig.14). The turbidites in the cycles of Middle Ridge, although similar to those of the valleys, are dissimilar in some characteristics: they do not display scour, but primarily deposition, and the terrigenous sand component is less than one percent. The resultant nonbiogenic sediment is all silt and clay. Studies on the Cascadia Deep-Sea Channel indicate that Holocene turbidity currents, which were smaller in volume than Late Pleistocene turbidity currents, may exhibit fine sediment plume (dilute cloud) effects 17 kilometres laterally and 120 metres vertically (Griggs and Kulm, 1970). Middle Ridge sediment is 135 metres above Middle Valley and West Ridge sediment is 800 meters above West Valley and 300 meters above

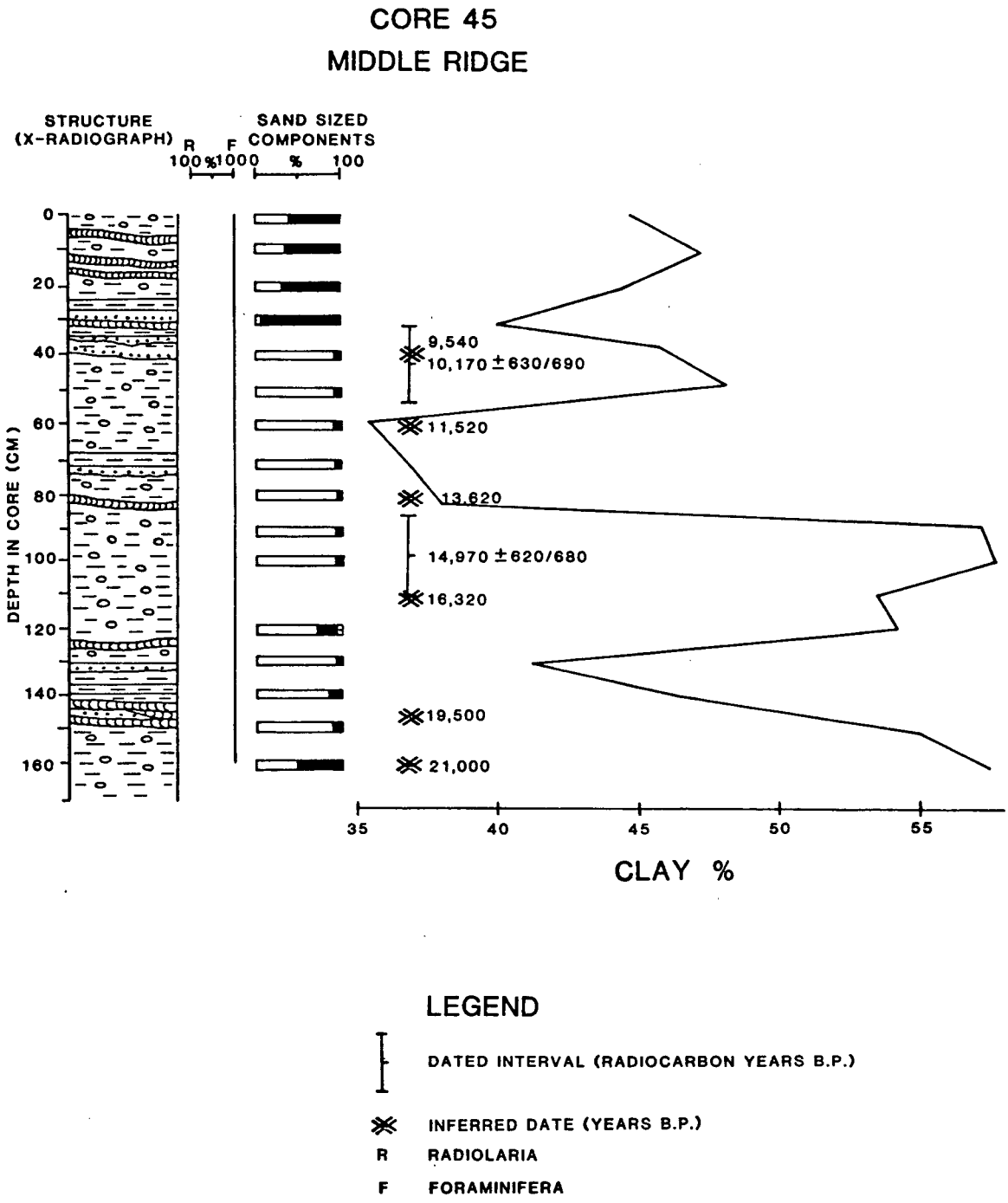

FIGURE 14. Core 45 from Middle Ridge with illustrated structure, components from the sand size fraction, clay percentages, foraminiferal to radiolarian ratios and radiocarbon dates. Symbols as in Figure 8 and Appendix II.

Middle Valley: These large differences in depth suggest that only major turbidity currents such as those of the Late Pleistocene could have contributed to sedimentation on the ridges, which was otherwise dominantly hemipelagic.

Abundant planktic foraminifera from the ridge-top cores supplied enough $CaCO_3$ for ^{14}C dating. A radiocarbon date indicates that sediment at the top of core 51 from West Ridge is 19,000 years old. This may imply a hiatus in sedimentation at the surface of West Ridge. Such a hiatus was not found on Middle Ridge (Fig.14). A comparable hiatus (17,440 B.P. to present) for the surface sediment of core 68PC16 at 2,020 m depth was observed from sediments of the Ontong-Java Plateau (Valencia, 1977). Variation in hemipelagic sedimentation of the biogenic component between West Ridge and Middle Ridge seems unlikely due to their proximity and common hydrography.

The foraminiferal fertility and preservation patterns obtained from the deep-sea sediments east and west of the Juan de Fuca Ridge indicate an abundance of planktic foraminifera until at least 12,000 B.P. (Nayudu, 1964; Duncan, Fowler and Kulm, 1970; Barnard and McManus, 1973). The reason for the age of the West Ridge surface sediments is unclear. One possible explanation is physical removal of sediment by local turbidity currents or slumping. Another is the disturbance of the surface sediment during coring. Yet another, as explained below, involves the position of sampled sediment at the top of West Ridge and temporal changes in the chemistry of ocean waters.

Extensive work on the dissolution by seawater of calcite and the position of the lysocline and carbonate compensation depth (CCD) in the

central and north Pacific has aided significantly in the interpretation of carbonate deep-sea stratigraphy (Peterson, 1966; Berger, 1967, 1970, 1976; Berger and Winterer, 1974; Pytkowicz, 1970; Ingle et al, 1973; Ingle, 1975). North-south hydrographic profiles show the lysocline at $2600^{\pm}$ 200 metres at 46^{o} north latitude (Berger, 1970). Projection of Berger's profile to 48^{o} north results in a lysocline position of $2100^{\pm}$ 200 metres.

During the Late Pleistocene the lowest glacial-eustatic sea level was around 20,000 B.P. (Clague, 1978) and stood approximately 80 to 110 metres deeper than the present lysocline thus impinging upon the site of core 51 on West Ridge, and enhancing carbonate preservation in the water column and sediments (Berger, 1970; Broecker, 1971; Morse and Berner, 1972). A subsequent rise in sea level and coincident rise in the lysocline to its present position would expose the biogenic carbonate of West Ridge surface sediment to enhanced rapid dissolution of undersaturated waters. It appears that the crucial rise in the lysocline and sea level began around 18,000 to 19,000 B.P., as evidenced by the 19,000 B.P. surface date of core 51. Middle Ridge sedimented carbonate is several hundred metres below the lysocline, and thus would not be affected by changes in the lysocline depth nor reflect the magnitude of dissolution inferred for core 51 from West Ridge.

The complexity of changes in the sea level, lysocline, and sedimentation processes during the Late Pleistocene make conclusions tentative.

Many workers have documented the preservation of foraminiferal-rich Late Pleistocene sediment on the seafloor below the CCD (Berger, 1967; Pytkowicz, 1970). It was postulated that dissolution of foraminifera in seawater undersaturated in calcite may be retarded by: (1) An organic coating on the shells which reduces the number of exchangeable Mg-Ca sites

(Lorens et al, 1977), (2) the formation of a layer of bottomwater saturated in carbonate adjacent to the carbonate-rich sediment, such that dissolution is by slow diffusion (Berger, 1967; Pytkowicz, 1970; Lorens et al, 1977) or (3) by rapid burial of carbonate during periods of high carbonate productivity, slumping or sedimentation from turbidity currents. Rapid sedimentation would remove the carbonate from corrosive open water circulation resulting in the equilibration of carbonate with pore waters and carbonate preservation.

Planktic productivity throughout the world's oceans was the highest during Late Pleistocene glacial intervals due to the enhanced atmospheric and corresponding surface water circulation (Nayudu, 1964; Broecker, 1971; Thiede, 1973; Emiliani and Shackleton, 1974; Valencia, 1977). Preservation of calcareous plankton in the water column and surface sediment is mainly dependent on deepwater chemistry (Berger, 1970). Since 19,000 B.P. productivity and preservation of foraminifera was highest in the central Pacific during the rapid melting of ice after approximately 15,000 B.P. (Berger and Killingsley, 1977). Foraminiferal abundance then decreased gradually until the end of the Late Pleistocene when productivity again increased around 10,000 B.P. (this study) followed by a major decrease in either or both productivity and preservation throughout the Holocene of the west-central and northeast Pacific (Barnard and McManus, 1973; Peng et al, 1979).

Foraminiferal abundance patterns are preserved for the Late Quaternary in Middle Ridge sediment while a post-19,000 B.P. hiatus exists for West Ridge sediment. The difference in carbonate stratigraphy between Middle and West Ridge is primarily attributed to "dilute cloud" turbidite sedimentation on Middle Ridge (absent on West Ridge) which rapidly buries

and preserves hemipelagic carbonate and, to a lessor extent, winnowing of West Ridge sediment that may disrupt the formation of carbonate saturated bottom waters and significantly remove hemipelagic fines. Changes in the lysocline position dependent on sea level, as previously discussed, may also have adversely influenced Late Quaternary carbonate sedimentation of West Ridge.

Stratigraphy Of Middle Ridge

Middle Ridge core 45 contains the best dated record of sedimentation for the northern end of Juan de Fuca Ridge (Fig.14). Based on a sedimentation rate of 11.1 cm/1000 years, determined from dated intervals, the deepest sediment is inferred to be approximately 21,000 years B.P. Three cycles of repeated turbidite "dilute cloud" and hemipelagic deposition occur throughout core 45. Each cycle is commonly composed of more than one turbidite sequence with a thick final massive sediment zone and in this respect is similar to turbidite-hemipelagic cycles discussed previously from adjacent valley sediments. Inferred dates indicate that the oldest (3), medial (2) and youngest (1) turbidite-hemipelagic cycles began near 19,500 B.P., 13,620 B.P. and 9,540 B.P. respectively. The top 10 to 15 cm of cored sediment appears hemipelagic in composition. The age of the surface sediment would be inferred at 6,000 B.P. or older if the sedimentation rate continued to be 11.1 cm/1000 yr. If a zero B.P. surface sediment age is assumed, a sedimentation rate of 4.3 cm/1000 yr results after 10,000 B.P. which includes the turbidites of cycle 1. Excluding the turbidites in cycle 1, a hemipelagic sedimentation rate of 1.0 to 2.3 cm/1000 yrs is obtained. Based on a 9,000 - 9,540 B.P. Holocene-Late Pleistocene boundary, only the hemipelagic sediment is Holocene, the remainder of the sediment is Late Pleistocene. A marked reduction in foraminiferal abundance exists

for Holocene sediment compared to Late Pleistocene sediment.

Late Pleistocene sedimentation rates on Gorda Ridge and the abyssal plain north of Cobb Seamount are 10.0 and 10.4 cm/1000 years respectively (Nayudu, 1964; Phipps, 1977), in good agreement with the 11.1 cm/1000 year sedimentation rate obtained from Middle Ridge. Benthic mixing and winnowing of sediment may obscure the actual sediment age (Selk, 1977; Peng et al, 1979). X-radiographs illustrate little bioturbation of surficial sediment for Middle Ridge although, as discussed earlier, some winnowing occurs. In this study sedimentation is assumed continuous for Middle Ridge and a Holocene hemipelagic sedimentation rate of 1.5 to 2.3 cm/1000 years is proposed.

Correlation Of Juan de Fuca Ridge Sediment

Radiocarbon dates are obtainable solely from ridge sediments. Correlation of ridge and valley stratigraphy is therefore based on assumption of synchronous sediment compositional changes across the Late Pleistocene-Holocene boundary. On Middle Ridge the boundary occurs at approximately 15 to 20 cm depth and in the valley sediments at approximately 40 to 50 cm depth. Late Pleistocene sediment is expressed in the valleys by more than one turbidite-hemipelagic cycle, coarser, more erosive (scoured) sediment, turbidity current entrained foraminifera, more abundant terrigenous plant debris and thicker pelite dominated pelite-hemipelagic intervals than exists for Holocene sediment. Middle Ridge Late Pleistocene sediment contains all the turbidite sequences, coarser sediment, more abundant terrigenous plant debris and substantially more foraminifera than Holocene sediment. The boundary therefore is marked by the changing of all patterns of sedimentation, turbidity current and hemipelagic.

Individual Late Pleistocene turbidite-hemipelagic cycles from West Valley may correlate with turbidite-hemipelagic cycles from Middle Ridge. Continent derived turbidity currents entering West Valley are partially blocked to the northeast by the confluence of the Sovanco Ridge and West Ridge (Davis and Lister, 1977a). Turbidity currents entering West Valley would therefore be dominated in form by "dilute cloud" sedimentation. Common final sequence thicknesses of turbidite and hemipelagic sediment (35 to 40 cm) occur for Middle Ridge cycle 2 and West Valley cycle III (Fig.15). Middle Ridge turbidites of cycle 1 and West Valley cycle II begin just below the Late Pleistocene-Holocene boundary and are overlain dominantly by Holocene hemipelagic sediments. West Valley Holocene cycle I is not continuous between cores and is believed locally derived. It is proposed that major periods of Late Pleistocene continent derived turbidite deposition occurred at the northern end of Juan de Fuca Ridge at 13,620 B.P. then again at 9,540 B.P. each followed by long periods of hemipelagic sedimentation. The 13,620 B.P. and 9,540 B.P. pulses of turbidite deposition are recorded as West Valley turbidites in cycle III and Middle Ridge cycle 2, and in West Valley cycle II and Middle Ridge cycle 1, respectively.

Correlation With Continental Glaciation

A comparison of Late Quaternary stratigraphy and sedimentation on the northern end of Juan de Fuca Ridge to the climatic glacials and interglacials documented for the same period from the continental Pacific Northwest demonstrates some unique associations (Fig.16). Periods of Late Pleistocene hemipelagic sedimentation on the Ridge are contemporaneous with maximum advances of continental glaciation. The same periods are also characterized

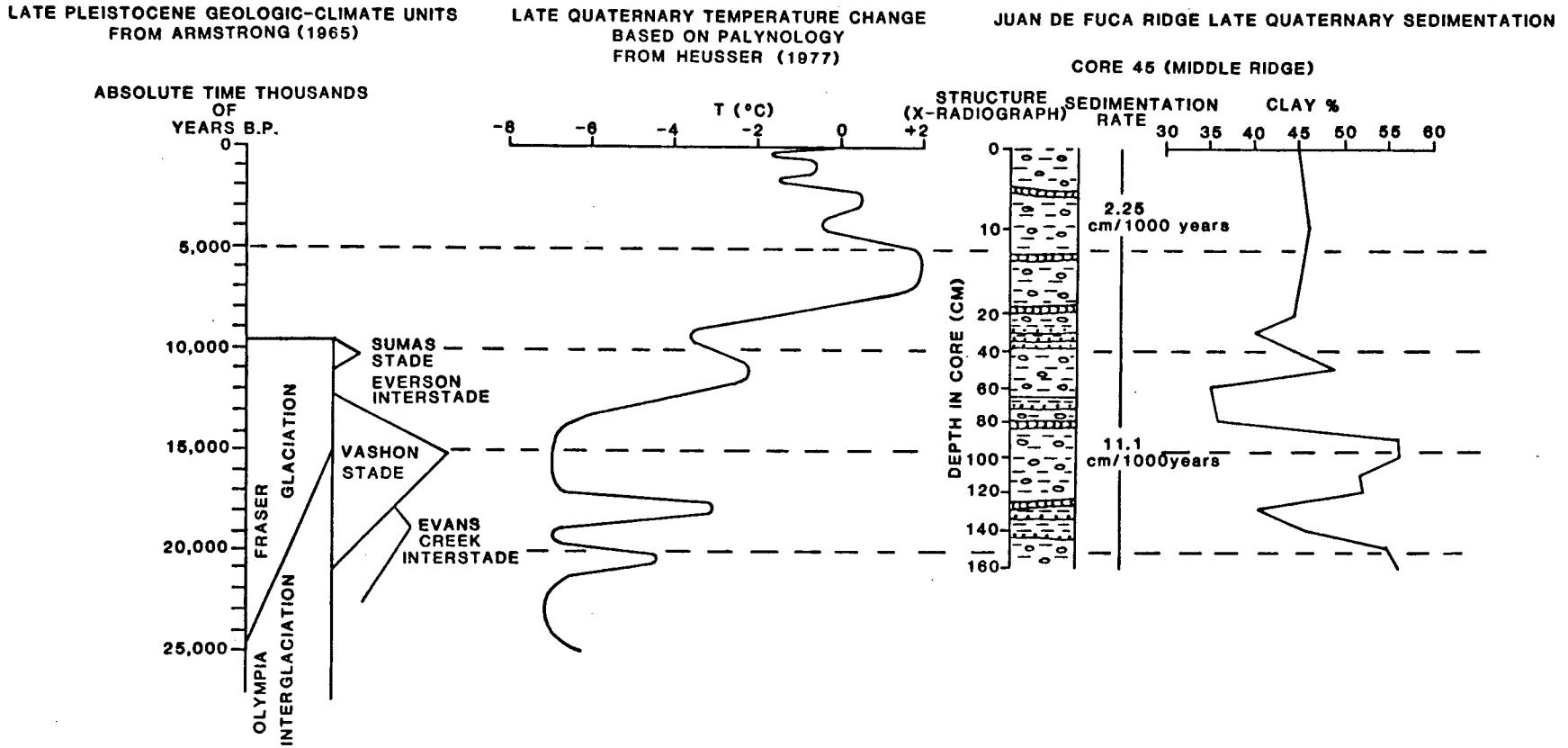

FIGURE 16. Stratigraphy of core 45 from Middle Ridge with sediment structure and percentage clay fluctuations compared to continental British Columbia and Washington Late Pleistocene to Recent geologic-climate units from Armstrong et al, (1965), and Late Quaternary temperature changes based on palynological studies from Heusser (1977).

in marine sediment by abundant well preserved planktic and benthic foraminifera. Following maximum advances of the ice during the Evans Creek, Vashon and Sumas stades, were rapid warming trends as shown by palynological studies in northwestern Washington (Heusser, 1977), during these times continentally initiated turbidity currents deposited turbidites on the northern end of Juan de Fuca Ridge. Thus the Late Pleistocene turbidite sequences of Juan de Fuca Ridge correlate directly with periods of maximum postglacial continental denudation (Mathews, 1979).

Late Pleistocene turbidity current deposition was replaced by hemipelagic sedimentation during the Holocene along deep-sea channels near Juan de Fuca Ridge (Griggs and Kulm, 1970; Nelson and Kulm, 1973). Coincident Holocene sedimentation at the northern end of Juan de Fuca Ridge was also predominantly hemipelagic. Those turbidites assigned to the Holocene from valley cores lack the terrigenous character and continuity of the Late Pleistocene turbidites and are considered local in source.

Source Of Late Pleistocene Turbidites

Mineralogy of turbidites and hemipelagic sediments in the study area is identical to that of sediments examined from Explorer Ridge (Béland, in prep.; Hanson, in prep.;). Major deep-sea channels nearest to and possibly influencing the sedimentation of the study area are Paul Revere Channel, to the north, Juan de Fuca and Vancouver Channels, to the east, all of which originate on the continental slope near Queen Charlotte Sound between Vancouver Island and the Queen Charlotte Islands. It is proposed that, during the lower sea level stand of the Late Pleistocene,

a large proportion of Queen Charlotte Sound was covered by glacial ice with glacial outwash deposited near the shelf edge (Mathews, 1981, oral commun.) Pulses of sediment were built up and released as turbidity currents during periods of major thawing coincident with flooding and abundant glacial outwash following the onset of glacial retreat (Armstrong et al, 1965; Clague, 1978; Mathews, 1979). Turbidity currents along deep-sea channels were sufficiently intense to strongly affect the sedimentation of the northern end of Juan de Fuca Ridge. The interruption of foraminiferal-rich hemipelagic deposition over Middle Ridge by "dilute cloud" turbidite deposits, preserved a datable stratigraphic record of deep-sea and associated continental Late Quaternary sedimentation. The presence of major turbidity current activity directly following the Sumas stade, which has not been observed in marine studies off the coast of Washington and Oregon, reflects the more northerly source of turbidites in the study area. The post-Sumas turbidite sequences of Middle Ridge coincides with the initial regression of a world-wide marine transgression (Armstrong et al, 1965). Sufficient sediment build-up on the lower shelf as a product of floodwater erosion may have produced the final turbidite sequences documented on Middle Ridge and throughout Juan de Fuca Ridge.

CONCLUSION

The sediments of the Juan de Fuca Ridge area demonstrate from their structure, grain size distribution and sand composition several dominant influences: (1) changed patterns in surface waters affected the hemipelagic-biogenic sediment, possibly dependent on the confluence of the West Wind Drift and the Northern Continental Current above the

study area; (2) turbidity currents, from the continental terrace eroded, resuspended and diluted the older sediment and due to the distal nature of the current, diluted the terrigenous character of the deposited load; (3) coincident and following the hemipelagic and turbidity current sedimentation was the reworking of such sediment by deep and bottomwater currents through winnowing and changes in flow, dependent on watermass density and seafloor configuration. All of these processes produced transitional phases in the sediment.

Middle Ridge sediment best presents the stratigraphy of the whole area. Recognition of synchronous sediment changes from all the physiographic areas is necessary for correlation. Detailed correlation was achieved primarily by defining the Late Pleistocene-Holocene boundary in the sediment and periods of synchronous turbidite-nonturbidite deposition. Good correlation exists for the Late Quaternary geologic -climate (Armstrong et al, 1965) changes of the continental northwest and the northern end of Juan de Fuca Ridge.

Chapter III

MINERALOGY

INTRODUCTION

Detailed studies on the mineralogy of Quaternary sediments in the northeast Pacific have been mainly directed at finding the provenance and stratigraphic variations of mineral species (Duncan et al, 1970; White, 1970; Stewart, 1976; Phipps, 1977; Selk, 1977). In deep-sea studies, complexity is introduced by the relatively great distance from terrigenous sources and by mixing during dispersal of sediment, which tends to obscure mineralogical variations in silt and clay. Mineralogical investigations have therefore been confined to large regions on or adjacent to the continental terrace (Duncan et al, 1970; White, 1970; Stoffers and Muller, 1972; Stewart, 1976; Karlin, 1980). Deep-sea studies of small areas commonly described stratigraphic changes in mineralogy but, due to the variety of poorly understood sedimentation parameters, defined mineralogical provenance with difficulty (Selk, 1977). Stratigraphic variations in mineralogy in the deeper parts of the northeast Pacific are best preserved on isolated hills and ridges (Phipps, 1977).

In this chapter, detailed mineralogy of sediment sampled from Juan de Fuca Ridge and Cascadia Basin is discussed, the aims being to define and compare gross changes in relative abundance of minerals which might be products of ridge-type hydrothermal activity (Fryer and Hutchison, 1976; Andrews and Fyfe, 1976).

One hundred and twenty samples taken from eleven cores, corresponding to those intervals analyzed for grain size, were analyzed in bulk.

Clay minerals were studied in thirty-nine subsamples selected at fifty centimetre intervals. Each gravity core produced three to five subsamples and Phleger cores typically yielded two subsamples.

METHODS

Bulk sediment samples of approximately one to two cubic centimetres were placed in Whirlpak bags with a stainless steel spatula, dried overnight at 70°C, gently crushed in an agate mortar, and stored in labelled glass vials until analyzed. Bulk sediment and slides for clay analysis were initially analyzed untreated. No attempt was made to remove organic components, carbonate, iron oxide or hydroxide on the premise that any modification of the sediment could alter the *in situ* mineralogy.

Analysis Of Bulk Sediment

A small amount of mixed dried sediment from a given sample was placed on a glass slide and mixed with several drops of acetone to form a quickly drying slurry.

Each sample was analyzed on a Philips X-Ray Diffractometer (Appendix V). The scanning speed was changed to 1°2θ/min., for all duplicate runs of samples from top surfaces of cores, and selected samples were also run to clarify mineral peak positions at a time constant of two.

Preparation And X-Ray Analysis Of Clays

Subsamples of the bulk sediment samples were placed in 50 ml glass beakers and mixed with 40 ml of distilled water to remove salts. The mixed sediment was left undisturbed for 72 hours to allow most of the clay size material to settle, the supernatant liquid was removed by pipete. This procedure was repeated, after which the beakers were filled with dis-

tilled water, thoroughly mixed with a glass stirring rod, and left undisturbed for eight hours until only the clay component ($< 9.7\emptyset$) remained in suspension (Folk, 1974). Several millilitres of suspension were removed from directly above the surface of settled sediment, pipeted onto a glass slide and allowed to air dry at room temperature. The process was repeated until oriented clay minerals with discernable peaks were evident on trial diffractograms.

Each oriented clay slide was X-rayed untreated, glycolated with ethylene glycol vapour in a humidity-controlled vacuum sealed jar at room temperature, heated in a muffle furnace at 300°C for two hours and reheated in a high temperature furnace at 550°C for two hours (MacEwan, 1961; Brindley, 1961; Biscaye, 1965; Carroll, 1970). X-ray diffractograms were obtained after each separate slide treatment.

Additional slides of oriented clays were prepared from sediment stirred then settled in 10% hydrochloric acid at 80°C (Brindley, 1961; Rateev et al, 1969; Carroll, 1970). After settlement periods of 3, 8, 12, and 72 hours, sediment-acid mixtures were washed in 100 ml of distilled water, centrifuged, as described in Chapter II methods for salt removal, for two hours and the supernatant decanted off. The procedure was repeated three times until the samples were well washed after which oriented slides were prepared and X-rayed before and after glycolation and heating.

Oriented clay diffractograms were run with the same diffractometer settings as previously described for the bulk sediment analysis except the scanning speed was altered to $1°2\emptyset$ /min., (Appendix V). Selected samples were run with time constants of both one and two.

Non-acidified slides were scanned from a $2\emptyset$ of 30° to 3.0° and 3.5°. Acidified slides were scanned from 40° to 3.5°.

Analysis Of Unknown Minerals

Two unknown minerals were separated and analyzed as follows:

Mineral "A" was a magnetic black silt sized mineral that coated the teflon surface of the magnetic stirring bar when sediment was prepared for grain size analysis. It occurred in all samples studied, including those of Cascadia Basin ranging from less than one percent to eight percent by weight. A concentrate was collected from the samples of one ridge core, washed in distilled water to remove excess sediment, air-dried, mixed with acetone, placed on a glass slide and X-rayed.

Mineral "B", commonly observed during optical analysis of the 63 μm sand fraction, occured in mineral aggregates with biogenic material in some cores and as irregular masses in others. The mineral was commonly brown, had a metallic to submetallic lustre and readily disaggregated into smaller clusters when disturbed. Aggregates of the material were hand-picked under a binocular microscope until a sufficient concentrate was available to produce identifiable mineral peaks on diffractograms.

Quantitative Analysis

The relative proportion of different groups of clay minerals in each sample was estimated by the method of Biscaye (1965). Peak areas were measured from the diffractograms of glycolated clay minerals using a Koizumi polar compensating planimeter. The clay mineral peak traces measured were at 17 Å, 10 Å and 7 Å for montmorillonite, illite and chlorite group minerals respectively. The areas were measured three to five times per peak and averaged. Biscaye's method requires the use of calibration factors with one times the montmorillonite peak area, four times the illite peak area and two times the chlorite peak area. The clay minerals are assumed to compose one hundred percent of the clay size fraction and the scaled mineral areas are adjusted to percentages.

RESULTS

Mineralogy Of Bulk Samples

Three minerals ∝-quartz, plagioclase feldspar and chlorite dominate each bulk sample (Fig.17). Diffractograms of samples from West and Middle Ridges contain prominent calcite peaks (Fig.17). Minor halite peaks in a few diffractograms reflect crystal formation during sample preparation. Any other minerals present do not produce peaks above the radiation background.

Clay Mineralogy

Three clay minerals and five other clay size minerals were determined in this study (Fig. 18). The clay minerals are montmorillonite, mica and chlorite. The other clay size minerals are ∝-quartz, plagioclase feldspar, calcite, cristobalite and amphibole.

Montmorillonite

In this study, montmorillonite is described in the sense of MacEwan (1961) Biscaye (1965), Rateev et al, (1969) and Carroll (1970). Identification is based on movement of the 12.5-13.5 Å d(001) reflection to a 17.0-17.2 Å position following glycolation. The peak is wide at the base and irregular, demonstrating poor crystallinity, amorphous nature of the clay, or both (Biscaye,1965; Carroll, 1970). Heating to 300°C resulted in disappearance of the 17.0-17.2 Å reflection, but the 9 Å peak that replaces it cannot be observed due to overlap by the d(001) mica peak.

Mica

The d(00ℓ) sequence of 10.2 Å and 5.0 Å are considered to be illite or mica, following Biscaye (1965), Duncan et al, (1970), Carroll (1970) and Selk (1977). Biscaye (1965) described identifiable 3.3 Å and 2.5 Å diffractogram peaks from Atlantic sediments in addition to the more

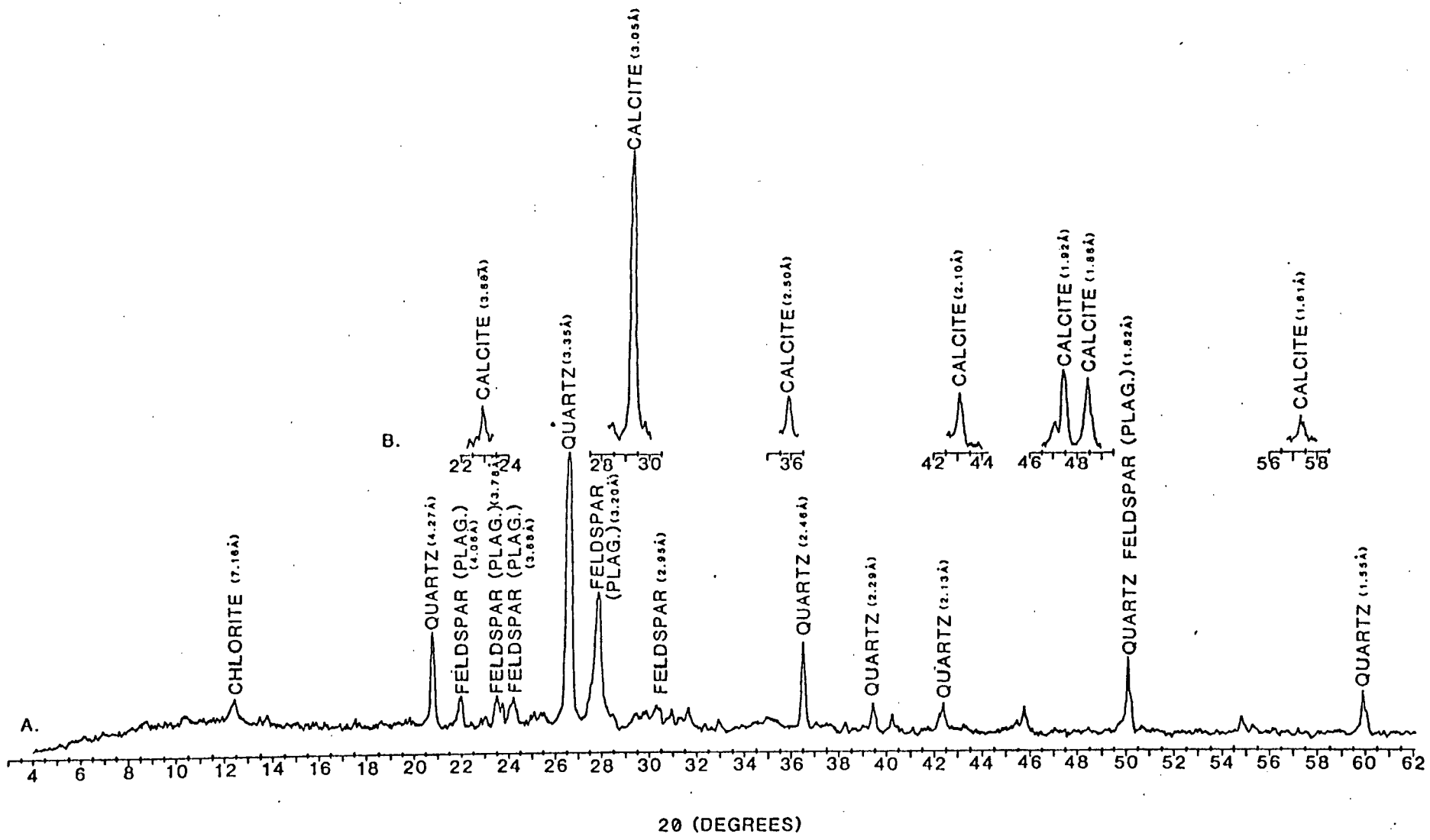

FIGURE 17. A. Diffractogram illustrating reflections from the three dominant, ubiquitous minerals in bulk sediment samples, ∝-quartz, plagioclase feldspar and chlorite (West Valley core 77-14-43).

B. Diffractogram illustrating peak traces from the mineral calcite which is common to ridge bulk sediments (West Ridge core 77-14-51).

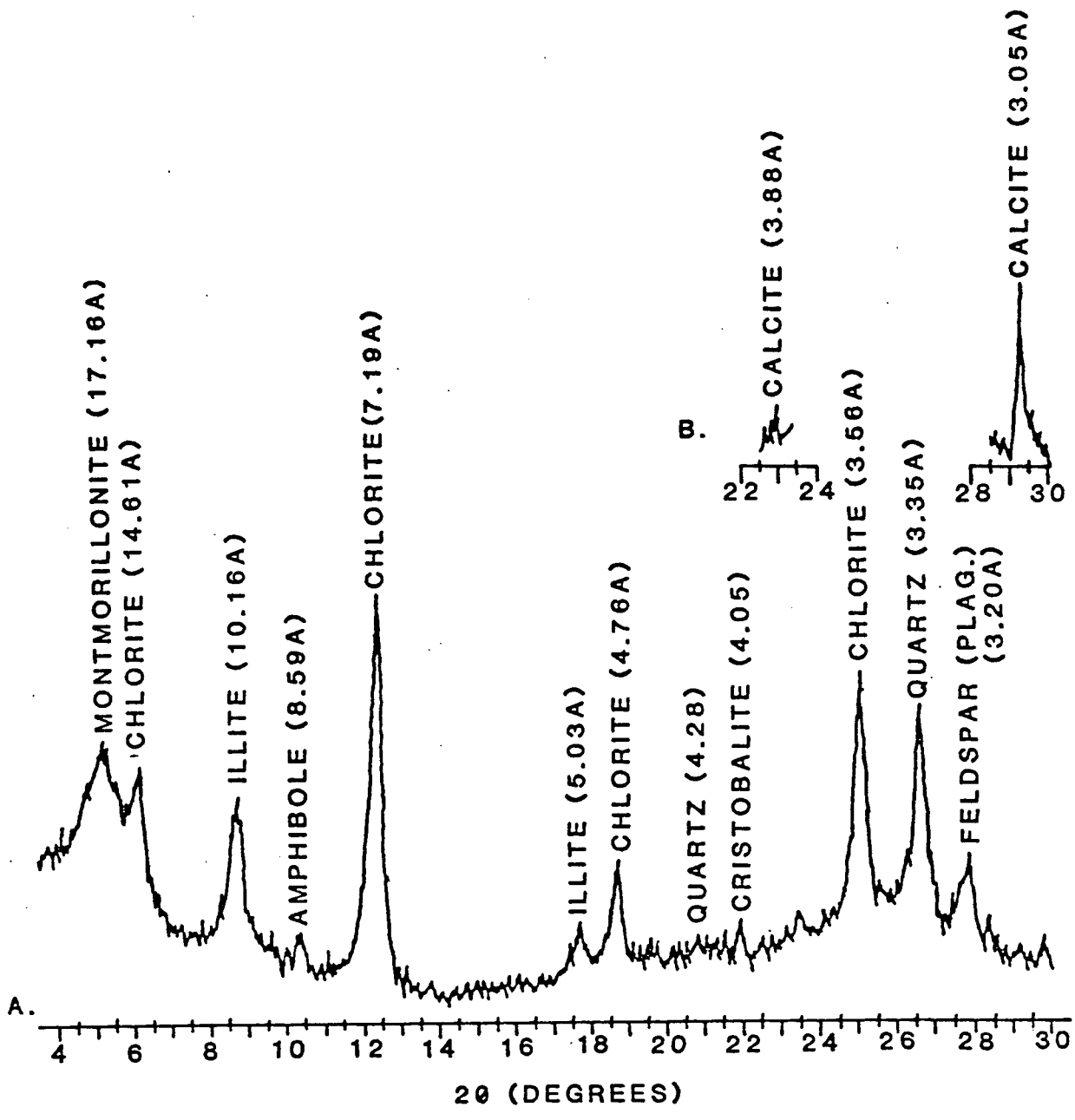

FIGURE 18. A. Diffractogram of the surface sediment (0 to 2 centimetres) from West Valley core 77-14-43 illustrating the clay minerals and clay sized minerals common to all samples studied.

B. Diffractogram peak traces of clay sized calcite from West Ridge core 77-14-51.

intense 10.0 Å and 5.0 Å peaks. Clays from Juan de Fuca Ridge contain ∝-quartz, which has an intense peak that obscures the 3.3 Å peak of illite. The 2.5 Å illite peak, although suggested where intense 001 illite diffractogram traces occur, is too weak and near background to be diagnostic.

The effect of glycolation, heating and acid treatment are negligible for the illite diffractogram peak traces.

Chlorite And Kaolinite

The peak at the 7.0-7.2 Å position, previously described in the section on mineralogy of bulk sediment, could be either chlorite or kaolinite. Basal spacings of chlorite are 14 Å (001), 7 Å (002), 4.7 Å (003) and 3.5 Å (004) (Brindley, 1961; Biscaye, 1964, 1965; Carroll, 1970), and of kaolinite, 7.15 Å (001), 3.57 Å (002), 2.35 Å (003) and 1.79 Å (004) (Carroll, 1970). Dominance of either clay mineral in oriented samples, obscures the presence of the other group in the resultant diffractogram. In diffractograms of deep-sea clay mineral assemblages, low intensities of the d(003) and d(004) kaolinite refractions (Carroll, 1970) make differentiation of the two groups even more difficult.

Biscaye (1964) developed an ultraslow X-ray diffraction scanning technique for oriented clay minerals that divides the 7 Å and 3.5 Å peaks into their chlorite and kaolinite components but this technique was not used for this study. Instead, samples were heated and treated with hydrochloric acid (Brindley, 1961; Biscaye, 1964; Carroll, 1970). Rateev et al, (1969) successfully applied the same procedure in their studies on northeast Pacific and Indian Ocean sediments.

The chlorite group minerals are selectively dissolved by warm dilute hydrochloric acid (Brindley, 1961; Carroll, 1970). Diffractograms

of acid-treated oriented samples illustrate decreased d(001) peak intensities (Fig.19). Weak vestigial 7 Å and 3.5 Å peaks persist in diffractograms of clay material treated with acid for 72 hours. The weak 7 Å and 3.5 Å peaks may be due to small amounts of kaolinite or well crystallized chlorite that resists rapid acid dissolution. Sediments of the Blanco Trough, Cascadia Basin and the continental terrace off Washington and Oregon, when analyzed by the method of Biscaye (1964), were chlorite-rich and kaolinite-poor (Duncan et al, 1970; Selk, 1977). Heat and acid treatments on the Juan de Fuca Ridge clays suggest the presence of either minor coarsely crystalline chlorite or minor kaolinite. Kaolinite, in the untreated Juan de Fuca Ridge diffractograms, is strongly if not completely dominated by the mineral chlorite.

Glycolation of the clay samples exposes the d(001) chlorite peak after the movement of the coincident montmorillonite d(001) spacing to 17 Å on the diffractogram. Examination of the chlorite peak intensities demonstrates strong d(002) and d(004) spacings with weaker d(001) and d(003) spacings, a relationship characteristic of iron-rich chlorites (Brindley, 1961; Carroll, 1970) (Fig. 19). Rateev et al, (1969)also observed iron-rich chlorite in the deep northeast Pacific.

Heating of clays to 300°C and 550°C produced marked reductions in size of the d(002), d(003) and d(004) chlorite peaks with the characteristic intensification of the d(001) chlorite peak at 14 Å after the 500°C heat treatment.

Identical chlorites were identified from Cascadia Basin (core 61).

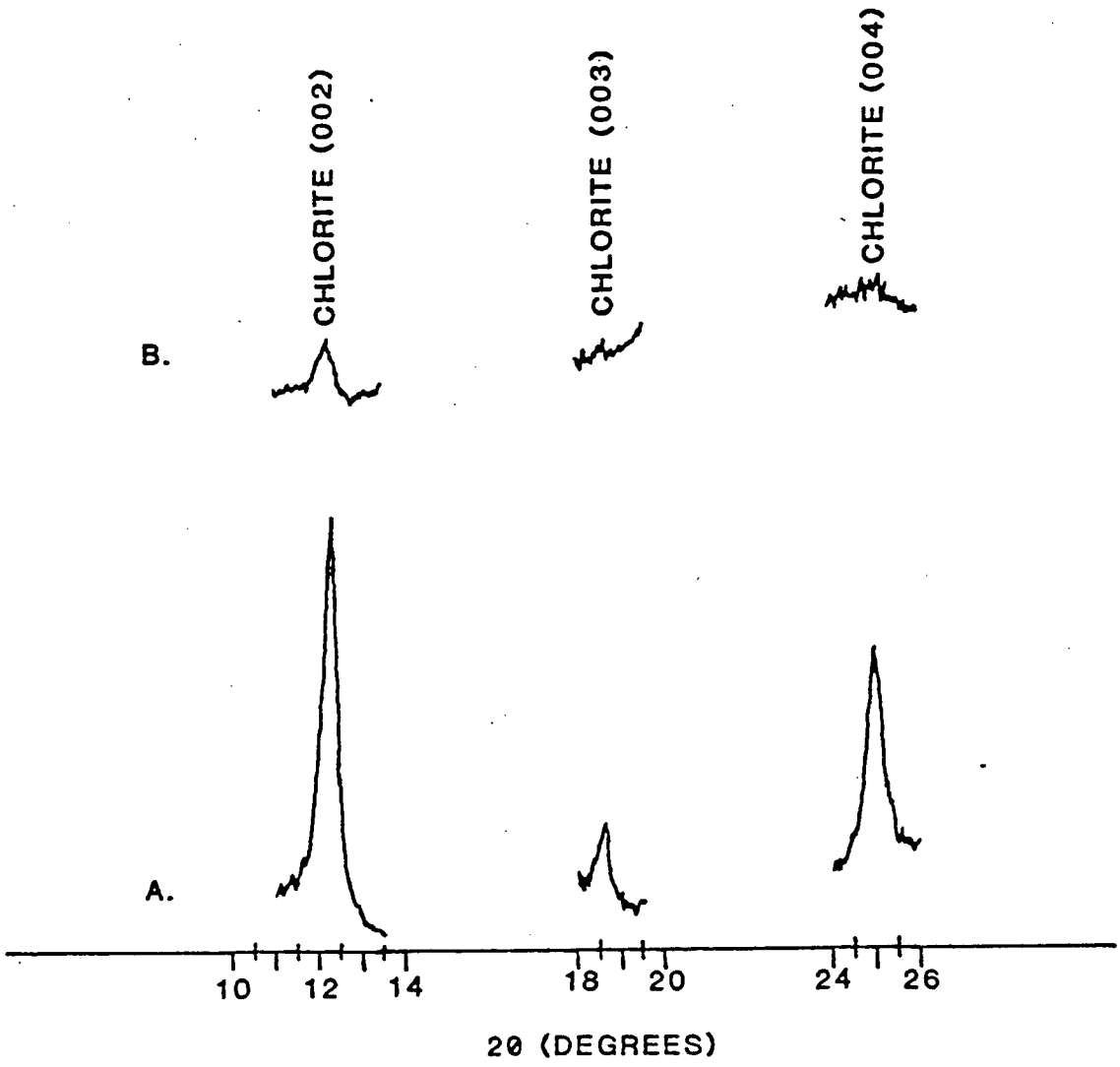

FIGURE 19. A. Diffractogram trace from West Valley core 77-14-43 showing untreated Fe-rich chlorite.

B. Chlorite peak removal after twelve hours of dissolution by warm (80°C) dilute (10%) hydrochloric acid.

Clay Sized Minerals

The dominant minerals described in the bulk sediment mineralogy are also present in the clay sized fraction. α-quartz and plagioclase feldspar produced prominent peaks in all oriented clay diffractograms (Fig.18). Weak peaks occur at 8.5 to 8.6 Å and 4.0 to 4.1 A in all clay X-ray traces. The 8.5 to 8.6 Å peak is due to the (110) plane of amphibole (Biscaye, 1965). Abundant amphibole should produce a weak 2.82 Å peak for the (330) plane. Although a 2.82 Å (330) peak just above background may exist in oriented clay diffractograms its presence cannot be strongly supported. An unoriented clay sample might better indicate the amphibole 330 crystal plane.

The 4.0 to 4.1 Å peak is produced by cristobalite (Carroll, 1970), which is widespread in the clays of the northeast Pacific and has been observed from Explorer Ridge, Juan de Fuca Ridge, Cascadia Basin and latitude 35°00'N, longitude 165°00'W (Carroll, 1970; Béland, in prep.; Price, in prep.).

Clay sized calcite is indicated by diffractogram peaks at 3.04 Å and 3.87 Å with the former peak being the largest (Fig.18). Samples from West and Middle Ridges have prominent calcite peaks, whereas West, Middle and East Valleys lack them. Clay sized calcite occurs wherever calcite is present in bulk sediment.

Treatment of the clay sediments by glycolation, heating and hydrochloric acid produced no change in the peak intensities or positions for any of the clay sized minerals except calcite. Heating to 550°C collapses the calcite peaks to the radiation background although heating to 300°C has no observable affect. Treatment of slides by warm dilute hydrochloric acid effects removal of calcite peaks.

Unknown Minerals

Diffractograms of mineral "A" indicate it is magnetite (Fig.20). Additional peaks are the result of minor amounts of quartz and feldspar in the concentrate.

The diffractogram of mineral "B" shows that the mineral is pyrite (Fig.21). Scanning electron microscophy illustrates the framboidal habit of the pyrite aggregates (Plate 5). Mineral "B" is most abundant in sediments from West Valley, West Ridge and Middle Ridge. Pyrite tends to be concentrated as a heavy mineral in the sediments when a direct association with the biogenic component is unclear. Its association was described in detail in Chapter II.

The presence of magnetite and pyrite in bulk sediment and clay sized samples is difficult to detect based on unconcentrated sample preparation prior to X-ray diffraction analysis. X-ray diffraction determination by a $CuK\alpha$ compared with an $FeK\alpha$ radiation source de-emphasizes the peaks of iron-rich minerals (Carroll, 1970), due to high mass absorption coefficients.

DISCUSSION

General Mineral Distribution

Except for calcite, the minerals in the bulk sediment samples and oriented clay subsamples are common to both the northern end of Juan de Fuca Ridge and Cascadia Basin. Calcite occurs most commonly on the ridges of the Juan de Fuca Ridge area and is noticeable absent from the valley sediment. Factors controlling occurrence of calcite are discussed in the preceding chapter.

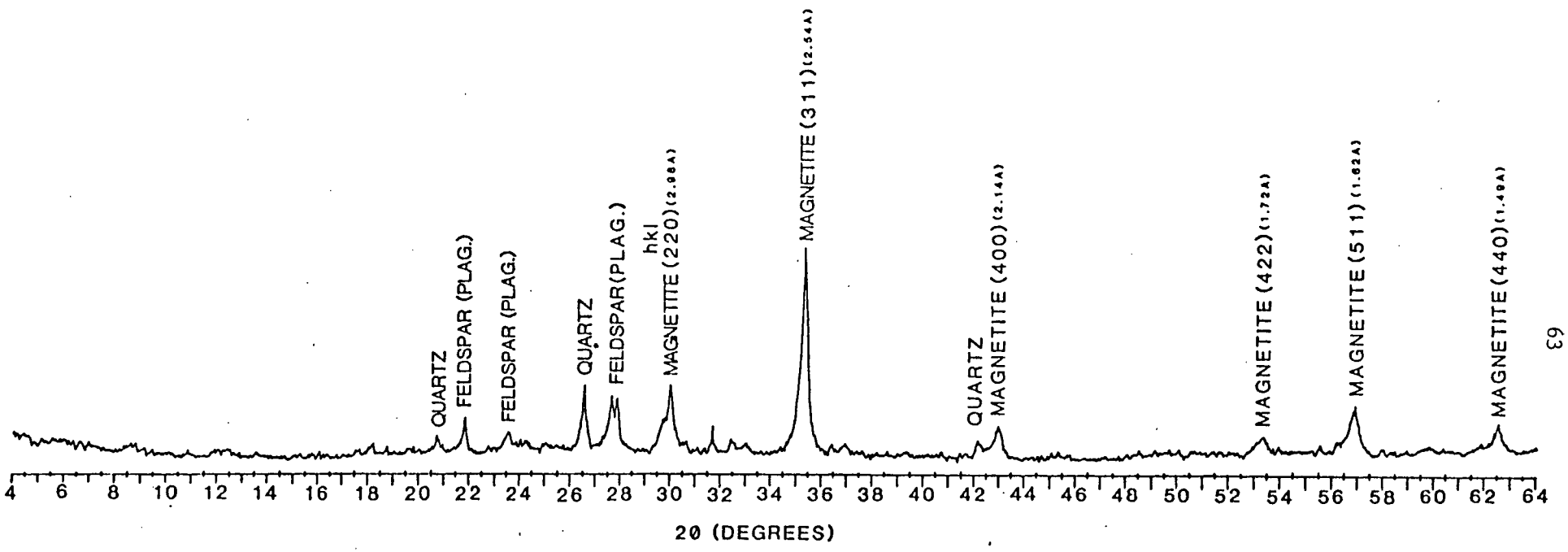

FIGURE 20. Magnetite (mineral"A") diffractogram trace. Minor ∝-quartz and plagioclase were collected unintentionally with the magnetite concentrate.

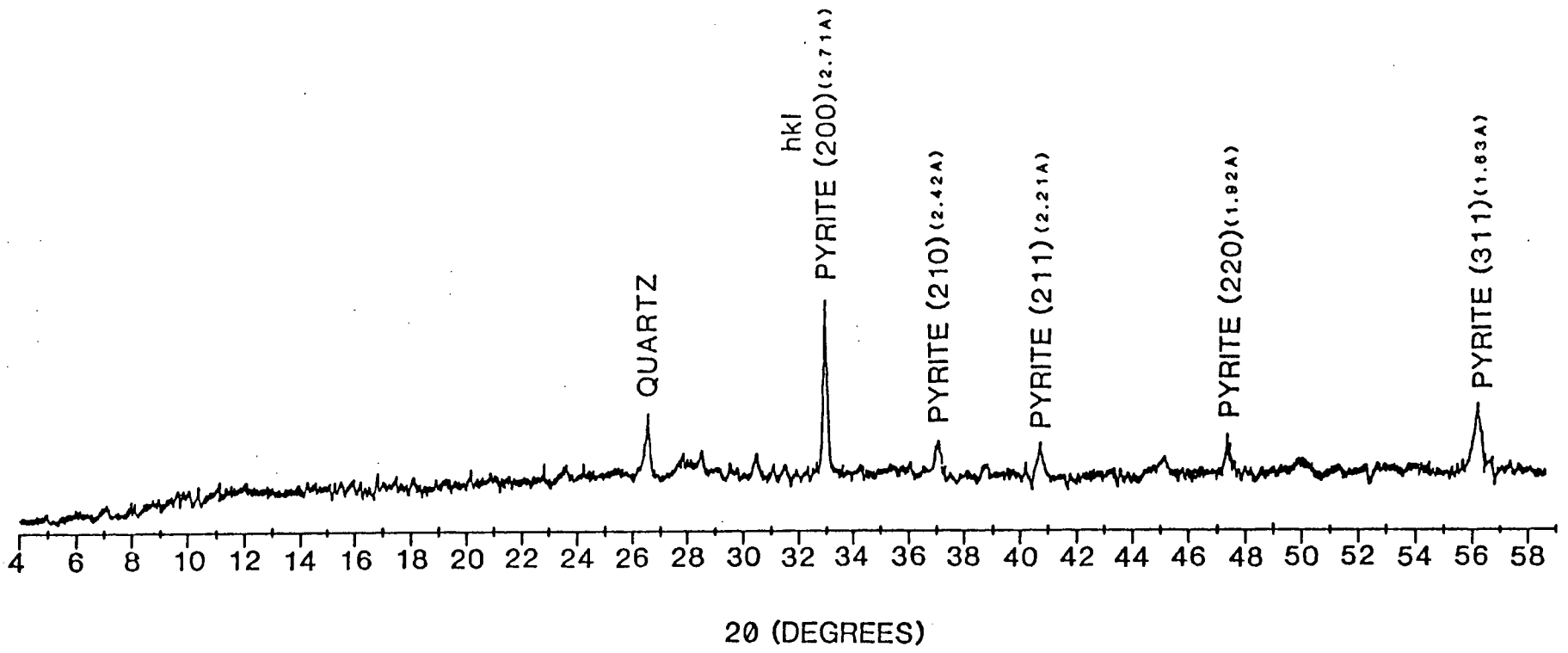

FIGURE 21. Authigenic pyrite (mineral"B") diffractogram trace. Minor ∝-quartz was collected with the concentrate.

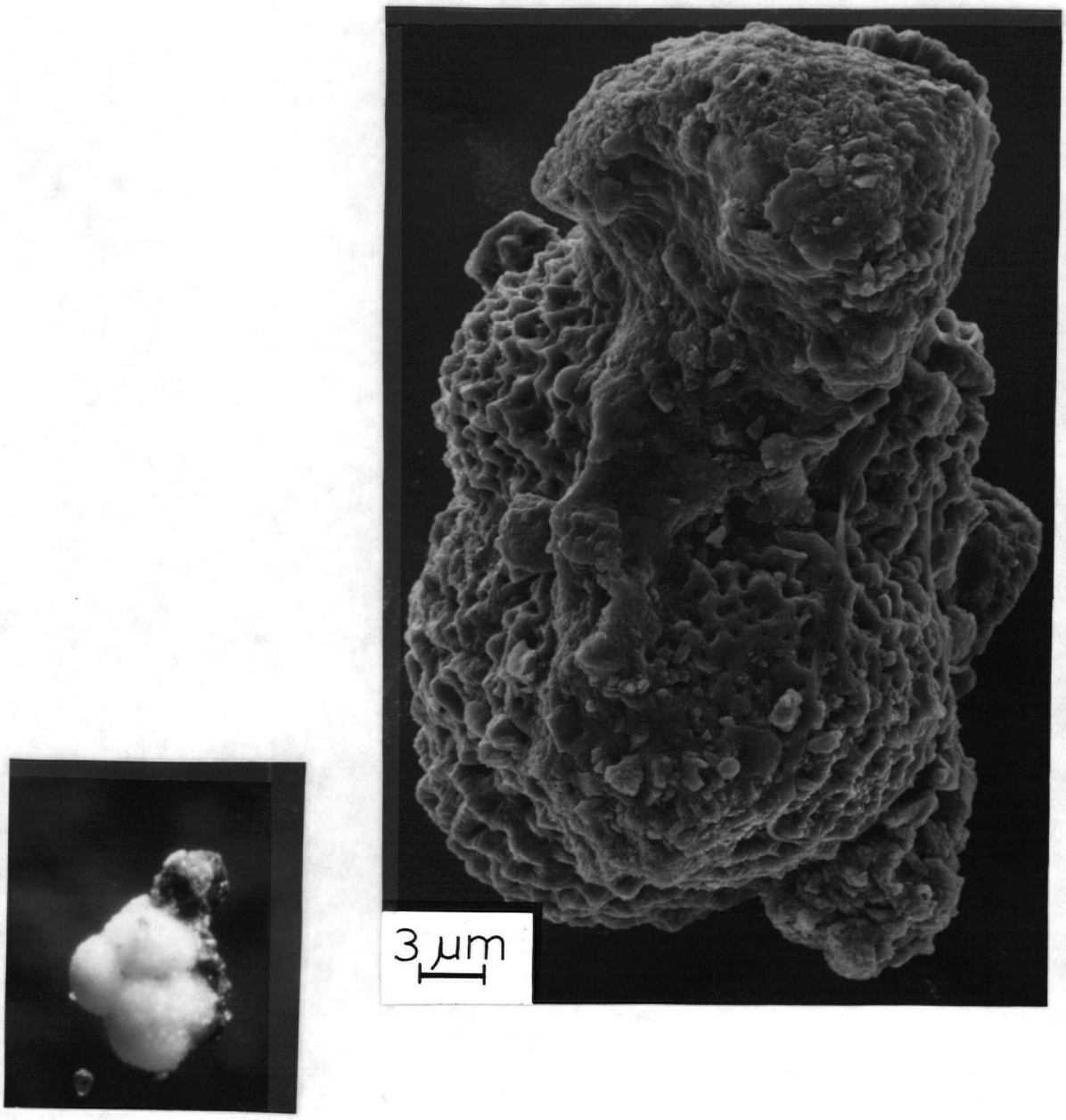

PLATE 5. Scanning electron micrograph showing pyrite aggregates externally attached to foraminiferal shell in Plate 3 (Mag. 200x).

Changes in the peak intensities of quartz and plagioclase feldspar occurred between samples, but no attempt at quantification was made.

Clay Mineral Abundances: Relation To Topography

The geographic location and small size of the area studied severely handicaps any conclusions on mineral provenance. Temporal changes in the distribution of clay minerals are discussed below based on the stratigraphic correlation of the ridge and valley sediments outlined in the preceding chapter. The most obvious variation exists between ridges and valleys, based on the semiquantitative estimation of average relative abundance in each core; montmorillonite is depleted on ridges and concentrated in valleys (Fig.22), whereas illite and to a lesser extent chlorite are concentrated on ridges and diluted in the valleys by montmorillonite (Fig.23). Chlorite does not vary as widely in abundance as do montmorillonite and illite. The same variations exist for surface sediments (Figs.22 and 23). Studies on the clay minerals dominating the various clay sizes of deep-sea sediment from Explorer Ridge show that montmorillonite dominates the finest clay sizes and is progressively depleted in the coarser clay sizes whereas chlorite and illite are least abundant in the very fine clay fraction with the abundance of illite greater than chlorite with increased clay size (Hanson, oral commun., 1981). In diffractograms of this study, montmorillonite peaks have wide bases and irregular boundaries, whereas illite and chlorite peaks have narrow bases and sharp boundaries. The character of peak boundaries and width of base reflect the degree of

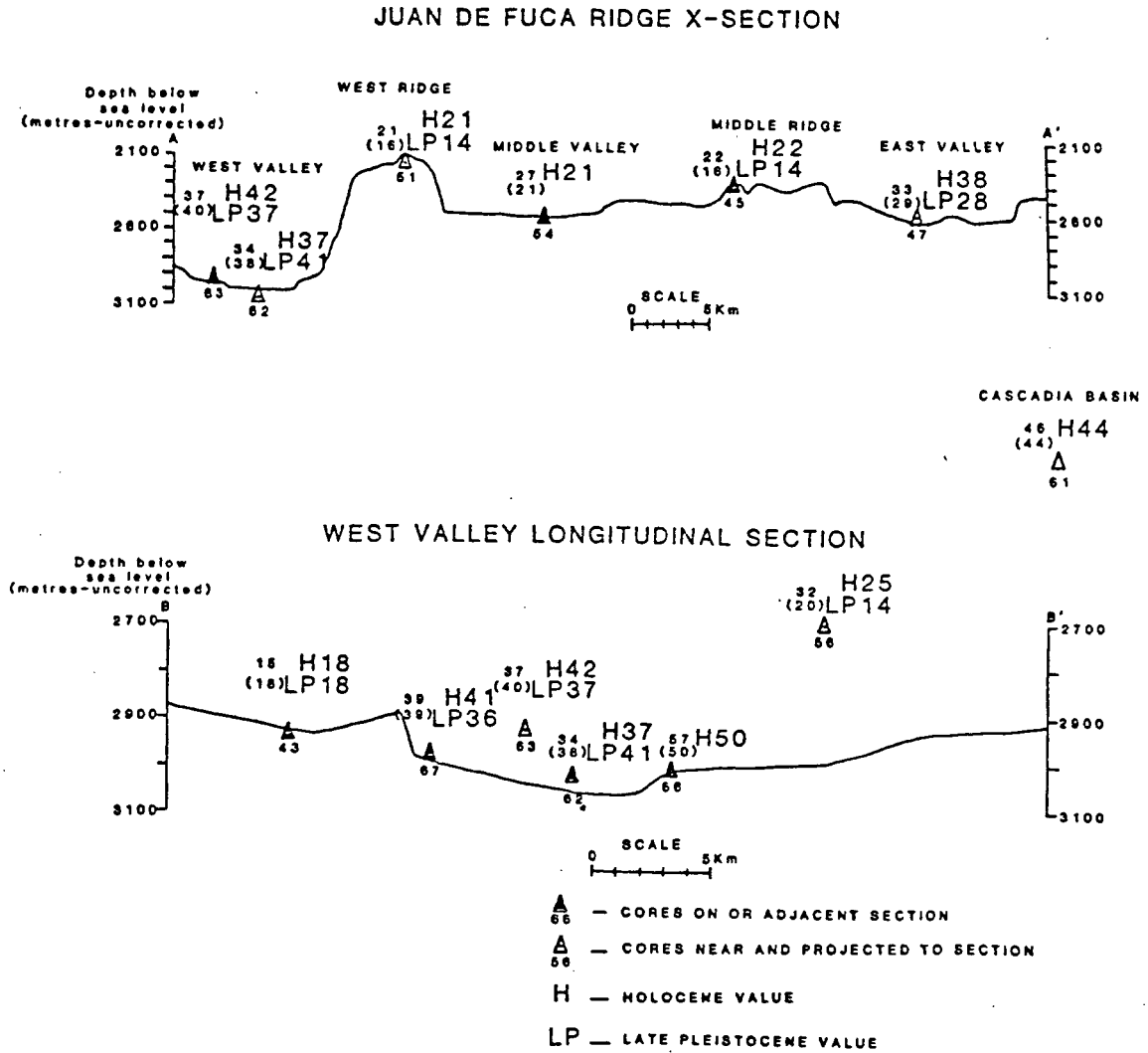

FIGURE 22. Bathymetric profiles of the northern end of Juan de Fuca Ridge AA' and BB' after Figure 4 , showing with small numbers the relative percentage of montmorillonite in surface samples and averaged through core (in parenthesis), large numbers show average relative percent montmorillonite in Holocene samples (H) and in Late Pleistocene samples (LP). Cascadia Basin core 77-14-61 is separately illustrated.

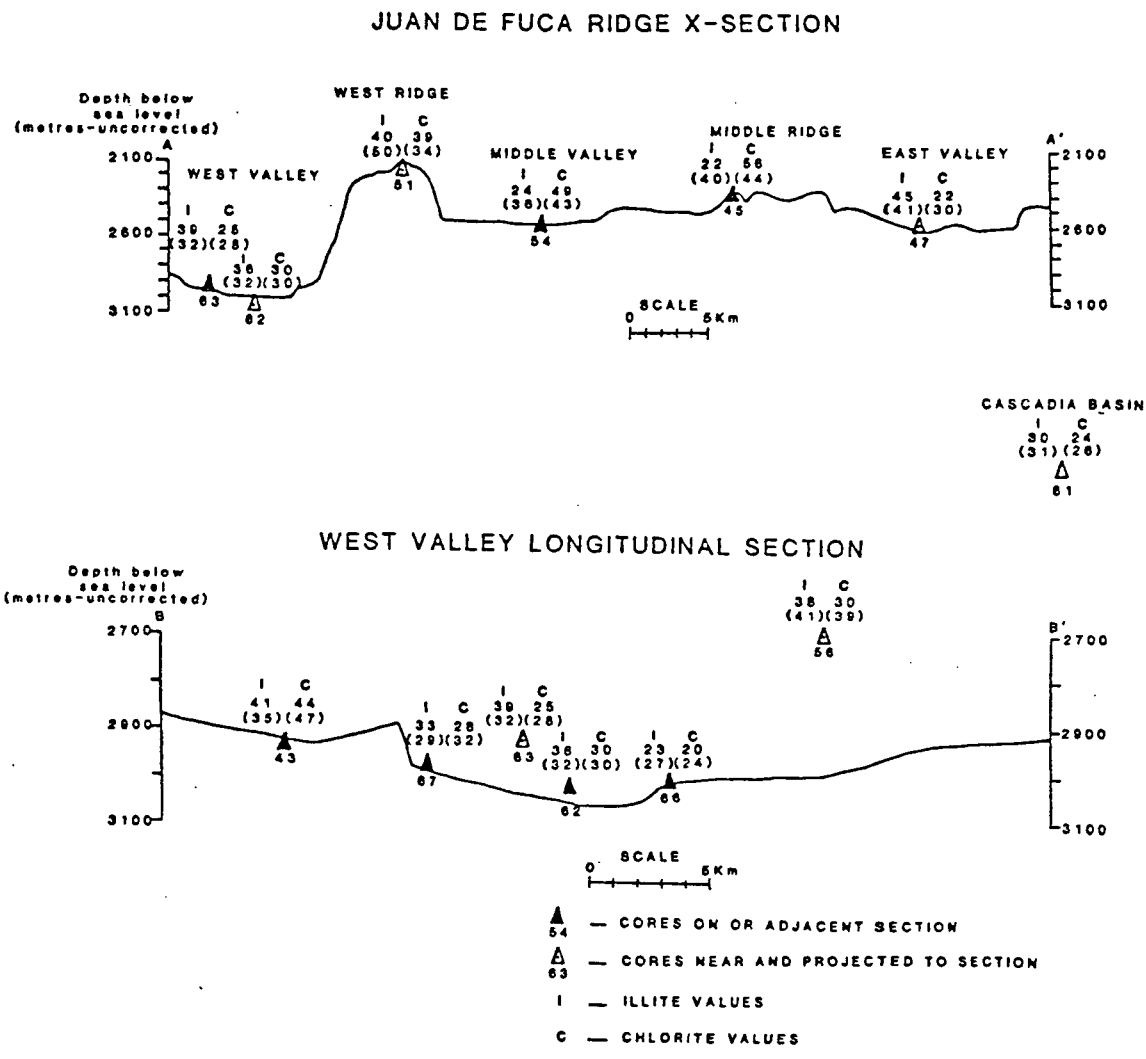

FIGURE 23. Bathymetric profiles AA' and BB' of the northern end of Juan de Fuca Ridge after Figure 4 , showing the distribution of the clay minerals illite (I) and chlorite (C), and the relative percentages of the clay minerals in surface samples and averaged through core (in parenthesis). Cascadia Basin core 77-14-61 sample values are separately indicated.

crystallinity of the clay mineral: the sharper the peak and the narrower the base the better crystallized the clay mineral species (Brindley, 1961; Carroll, 1970). Thus, montmorillonite is not as well crystallized as chlorite or illite.

Dominance of fine poorly crystalline montmorillonite in valleys and of coarser better crystallized illite and chlorite on ridges could be the result of winnowing. The occurrence of winnowed sediment on the topographic highs was observed in the previous chapter. Winnowing removes the finer sized clay component to the valleys, while a residual concentration of the coarser clay sizes remains on the ridges. A gradation exists between valleys and ridges.

Temporal Variation In Clay Mineral Abundances

A change in the abundance of clay minerals from the Late Pleistocene to the Holocene has been observed in the northeast Pacific by Duncan, Kulm and Griggs (1970), and Duncan and Kulm (1970). A similar change is observed in this study. Core length plots of relative clay mineral abundances and ratios of montmorillonite to illite and chlorite to illite demonstrate consistent temporal clay mineral fluctuations (Figs.24 and 25). The Late Pleistocene-Holocene boundary, as discussed in Chapter II for this study, at 9,000 to 9,540 years B.P., is shown on the plots. In general the montmorillonite to illite ratio increases from the basal cored sediment to the approximated boundary, then decreases above it. The average percentage of montmorillonite increases for all physiographic areas of the Juan de Fuca Ridge from the Late Pleistocene to the Holocene (Fig.22). A similar result was found for the ratio of montmorillonite to illite in the northeast Pacific by Duncan, Kulm and Griggs, (1970). A corresponding change in the abundance of chlorite and

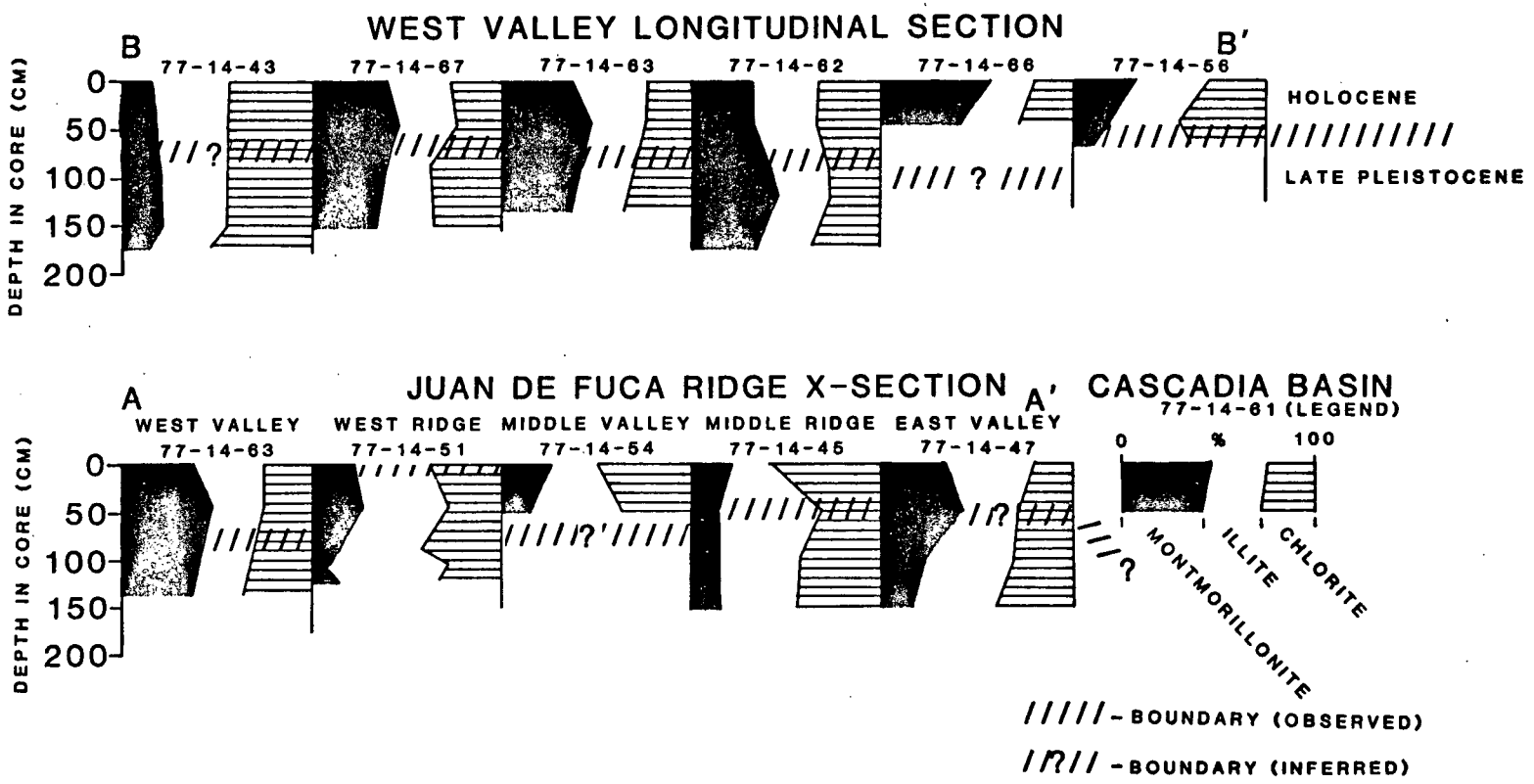

FIGURE 24. Relative percentage of clay minerals montmorillonite, chlorite and illite plotted against depth in core (centimetres) for Juan de Fuca Ridge section AA' and West Valley section BB'. Cascadia Basin core 77-14-61 is illustrated with legend.

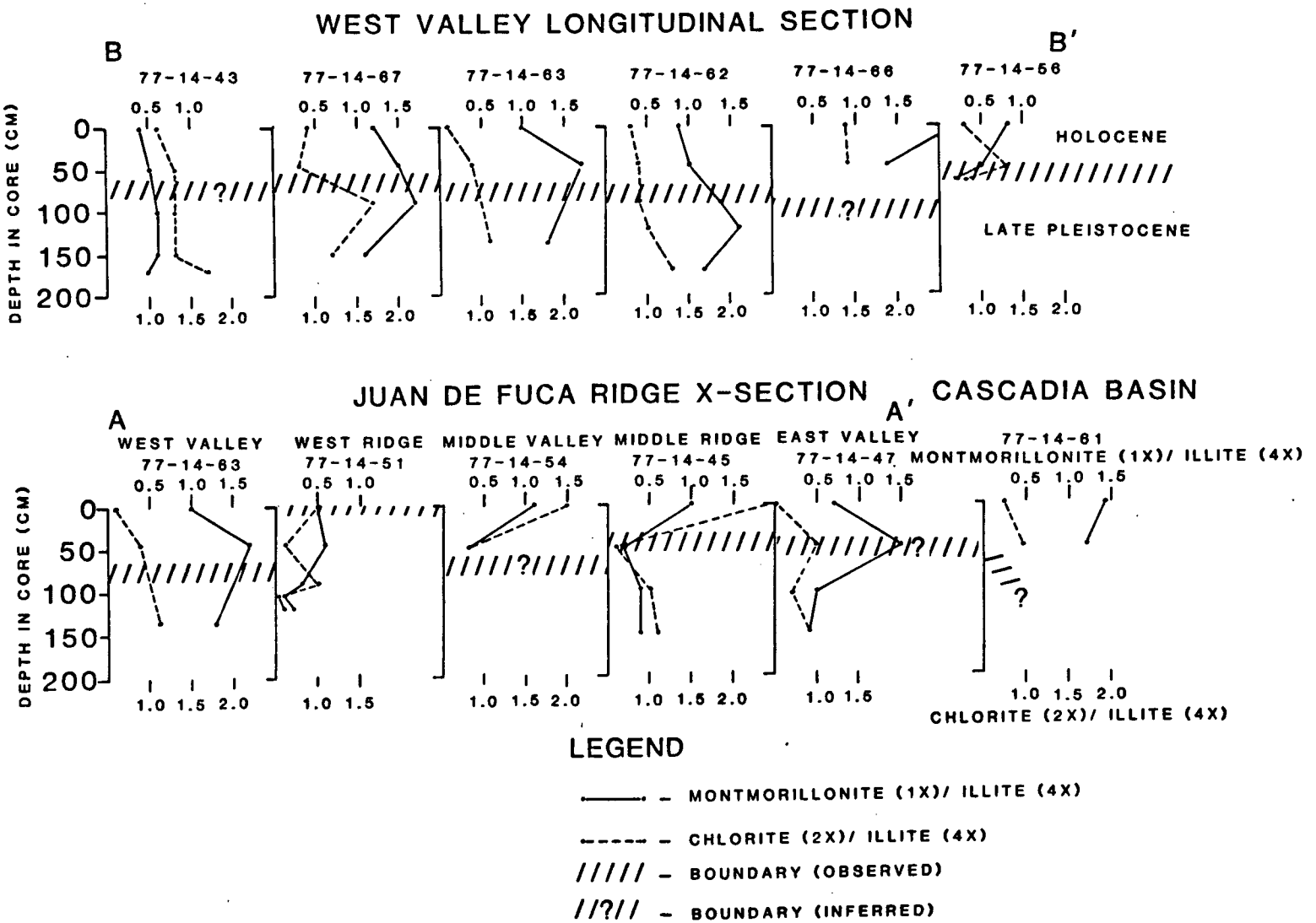

FIGURE 25. Ratioed relative percentage of clay minerals, with montmorillonite (1x) / illite (4x) and chlorite (2x) / illite (4x) plotted against depth in core (centimetres) for Juan de Fuca Ridge section AA' and West Valley section BB'. Cascadia Basin core 77-14-61 is also illustrated.

illite occurs from the Late Pleistocene to the Holocene for the Juan de Fuca Ridge area but the changes are physiographically variable (Fig.26). Chlorite decreased in abundance in the valleys and increased on the ridges from the Late Pleistocene to the Holocene whereas illite shows the opposite trend.

The interrelationship of the three clay minerals during the Late Pleistocene is explained by the widespread reduction in montmorillonite discussed earlier. The observed decrease in montmorillonite and corresponding increase in illite and chlorite may primarily reflect the dominance of sedimentation by turbidity currents during the Late Pleistocene. Sediments, as discussed in Chapter II, are dominated by terrigenous turbidites which contain abundant micaceous and chloritic minerals. Moreover, during the Late Pleistocene, winnowed chlorite appears to have diluted the clay minerals of the topographic lows leaving a residuum of illite on the ridges and topographic highs (Fig.26). During the Holocene, montmorillonite abundance generally increased, or chlorite and illite abundance decreased compared to Late Pleistocene abundances, and montmorillonite was preferentially winnowed from ridges to dilute the sediment of the valleys, chlorite remained with illite as a lag deposit on the ridges (Figs.26 and 27).

Is the observed change in the relative clay mineral distribution diagenetic? The shortness of the cores sampled for this study, the radiocarbon ages and the general moist unconsolidated character of the sediment indicates that only the earliest stage of diagenesis can have taken place. The early stage of marine diagenesis is marked by the stability of the clay minerals (DeSegonzac, 1970; Eberl and Hower, 1976). A diagenetic

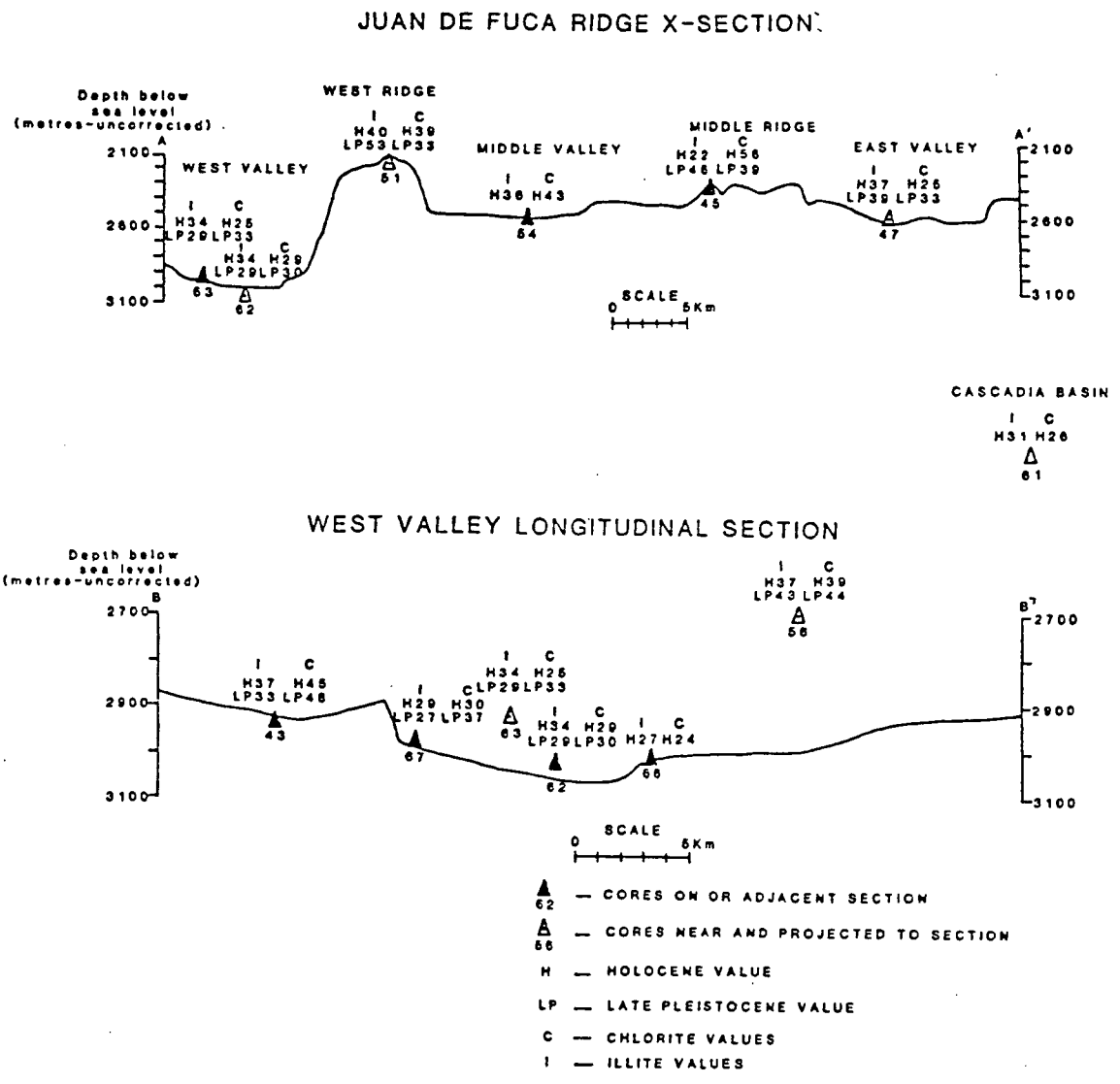

FIGURE 26. Bathymetric profiles AA' and BB' of the northern end of Juan de Fuca Ridge after Figure 4 , showing the distribution of average relative percentage values for illite (I) and chlorite (C) in Holocene samples (H) and Late Pleistocene samples (LP). Cascadia Basin core 77-14-61 is separately illustrated.

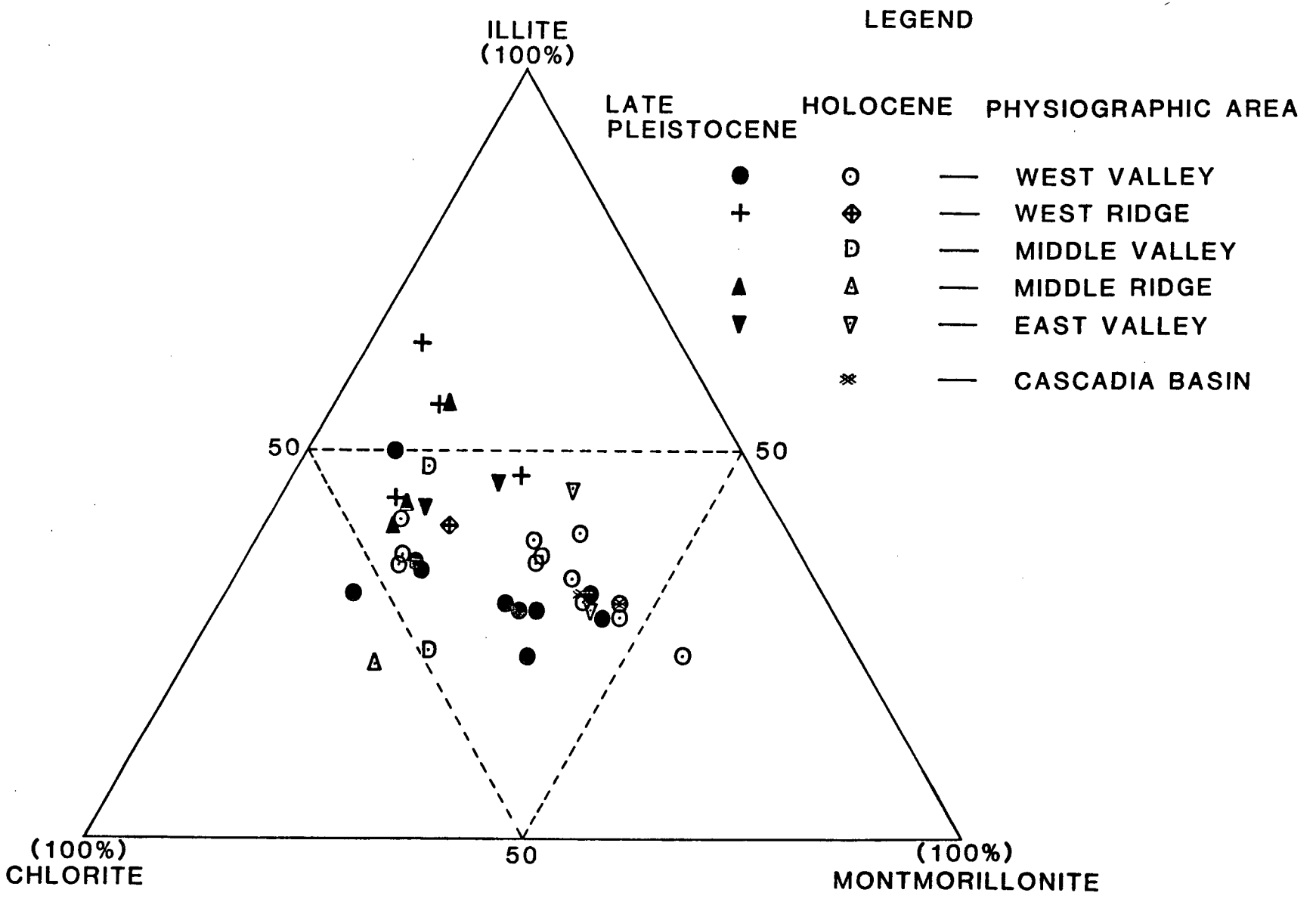

FIGURE 27. Ternary plot illustrating changes in relative percentages of clay minerals within different physiographic areas for the Late Pleistocene and Holocene Epochs.

explanation for the observed Late Pleistocene to Holocene deep-sea clay mineral fluctuations was discounted by Duncan, Kulm and Griggs (1970), and this writer holds the same opinion.

In summary, the observed downcore changes in mineral abundance are believed the result of interacting local and regional hydrographic and sedimentation factors effective during the Late Quaternary.

CONCLUSION

Provenance Of Minerals

The detrital minerals detected from each sample are ubiquitous to all the analyzed sediment from the study area. Certain minerals have distinct relationships: calcite, abundant in the tests of planktic and benthic foraminifera, is biogenic, while framboidal pyrite has a biogenic association.

The same suite of clay minerals, except for calcite, was detected both from Juan de Fuca Ridge and Cascadia Basin. Cascadia Basin sediments contain abundant montmorillonite, a feature that characterizes Holocene rather than Late Pleistocene sediments. The change in clay abundance from the Late Pleistocene to the Holocene suggests a relative increase in supply of montmorillonite, a relative decrease in supply of chlorite and illite, or both.

Clay mineral abundances throughout the world's oceans demonstrate strong latitudinal-climatic zonations, a feature primarily the result of aeolian and fluvial distribution patterns (Biscaye, 1965; Rateev *et al*, 1969; Keller, 1970). Chloritic and illitic clays are most plentiful in northern latitudes. Chlorite and illite dominate temperate high latitude soils where chemical weathering is of lesser intensity than in lower

latitudes (Rateev et al, 1969). Montmorillonite in the deep-sea may be an alteration product of: volcanic ash where occurrence with pyroclastic minerals and phillipsite suggests a volcanic association, basalts associated with hydrothermal circulation (Seyfried and Bischoff, 1981) and low latitude, arid, acidic, poorly drained, terrestrial lateritic soils. Pyroclastic minerals and phillipsite were not detected in the clays or the bulk sediments of this study, so a volcanic source is not apparent and the wide areal distribution and abundance changes for montmorillonite both for the study area and Cascadia Basin lend doubt to a ridge-type hydrothermal source. A temporal variation in montmorillonite for deep-sea sediments in the northeast Pacific was proposed by Duncan, Kulm and Griggs (1970), and was attributed to fluctuations in the Columbia River sediment load. Chlorite and illite-rich sediments come from the northern part of the river basin. The increase in sediment from the northern basin and its domination of the montmorillonite-rich southern Columbia drainage basin was the result of severe glacial erosion to the north in the Late Pleistocene. Subsequent glacial recession has caused the Columbia River system to produce a load with higher montmorillonite and lower chlorite and illite abundances during the Holocene. The influence of such a change in clay mineral abundance in the load of the Columbia River may be sufficiently large to affect the observed clay mineral abundances at the northern end of Juan de Fuca Ridge. However, the proposed source for turbidity currents affecting the study area is Queen Charlotte Sound. No known mineralogical studies on the sediments of the Sound have been conducted. Rivers presently contributing sediment to the Sound, drain basins that during the Late Pleistocene experienced glacial erosion and deposition. Sediment source areas contain outcrops

of primarily quartz diorite, granodiorite and diorite of the Coast Plutonic Complex to the east and basalts, pillow lavas and granodiorites of Vancouver Island to the south (G.S.C. Map 1386A, 1979). The Coast Plutonic Complex covers far more area than the mafic rocks of Vancouver Island, and should thus have been the major contribution to the Late Pleistocene glacial outwash. Clay minerals from the weathered intrusives would be dominated by muscovite and to a lesser extent chlorite derived from sericitic and propylitic alteration products (Sillitoe, 1973). Turbidity currents initiated from Queen Charlotte Sound, generated during glacial recession, would carry clays whose proportions would reflect provenance from the Coast Plutonic Complex.

In conjunction with or as an alternative to the preceding scenarios is one involving a change in clay mineral sedimentation dependent on differences in climate and soil mineralogy between the Late Pleistocene and Holocene. The correlation between terrestrial and marine chlorite and illite clay minerals at high latitudes was previously mentioned, while a comparable abundance exists for montmorillonite at lower latitudes. The Late Pleistocene was colder than the Holocene and the isotherms were further south (Clague, 1978). Possibly during the Late Pleistocene, soils from mid-latitudes that presently weather under warm, dry conditions experienced higher humidity and cooler climates that emphasized an increased production of chlorite and illite at the expense of montmorillonite clays. The result of a latitudinal shift in soil clay mineralogy between the Late Pleistocene and Holocene would be reflected in the neighbouring deep-sea environment.

It can be concluded that the shift in relative clay mineral abundances between the Late Pleistocene and Holocene epochs for the northern

end of Juan de Fuca Ridge primarily reflects changes from turbidity current deposition initiated from Queen Charlotte Sound to nonturbidity current deposition with possible secondary influence from changing continental soil weathering patterns and Columbia River sediment discharge.

Minerals described in this study are biogenic, authigenic or terrigenous. Minerals of a clearly hydrothermal affinity were not discovered in any of the samples analyzed. It is believed that due to the local character of known hydrothermal occurrences, surface vessels without deep-diving submersibles or drilling capability are unlikely to discover hydrothermal deposits (Hekinian et al, 1978, Franchteau et al, 1979). Detection of hydrothermal minerals will be complicated in an area such as the northern end of Juan de Fuca Ridge by dilution with non-hydrothermal sediment.

CHAPTER IV

SUMMARY AND CONCLUSIONS

Sediments from the northern end of Juan de Fuca Ridge possess characteristics as summarized below.

1. Gravity cores at all sites penetrate the Late Pleistocene-Holocene boundary. Late Pleistocene sediment is dominantly turbidite, whereas Holocene sediment is chiefly hemipelagic, with minor turbidite.

2. The Late Pleistocene turbidites are of the distal type, are terrigenous in character and are dominated by " dilute cloud " pelite. Turbidites and hemipelagic sediments are present at all physiographic sites studied except West Ridge. The valley sediments possess a stronger turbidite and weaker reworked hemipelagic character than do the ridges. Excluding the biogenic component, the differences in sediment between valleys and ridges are small.

3. The Late Pleistocene-Holocene boundary is not marked by a transition from foraminiferal to radiolarian dominated sediment, which was therefore time-transgressive. Interbedded hemipelagic sediments and turbidites of the valleys contain more radiolaria than foraminifera except where entrained foraminifera occur in the basal coarse sediment of the turbidite sequences. Foraminifera are dominant throughout the sediment of the ridges, with a decreased abundance from the Late Pleistocene to the Holocene.

4. Sedimentation rates for the Late Pleistocene based on radiocarbon dates, are 11.1 cm/1000 years for Middle Ridge and 16.5 cm/1000 years for West Ridge. Holocene sedimentation rates of 1.5 to 2.3 cm/1000 years are inferred for Middle Ridge.

5. Ubiquitous minerals for the Juan de Fuca Ridge and Cascadia Basin as determined by X-ray diffraction are: α-quartz, plagioclase, montmorillonite, illite, iron-rich chlorite, amphibole and cristobalite. Calcite was found in all analyzed samples from West and Middle Ridges. Magnetite is ubiquitous, and

pyrite was identified in concentrates from West Valley, West Ridge and Middle Ridge sediments.

6. Montmorillonite is relatively more abundant in the valleys and chlorite and illite on the ridges, the probable result of ridge sediment reworking. Montmorillonite shows a widespread relative increase and chlorite and illite a corresponding decrease from the Late Pleistocene to the Holocene.

7. Radiocarbon dates, inferred ages and cycles of sedimentation enables the stratigraphy of Juan de Fuca Ridge to be determined. Three cycles of interbedded turbidite-hemipelagic sediment were recognized from Middle Ridge and similar cycles are present in valley sediments. Turbidity current deposition appears episodic. Cycles in valley sediment contain compositional changes, recognized as Late Pleistocene, Holocene and transitional Late Pleistocene-Holocene in studies of the Cascadia Abyssal Plain and inclusive deep-sea channels (Griggs and Kulm, 1970). Postulation of a Late Pleistocene-Holocene boundary in the sediment of the valleys enables correlation of sedimentation cycles throughout the study area. Coincident changes in the relative abundances of clay minerals agree with the postulated boundary position.

8. A radiocarbon date of 19,000 years B.P. from surface sediment and a date of 23,660 years B.P. from deeper sediment, places stratigraphy of a core from West Ridge wholly within the Late Pleistocene. The hiatus since 19,000 years B.P. in foraminiferal-rich sediment in this core from West Ridge may be explained by: (a) Reworking of hemipelagic sediment, (b) lack of deposition from turbidity currents or (c) changes in both the foraminiferal fertility patterns of surface waters and the position of the lysocline relative to the core site during the Late Quaternary.

9. Enhanced preservation of Middle Ridge planktic foraminifera by episodic deposition of turbidites from " dilute clouds ", associated with turbidity currents originating at the continental terrace, has enabled good correlation

of geologic-climate events for Juan de Fuca Ridge and the continental Pacific Northwest.

10. The source area for Late Pleistocene turbidites on the Juan de Fuca Ridge was Queen Charlotte Sound. This conclusion is based on (a) the mineralogy of the turbidites which indicates provenance from a terrain of intermediate plutons ie., the Coast Plutonic Complex (b) the fact that deep-sea channels nearest the study area originate on the continental slope immediately west of Queen Charlotte Sound and (c) the presence, in ridge sediments, of post-Sumas stade turbidites not reported in studies of sediments from Cascadia Abyssal Plain.

It is concluded, based on structure, grain size distribution, radiocarbon dates and mineralogy that the sediments from the northern end of Juan de Fuca Ridge contain the Late Pleistocene-Holocene boundary, are correlatable between physiographic sites, and are correlatable with synchronous continental geologic-climate changes. A hydrothermal input into the sediments was not detected.

BIBLIOGRAPHY

Andrews, A. J., and W. S. Fyfe. 1976. Metamorphism and massive sulphide generation in oceanic crust. Geoscience Canada 3: 84-94.

Armstrong, J. E., D. R. Crandell, D. J. Easterbrook, and J. B. Noble. 1965. Late Pleistocene stratigraphy and chronology in southwestern British Columbia and northwestern Washington. Bull. Geol. Soc. Am. 76: 321-330.

Atwater, T. 1970. Implications of plate tectonics for the Cenozoic tectonic evolution of western North America. Bull. Geol. Soc. Am. 81: 3513-3536.

Barnard, W. D., and S. A. McManus. 1973. Planktonic foraminiferan-radiolarian stratigraphy and the Pleistocene-Holocene boundary in the northeast Pacific. Bull. Geol. Soc. Am. 84: 2097-2100.

Barr, S. M., 1972. Geology of the northern end of Juan de Fuca Ridge and adjacent continental slope. Ph.D. dissertation, University of British Columbia, 287 pp.

Barr, S. M., and R. L. Chase. 1973. Geology of the northern end of Juan de Fuca Ridge and sea-floor spreading. Can. J. Earth Sci. 10: 1384-1406.

Berger, W. H., 1967. Foraminiferal ooze: Solution at depths. Science 156: 383-385.

1970. Biogenous deep-sea sediments: Fractionation by deep-sea circulation. Bull. Geol. Soc. Am. 81: 1385-1402.

1971. Planktonic foraminifera: Sediment production in an oceanic front. J. Foram. Res. 1: 95-118.

1976. Biogenous deep-sea sediments: Production, preservation and interpretation in Chemical Oceanography, J. P. Riley and R. Chester, Ed. Academic Press, 5: 265-388.

Berger, W. H., and J. S. Killingley. 1977. Glacial-Holocene transition in deep-sea carbonates: Selective dissolution and the stable isotope signal. Science 197: 563-565.

Berger, W. H., and E. L. Winterer. 1974. Plate stratigraphy and the fluctuating carbonate line in Pelagic Sediments on Land and Under the Sea. International Association of Sedimentology Special Publication 1: 11-48.

Biscaye, P. E., 1964. Distinction between kaolinite and chlorite in Recent sediments by X-ray diffraction. Am. Min. 49: 1281-1289.

Biscaye, P. E., 1965. Mineralogy and sedimentation of Recent deep-sea clay in the Atlantic Ocean and adjacent seas and oceans. Bull. Geol. Soc. Am. 76: 803-832.

Blatt, H., G. Middleton, and R. Murray. 1972. Origin Of Sedimentary Rocks. Prentice-Hall, Inc., New Jersey: 634 pp.

Bouma, A. H., 1962. Sedimentology of some flysch deposits. Elsevier Amsterdam, Publ. 168 pp.

Bouma, A. H. and C. D. Hollister. 1973. Deep ocean basin sedimentation in Turbidites and Deepwater Sedimentation S. E. P. M. Pacific Short Course, Anaheim. 79-118.

Brindley, G. W., 1961. Chlorite minerals in Identification And Crystal Structures Of Clay Minerals, G. Brown, Ed. Mineralogical Society: 242-296.

Broecker, W. S., 1971. Calcite accumulation rates and glacial to interglacial changes in oceanic mixing in Late Cenozoic Glacial Ages: New Haven, Yale Univ. Press: 239-265.

Carroll, D., 1970. Clay minerals: A guide to their X-ray identification. Geol. Soc. Am. Special Paper 126: 80 pp.

Carson, B., 1971. Stratigraphy and depositional history of Quaternary sediments in northern Cascadia Basin and Juan de Fuca Abyssal Plain, Northeast Pacific Ocean. Ph.D. dissertation, Univ. of Washington, Seattle.

Carson, B., and D. A. McManus. 1971. Analysis of turbidite correlation in Cascadia Basin, northeast Pacific Ocean, Deep-Sea Res. 18: 593-604.

Clague, J. J., 1978. Mid-Wisconsinan climates of the Pacific Northwest in Current Research, Part B, Geol. Surv. Can., Paper 78-IB: 95-100.

Davis, E. E., and C. R. B. Lister. 1977a. Tectonic structures on the Juan de Fuca Ridge. Bull. Geol. Soc. Am. 88: 346-363.

Davis, E. E., and C. R. B. Lister. 1977b. Heat flow over the Juan de Fuca Ridge: Evidence for widespread hydrothermal circulation in a highly heat transportative crust. J. Geophys. Res. 82: 4845-4860.

DeSegonzac, G. D., 1970. The transformation of clay minerals during diagenesis and low-grade metamorphism: A review. Sedimentology 15: 281-346.

Duncan, J. R., G. A. Fowler, L. D. Kulm. 1970. Planktonic foraminiferan-radiolarian ratios and Holocene-Late Pleistocene deep-sea stratigraphy off Oregon. Bull. Geol. Soc. Am. 81: 561-566.

Duncan, J. R., and L. D. Kulm. 1970. Mineralogy, provenance and dispersal history of Late Quaternary deep-sea sands in Cascadia Basin and Blanco Fracture Zone off Oregon. J. Sed. Pet. 40: 874-887.

Duncan, J. R., L. D. Kulm, and G. B. Griggs. 1970. Clay mineral composition of Late Pleistocene and Holocene sediments of Cascadia Basin, northeastern Pacific Ocean. J. Geol. 78: 213-221.

Eberl, D., and J. Hower. 1976. Kinetics of illite formation. Bull. Geol. Soc. Am. 87: 1326-1330.

Elverhøi, A., 1977. Origin of framboidal pyrite in clayey Holocene sediments and in Jurassic black shale in the northwestern part of the Barents Sea. Sedimentology 24: 591-595.

Emiliani, C., 1971. The amplitude of Pleistocene climatic cycles at low latitudes and the isotopic composition of glacial ice in Late Cenozoic Glacial Ages: New Haven, Yale Univ. Press: 183-197.

Emiliani, C., and N. J. Shackleton. 1974. The Brunhes Epoch: Isotopic paleotemperatures and geochronology. Science 183: 511-514.

Farrand, M., 1970. Framboidal sulphides precipitated synthetically. Min. Deposita 5: 237-247.

Folk, R. L., 1974. Petrology of sedimentary rocks. Univ. of Texas, Austin: 182 pp.

Folk, R. L., and W. C. Ward. 1957. Brazos River bar: A study in the significance of grain size parameters. J. Sed. Pet. 27: 3-26.

Francheteau, J., H. D. Needham, P. Choukroune, T. Juteau, M. Seguret, R. D. Ballard, P. J. Fox, W. Normark, A. Carranza, D. Cordoba, J. Guerrero, C. Rangin, H. Bougault, P. Cambon, and R. Hekinian. 1979. Massive deep-sea sulphide ore deposits discovered on the East Pacific Rise. Nature 277: 523-528.

Frerichs, W. E., 1968. Pleistocene-Recent boundary and Wisconsin glacial biostratigraphy in the northern Indian Ocean. Science 159: 1456-1458.

Fryer, B. J., and R. W. Hutchinson. 1976. Generation of mineral deposits on the seafloor. Can. J. Earth, Sci. 13: 126-135.

Griggs, G. B., and L. D. Kulm. 1970. Sedimentation in Cascadia Deep-Sea Channel. Bull. Geol. Soc. Am. 81: 1361-1384.

Hekinian, R., B. R. Rosendahl, D.S. Cronan, Y. Dmitriev, R. V. Fodor, R. M. Goll, M. Hoffert, E. E. Humphris, D. P. Mattey, J. Natland, N. Petersen, W. Roggenthen, E. L. Schrader, R. K. Srivastava, N. Warren. 1978. Hydrothermal deposits and associated basement rocks from the Galapagos spreading center Oceanologica Acta 1: 473-482.

Heusser, C. J. 1977. Quaternary palynology of the Pacific slope of Washington Quat. Res. 8: 282-306.

Horn, D. R., M. Ewing, M. N. Delach, and B. M. Horn. 1971. Turbidites of the northeast Pacific. Sedimentology 16: 55-69.

Horn, D. R., J. I. Ewing, and M. Ewing. 1971. Graded-bed sequences emplaced by turbidity currents north of 20°N in the Pacific, Atlantic and Mediterranean. Sedimentology 18: 247-275.

Imbrie, J., and N. G. Kipp. 1971. A new micropaleontological method for quantitative paleoclimatology: Application to a Late Pleistocene Caribbean core in Late Cenozoic Glacial Ages: New Haven, Yale Univ. Press: 71-181.

Ingle, S. E., 1975. Solubility of calcite in the ocean. Mar. Chem. 3: 301-319.

Ingle, S. E., C. H. Culberson, J. E. Hawley, and R. M. Pytkowicz. 1973. The solubility of calcite in seawater at atmospheric pressure and 35 °/oo salinity. Mar. Chem. 1: 295-307.

Karlin, R., 1980. Sediment sources and clay mineral distributions off the Oregon coast. J. Sed. Pet. 50: 543-560.

Keller, W. D., 1970. Environmental aspects of clay minerals. J. Sed. Pet. 40: 788-854.

Kent, D., N. D. Opdyke, and M. Ewing, 1971. Climate change in the north Pacific using ice-rafted detritus as a climatic indicator. Bull. Geol. Soc. Am. 82: 2741-2754.

Kido, K., 1974. Latitudinal distribution and origin of particulate silica in the surface water of the north Pacific. Mar. Chem. 2: 277-285.

Kulm, L. D., R. C. Roush, J. C. Harlett, R. H. Neudeck, D. M. Chambers, and E. J. Runge. 1975. Oregon continental shelf sedimentation: interrelationships of facies distribution and sedimentary processes. J. Geol. 83: 145-175.

Kulm, L. D., R. vonHuene, et al. 1973. Initial reports of the deep-sea drilling project, 18, Washington (U. S. Government Printing Office) 1077 pp.

Lisitizin, A. P., 1972. Sedimentation in the world ocean. Soc. Econ. Paleon. Min. Special Publication 17: 218 pp.

Lorens, R. B., D. F. Williams, and M. L. Bender. 1977. The early nonstructural chemical diagenesis of foraminiferal calcite. J. Sed. Pet. 47: 1602-1609.

Lucas, W. H., 1972. Juan de Fuca Ridge and Sovanco Fracture Zone. RP-5-OC-71, N. O. A. A. Technical Report ERL234-POL11, Boulder, Colo. 39 pp.

MacEwan, D. M. C., 1961. Montmorillonite minerals in The X-Ray Identification and Crystal Structures of Clay Minerals. G. Brown, Ed. Min. Soc. 143-207.

Mathews, W. H., 1979. Late Quaternary environmental history affecting human habitation of the Pacific Northwest. Can. J. Arch. 3: 145-156.

McManus, D. A., M. L. Holmes, B. Carson, and S. M. Barr. 1972. Late Quaternary tectonics, northern end of Juan de Fuca Ridge (northeast Pacific). Mar. Geol. 12: 141-164.

Micromeritics Instrument Corporation Instruction Manual. 1973. Sedigraph 5000 particle size analyzer. Micromeritics Instrument Corporation, Atla., Georgia. 87 pp.

Middleton, G. V., and M. A. Hampton. Sediment gravity flows: Mechanics of flow and deposition in Turbidites And Deepwater Sedimentation, S. E. P. M. Pacific Section Short Course, Anaheim, 1-38.

Morse, J. W., and R. A. Berner. 1972. Dissolution of calcium carbonate in seawater: A kinetic origin for the lysocline. Am. J. Sci. 272: 840-851.

Nayudu, Y. R., 1964. Carbonate deposits and paleoclimatic implications in the northeast Pacific Ocean. Science 146: 515-517.

Nelson, C. H., L. D. Kulm, P. R. Carlson, and J. R. Duncan. 1968. Mazama ash in the northeastern Pacific. Science 161: 47-49.

Nelson, C. H., and L. D. Kulm. 1973. Submarine fans and deep-sea channels in Turbidites And Deepwater Sedimentation, S. E. P. M. Pacific Short Course, Anaheim: 39-78.

Peng, T. H., W. S. Broecker, and W. H. Berger. 1979. Rates of benthic mixing in deep-sea sediment as determined by radioactive tracers. Quat. Res. 11: 141-149.

Peterson, M. N. A., 1966. Calcite: Rates of dissolution in a vertical profile in central Pacific. Science 154: 1542-1544.

Phipps, J. B., 1977. Late Quaternary variations in the silt mineralogy of deep-sea cores from the Gorda Ridge, northeast Pacific. J. Geol. 85: 619-624.

Prell, W. L., 1977. Winnowing of Recent and Late Quaternary deep-sea sediments sediments: Colombia Basin, Caribbean Sea. J. Sed. Pet. 47: 1583-1592.

Pytkowicz, R. M., 1970. On the carbonate compensation depth in the Pacific Ocean. Geochim. Cosmochim. Acta 34: 836-839.

Rateev, M. A., Z. N. Gorbunova, A. P. Lisitzyn, and G. L. Nosov. 1969. The distribution of clay minerals in the oceans. Sedimentology 13: 21-43.

Selk, B. W., 1977. The manganese-enriched sediments of the Blanco Trough: Evidence for hydrothermal activity in a fracture zone. M.Sc. dissertation Oregon State Univ., Corvallis, 137 pp.

Seyfried, Jr. W. E., and J. L. Bischoff. 1981. Experimental seawater-basalt interaction at 300 ^{o}C, 500 bars, chemical exchange, secondary mineral formation and implications for the transport of heavy metals. Geochim. Cosmochim. Acta 45: 135-147.

Siesser, W. G., and Rogers. 1976. Authigenic pyrite and gypsum in southwest African continental slope sediments. Sedimentology 23: 567-577.

Sillitoe, R. H., 1973. The tops and bottoms of porphry copper deposits. Econ. Geol. 68: 799-815.

Stewart, R. J., 1976. Turbidites of the Aleutian Abyssal Plain: Mineralogy, provenance and constraints for Cenozoic motion of the Pacific plate. Bull. Geol. Soc. Am. 87: 793-808.

Stoffers, P., and G. Muller. 1972. Clay mineralogy of Black Sea sediments. Sedimentology 18: 113-121.

Thomson, R. E., 1973. The distribution and variability of physical oceanographic properties along Line P, May 8-18, 1972. Pacific Marine Science Report 73-6. 155 pp.

Turekian, K. K., and M. Stuiver. 1964. Clay- and carbonate-accumulation rates in three south Atlantic deep-sea cores. Science 146: 55-56.

Valencia, M. J., 1977. Pleistocene stratigraphy of the western equatorial Pacific. Bull. Geol. Soc. Am. 88: 143-150.

vonHuene, R., J. Crouch, and E. Larson. 1976. Glacial advance in the Gulf of Alaska area implied by ice-rafted material. Mem. Geol. Soc. Am. 145: 411-422.

Wakeham, S. E. 1977. Petrochemical patterns in young pillow basalts dredged from Juan de Fuca and Gorda Ridges. M.Sc. dissertation, Oregon State Univ., Corvallis, 95 pp.

Walker, R. G., and Mutti. 1973. Turbidite facies and facies associations in Turbidites And Deepwater Sedimentation, S. E. P. M., Pacific Section Short Course, Anaheim: 119-158.

White, S. M., 1970. Mineralogy and geochemistry of continental shelf sediments off the Washington-Oregon coast. J. Sed. Pet. 40: 38-54.

Windom, H. L., 1969. Atmospheric dust records in permanent snowfields: Implications to marine sedimentation. Bull. Geol. Soc. Am. 80: 761-782.

Windom, H. L., 1976. Lithogenous material in marine sediments in Chemical Oceanography, J. P. Riley and R. Chester, Ed. Academic Press, 5: 103-135.

APPENDIX I

Location, Bathymetric Depth And Length Of Analyzed Cores

Core No.	Location		Depth (m)	Length (cm)
	Latitude	Longitude		
77-14-43	48° 39.8'	128° 55.9'	2935	172
77-14-45	48° 27.5'	128° 37.0'	2350	160
77-14-47	48° 28.9'	128° 25.6'	2585	150
77-14-51	48° 30.6'	128° 52.0'	2180	124
77-14-54	48° 30.0'	128° 45.5'	2520	53
77-14-56	48° 29.6'	129° 04.5'	2700	69
77-14-61	48° 34.0'	127° 44.6'	2600	68
77-14-62	48° 33.4'	128° 52.4'	3025	172
77-14-63	48° 34.6'	129° 00.2'	2925	148
77-14-66	48° 31.2'	128° 58.8'	3010	46
77-14-67	48° 36.4'	128° 55.7'	2975	164

APPENDIX II

Core Structure And Clay Size Distribution

LEGEND

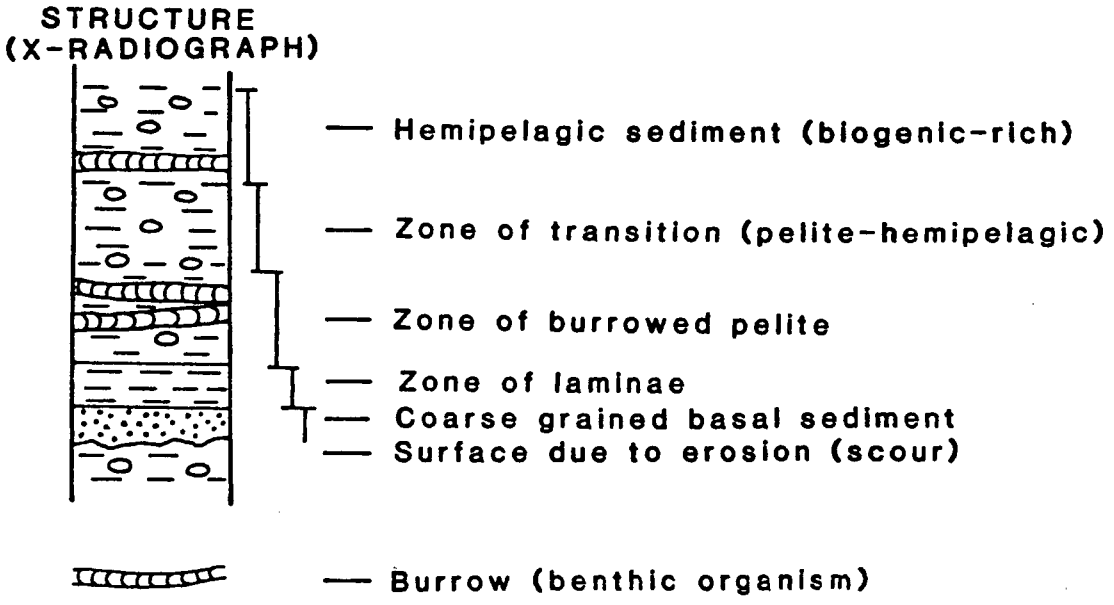

WEST VALLEY
CORE 77-14-43

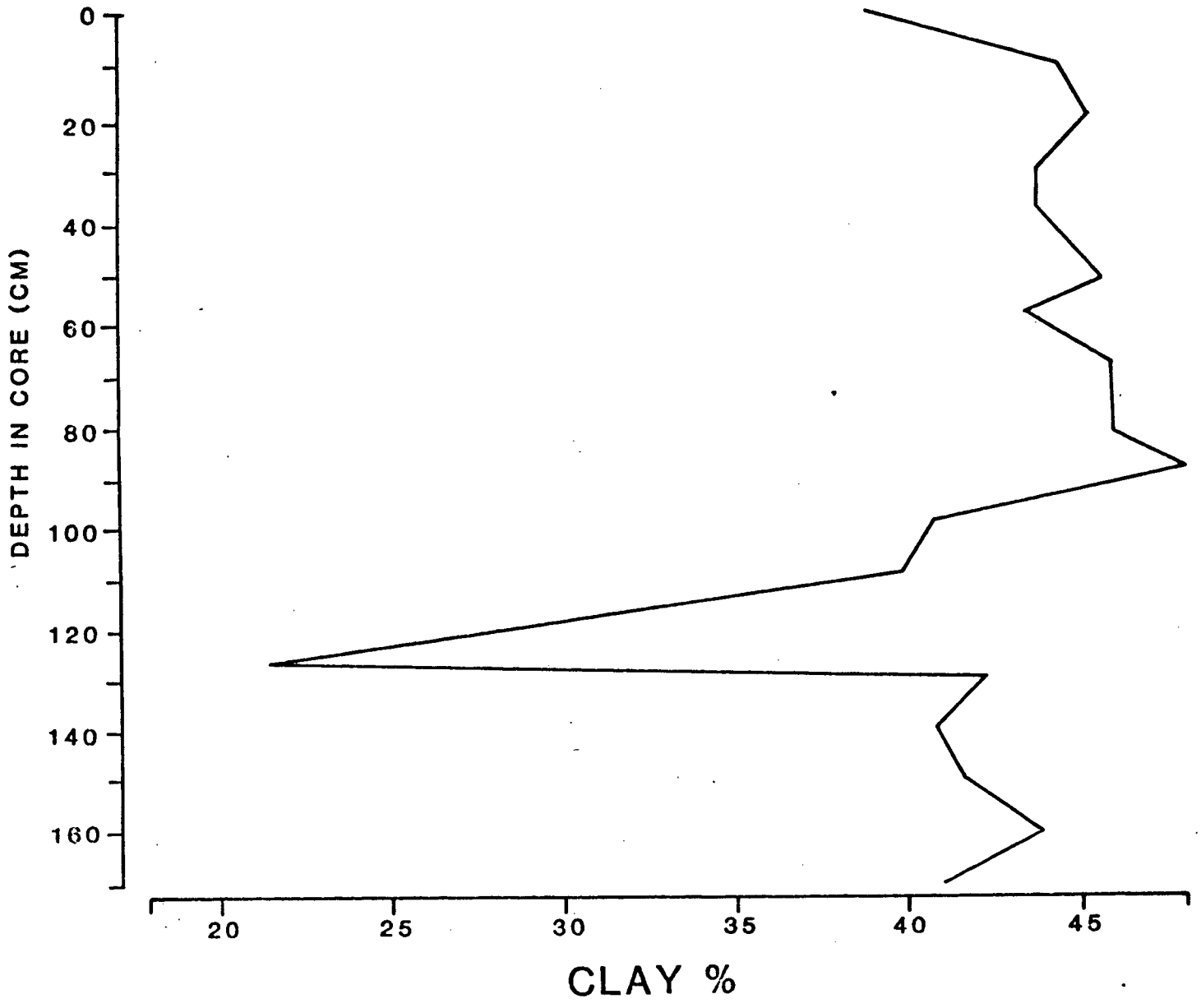

MIDDLE RIDGE
CORE 77-14-45

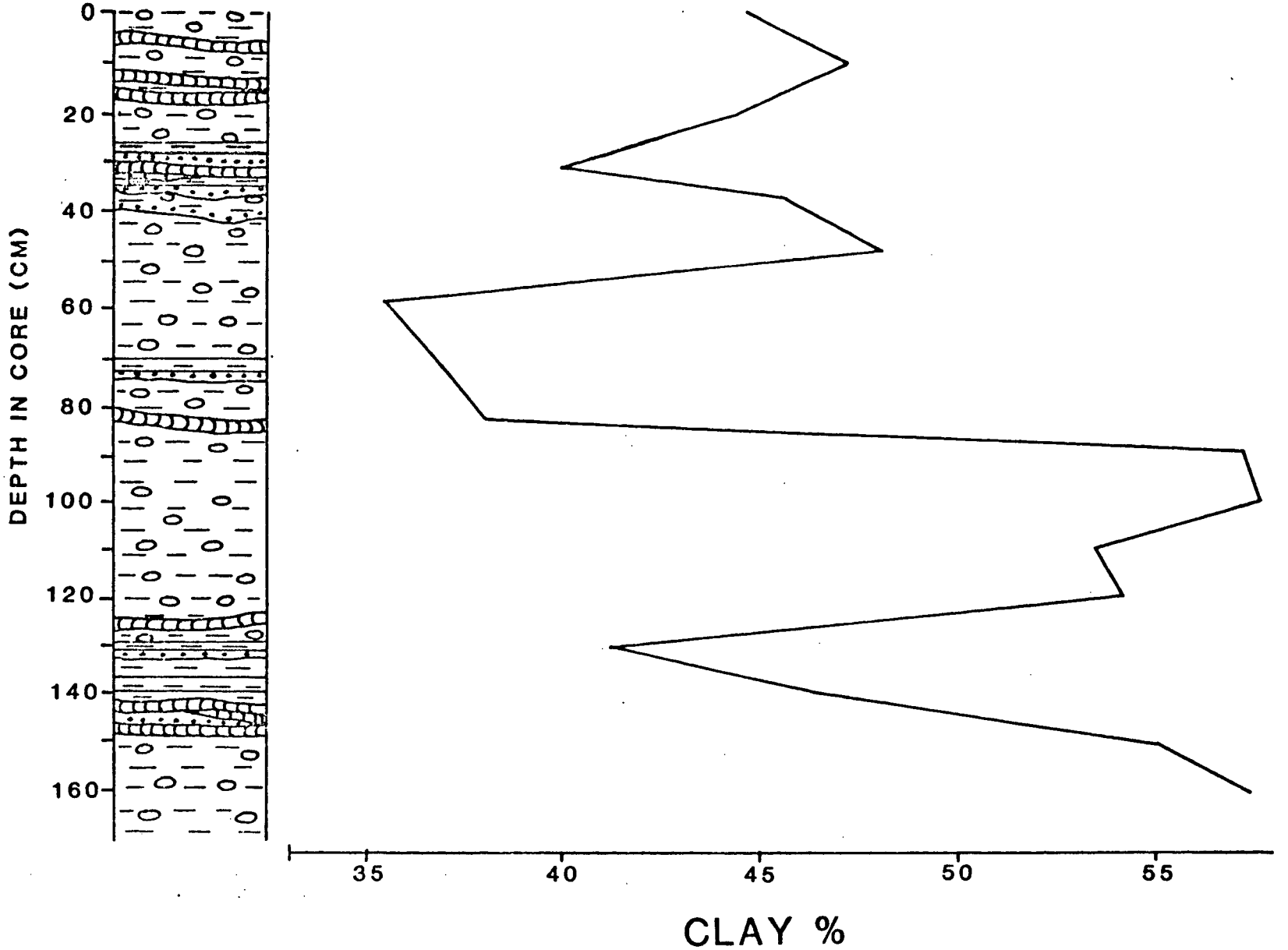

EAST VALLEY
CORE 77-14-47

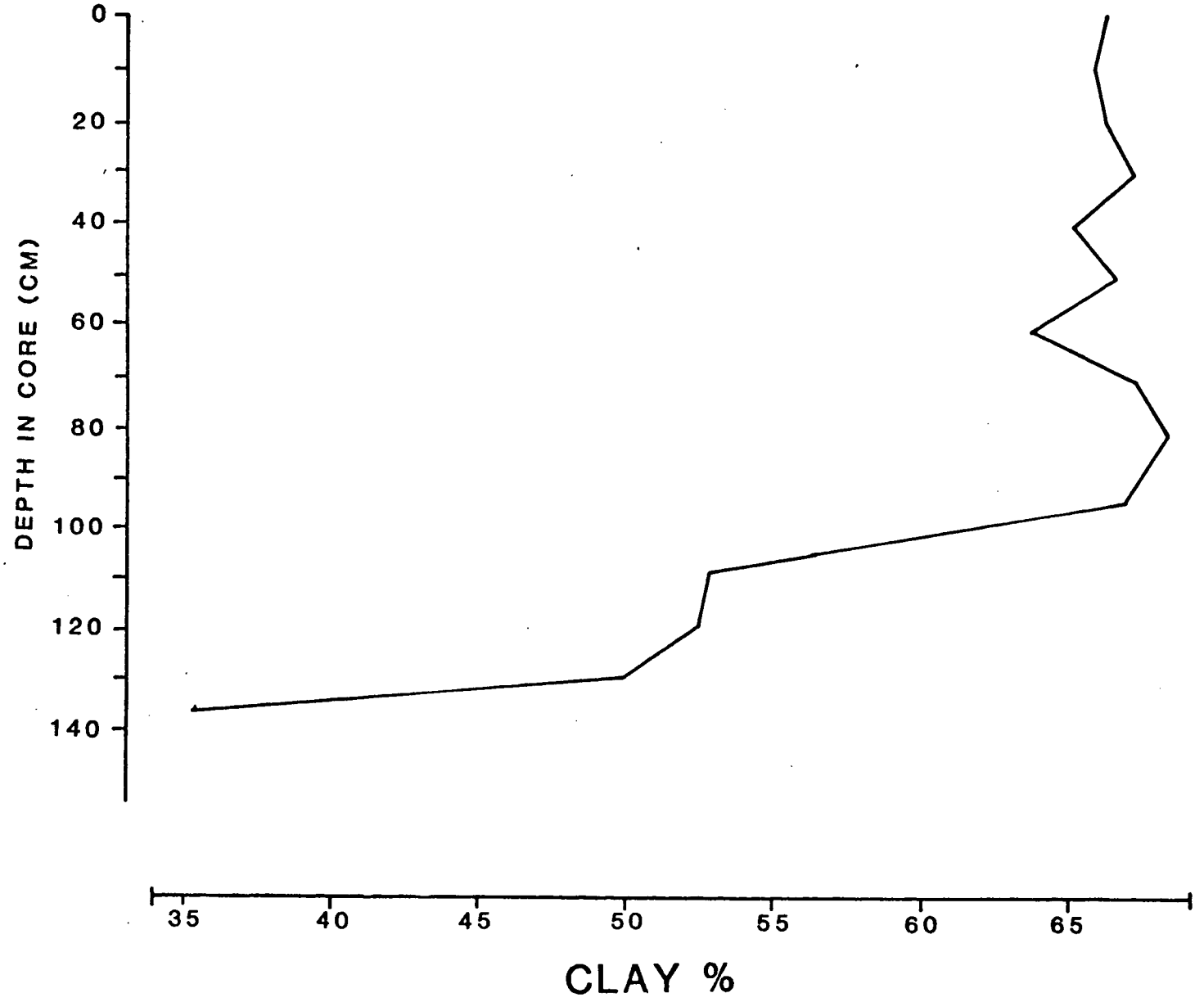

WEST RIDGE
CORE 77-14-51

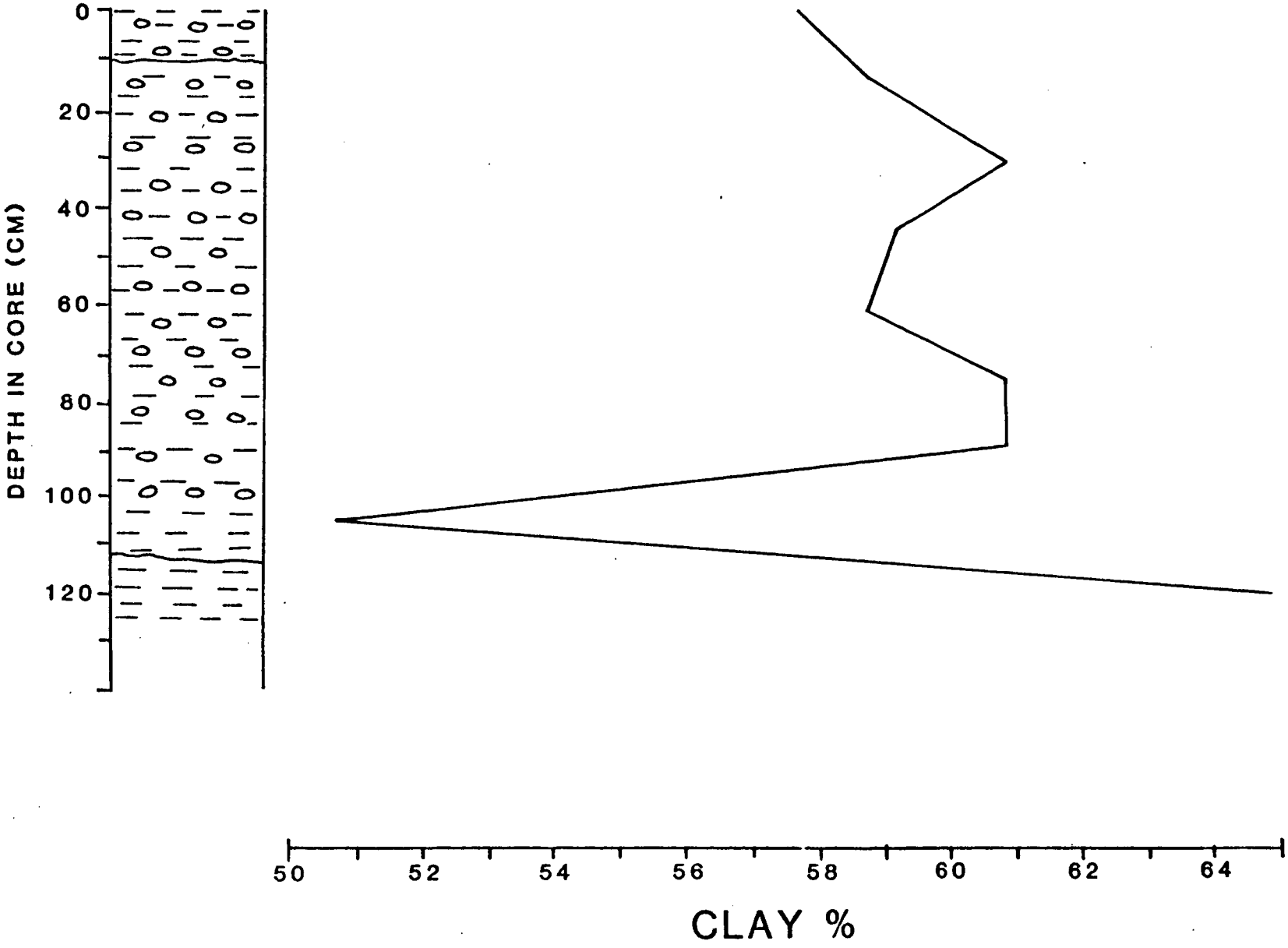

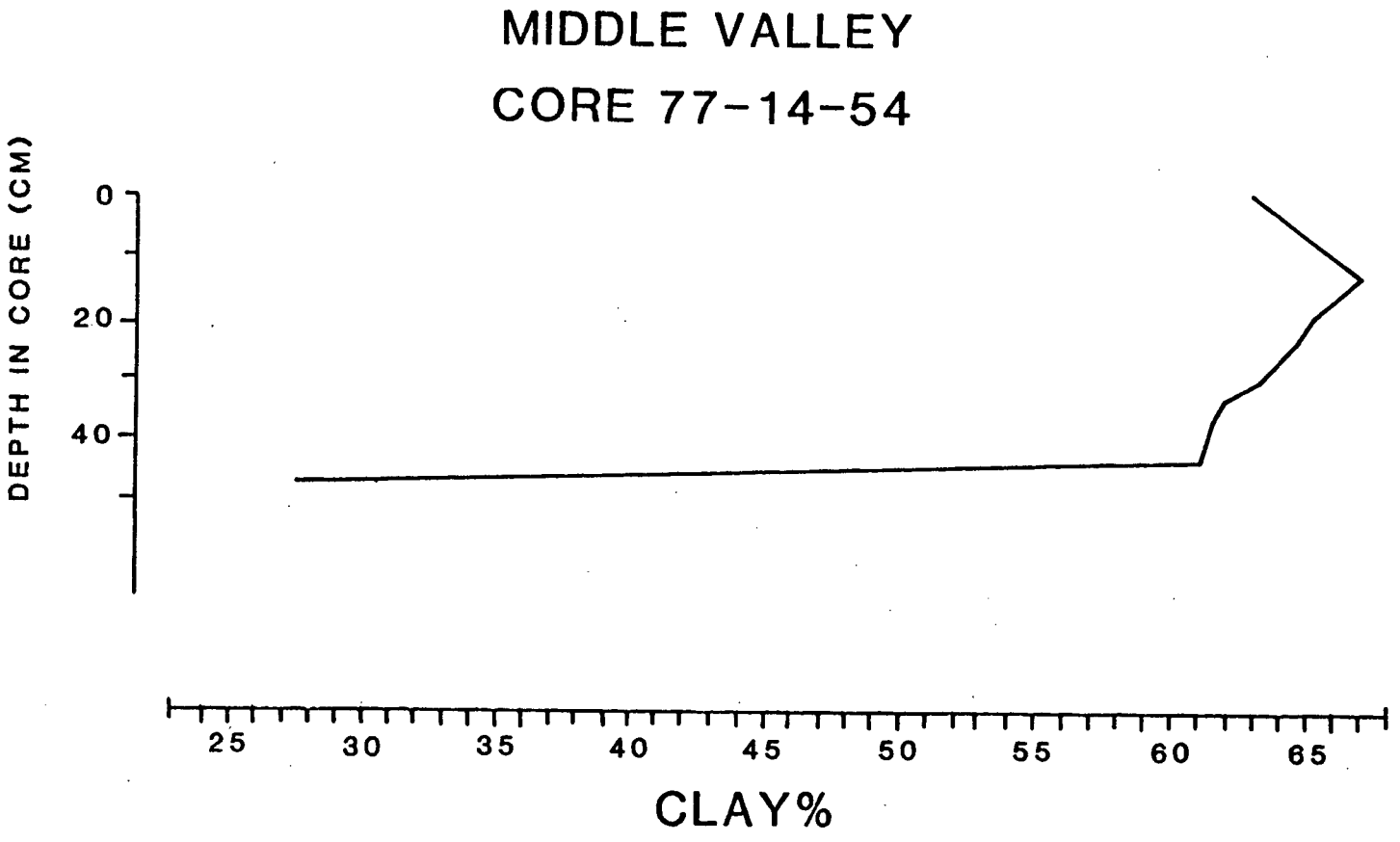
MIDDLE VALLEY
CORE 77-14-54
DEPTH IN CORE (CM)
0
20
40
25
30
35
40
45
50
55
60
65
CLAY%

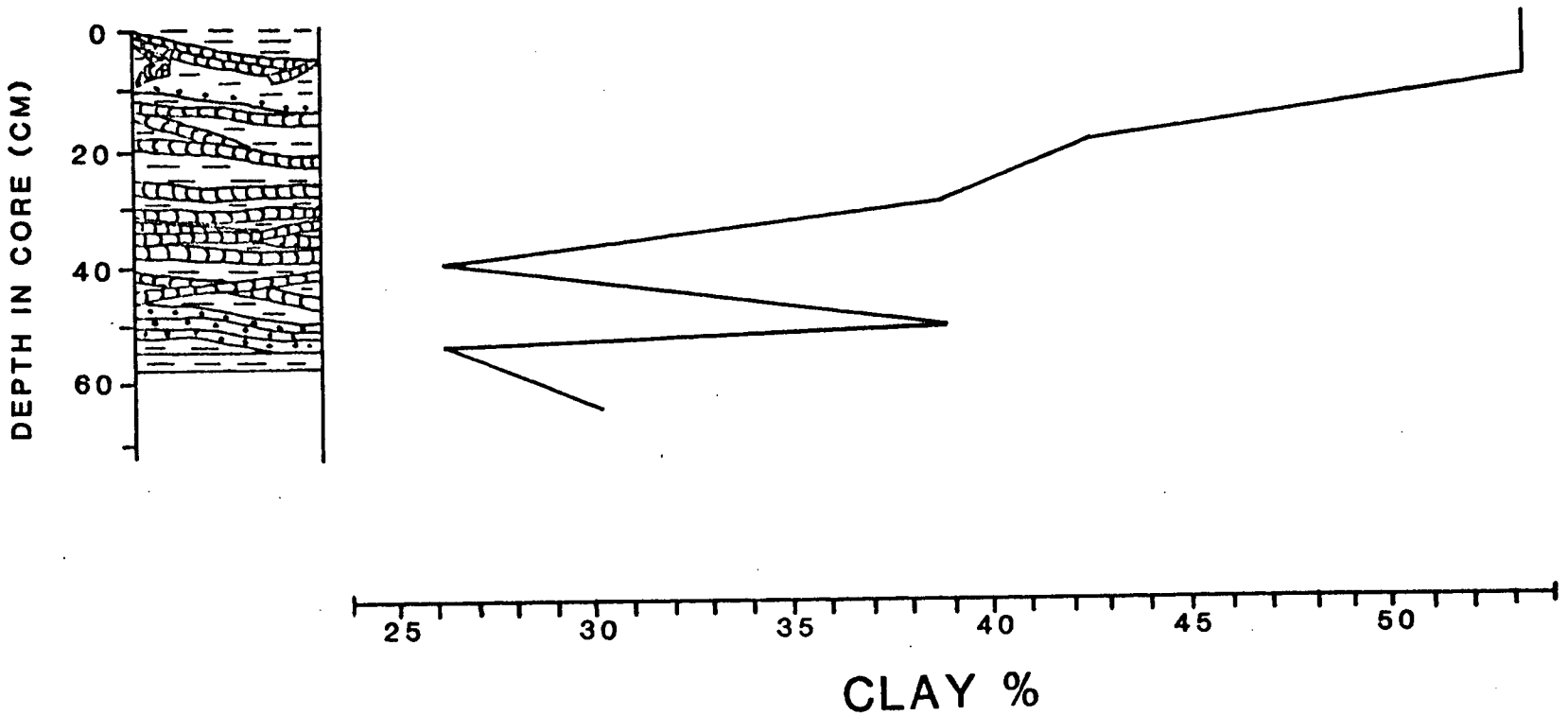
WEST VALLEY
CORE 77-14-56
DEPTH IN CORE (CM)
0
20
40
60
25
30
35
40
45
50
CLAY %

CASCADIA BASIN
CORE 77-14-61

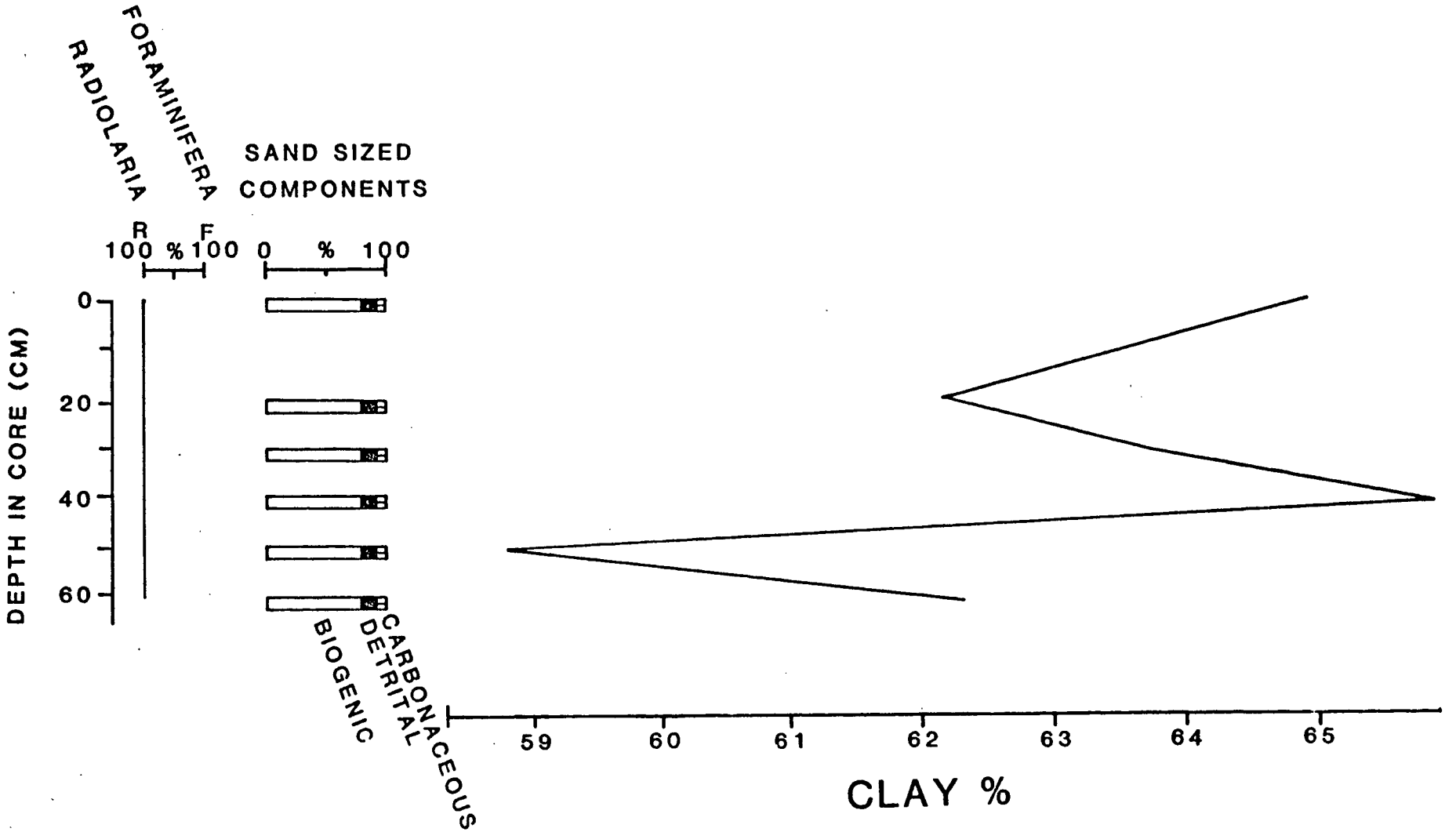

WEST VALLEY
CORE 77-14-62

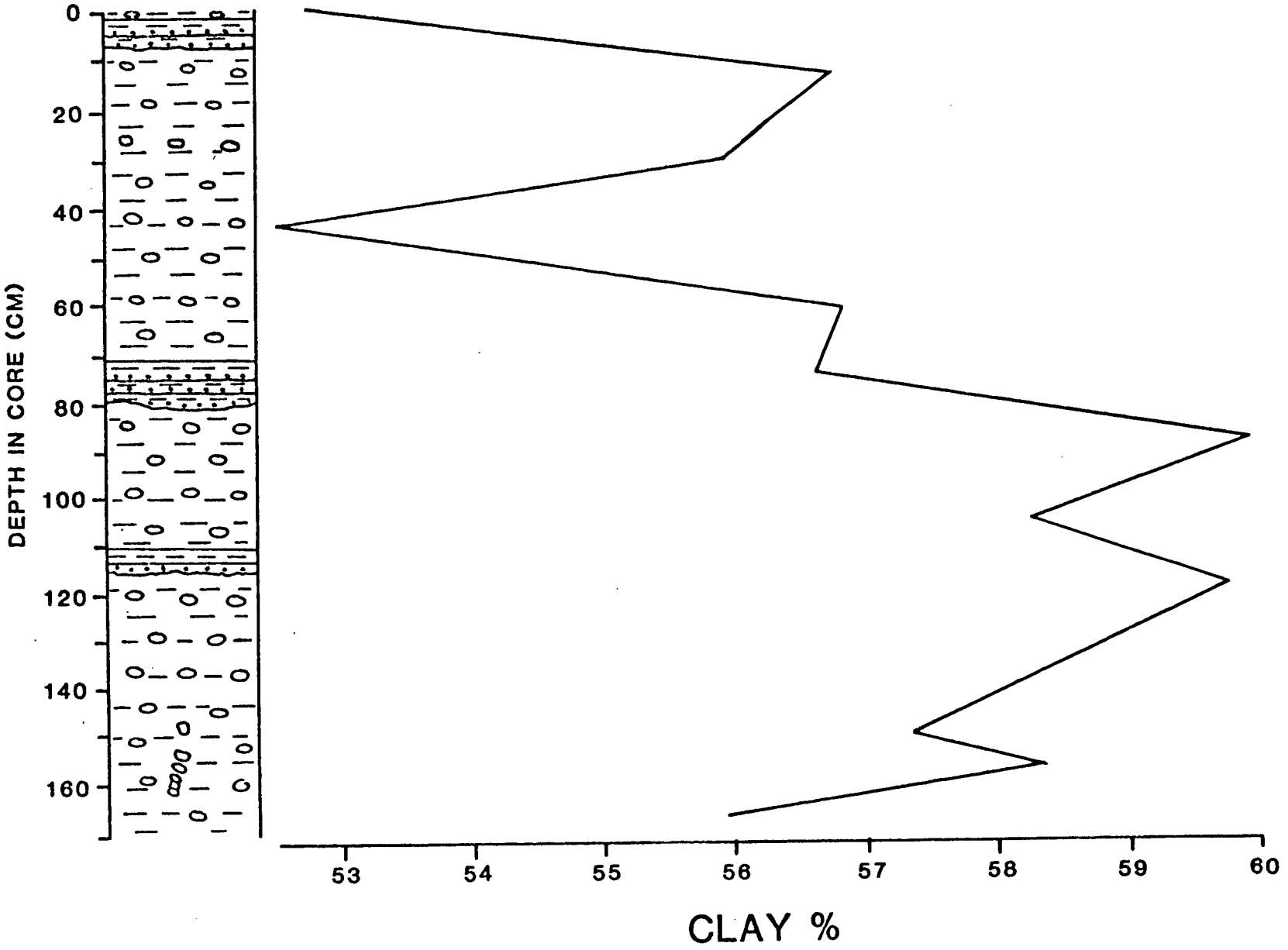

WEST VALLEY
CORE 77-14-63

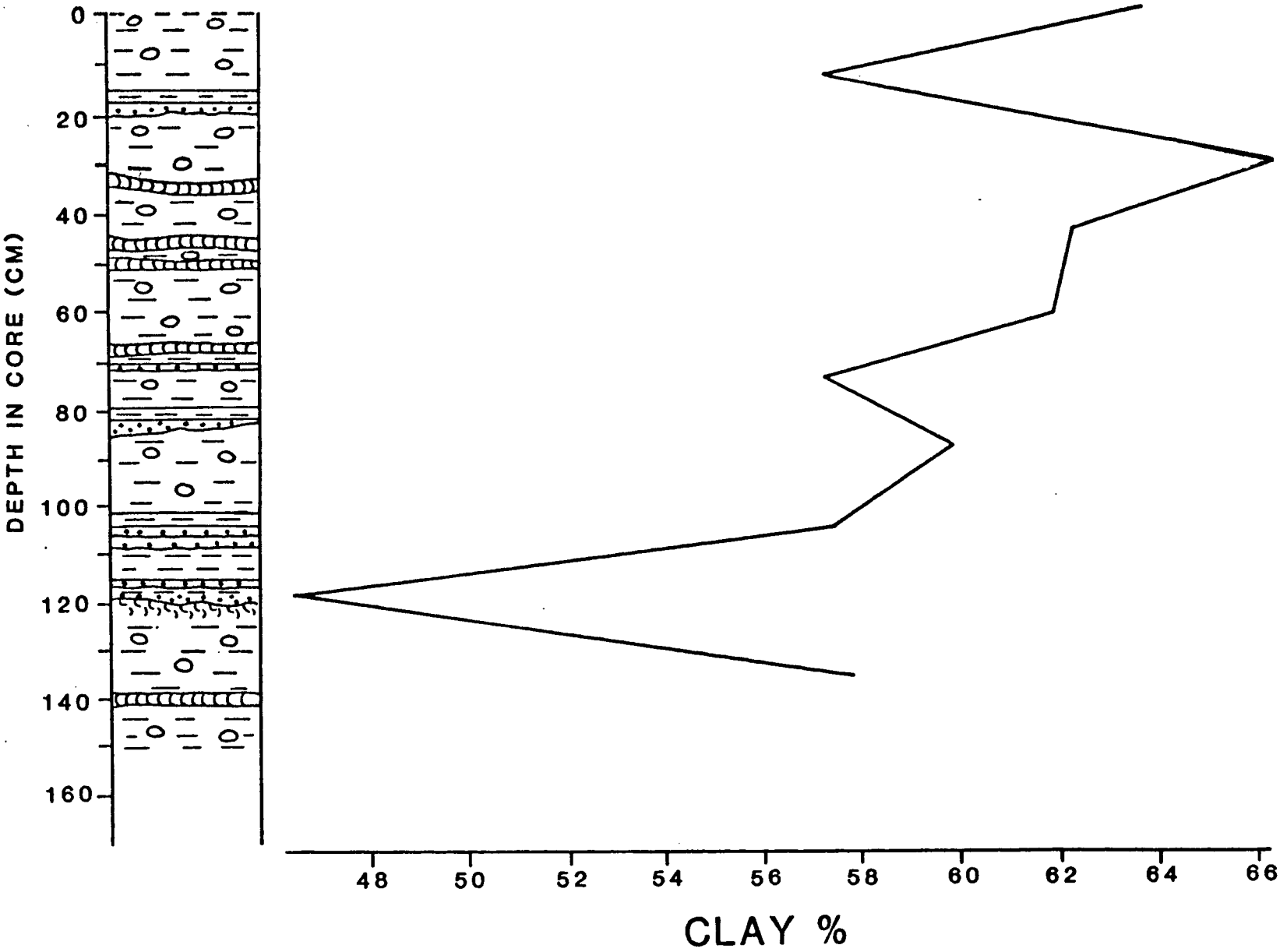

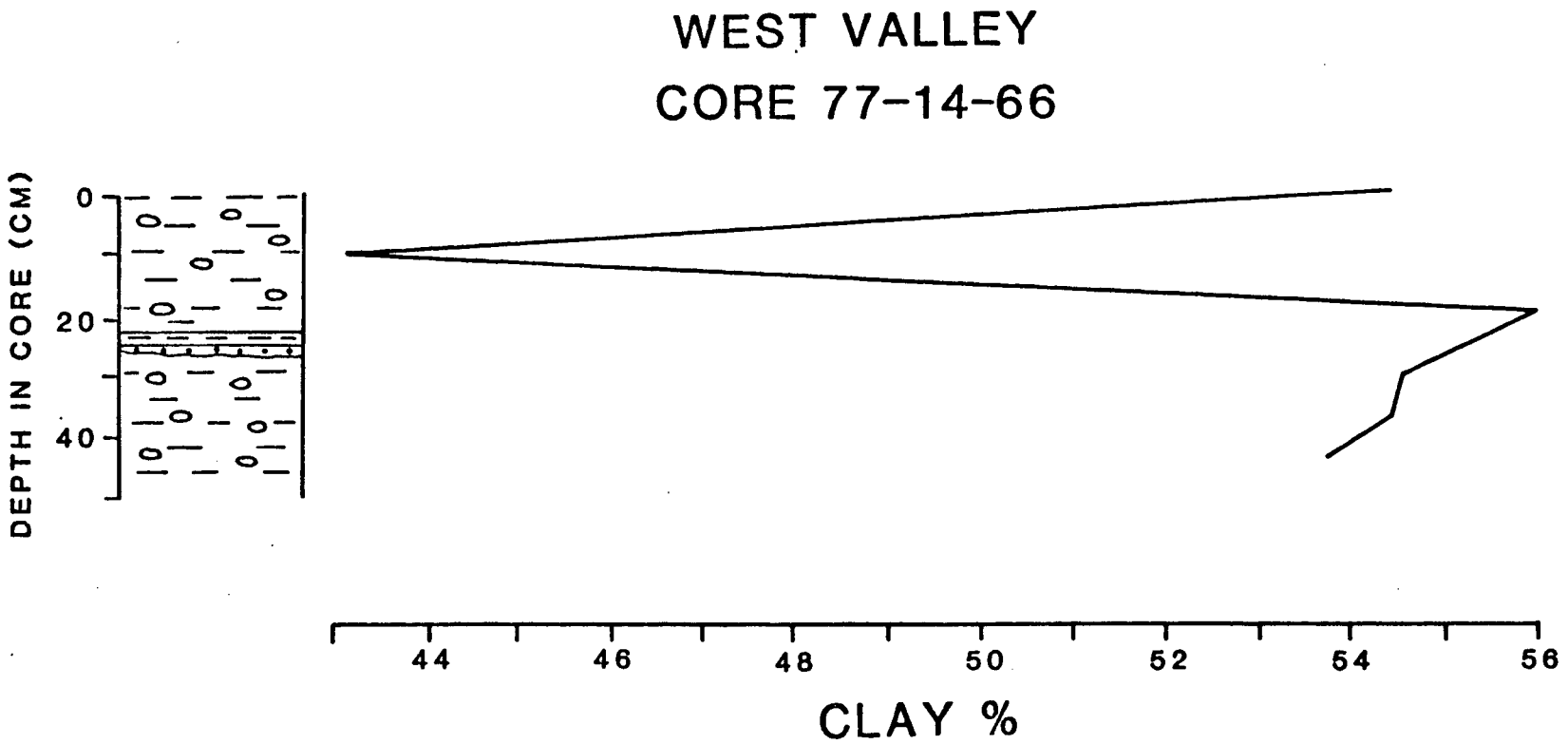
WEST VALLEY
CORE 77-14-66
DEPTH IN CORE (CM)
0
20
40
44
46
48
50
52
54
56
CLAY %

WEST VALLEY
CORE 77-14-67

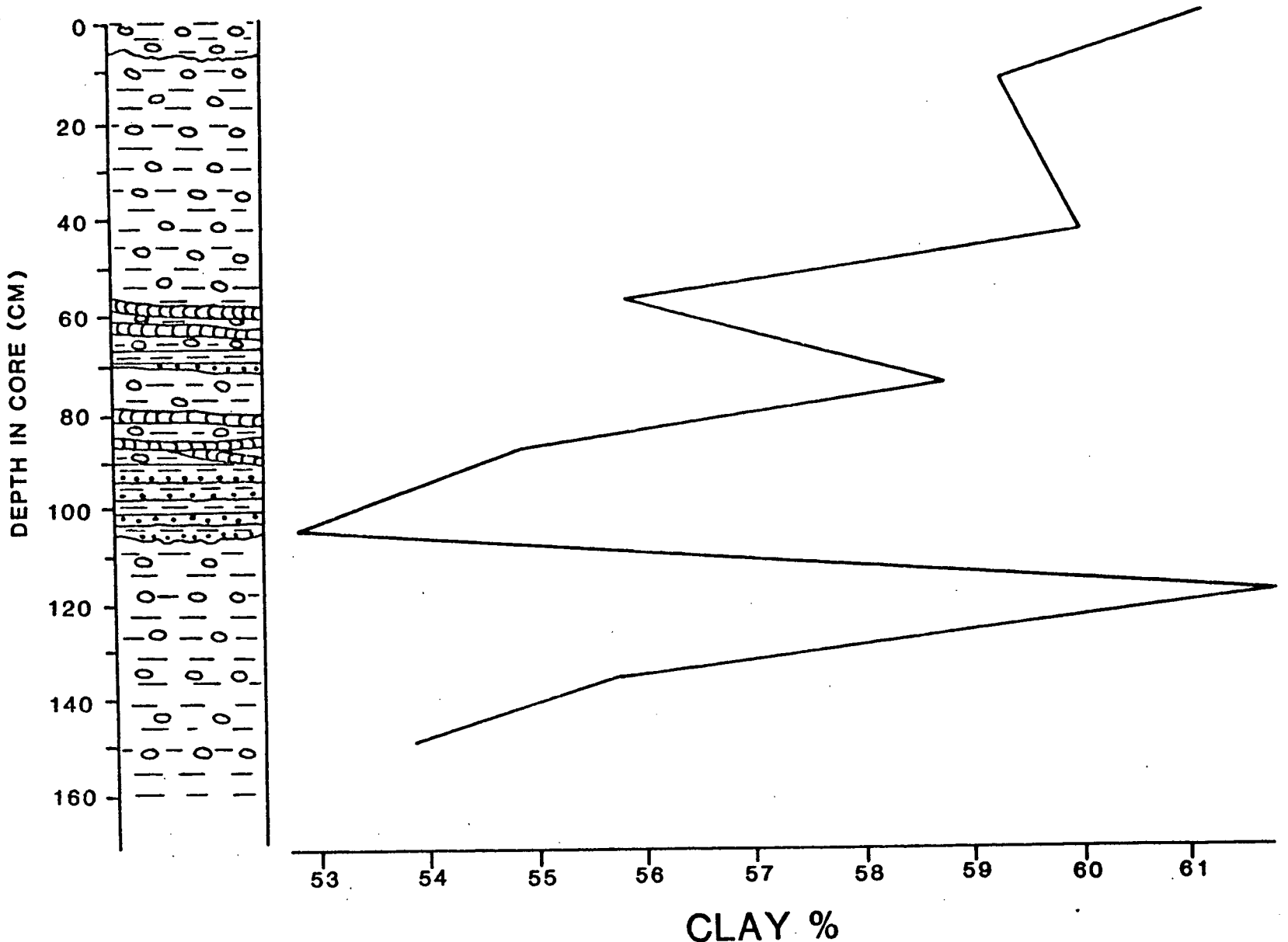

APPENDIX III

Radiocarbon Data

Core 77-14-45

Sample Interval (centimetres)				33-54	85-109
Combustion	Amount CO2 (inches Hg)			20 @ 1T	20 @ 2T
	Amount Lithium (grams)			4	5
	Weight Benzene (grams)			.2900	.4550
	Weight Carbon (grams)			.2675	.4197
Calculation	Background	Counts/min.		3.166	3.155
		σ		.024	.024
	Modern Standard	Counts/min.		8.054	8.054
		σ		.024	.024
	Sample	Counts/min.		3.773	3.679
		σ		.043	.034
		Specific Activity (c/m.g.)		2.2710 ± .185	1.250 ± .100
		"Q" ratio $\frac{A\ (Mod.\ Std.)}{A\ \ Sample}$		3.544	6.441
		σQ ±		.289	.519
		Age: 8035 ln ("Q" ratio)		10170 B.P.	14970
		Age Statistics +		10800-10170 = 630	15590-14970 = 620
		−		10170- 9480 = 690	14970-14290 = 680
		Sample Age (B.P.)		10170 + 630/690	14970 ± 620/680

APPENDIX III continued.

Radiocarbon Data

Core 77-14-51

Sample Interval (centimetres)			0-12	79-87
Combustion	Amount CO2 (inches Hg)		20 @ 2T	15 @ 1T
	Amount Lithium (grams)		5	5
	Weight Benzene (grams)		.5980	.6000
	Weight Carbon (grams)		.5517	.5535
Calculation	Background	Counts/min.	3.155	3.155
		σ	.024	.024
	Modern Standard	Counts/min.	8.054	8.054
		σ	.024	.024
	Sample	Counts/min.	3.572	3.389
		σ	.038	.035
		Special Activity (c/m.g.)	.756 ± .082	.423 ± .077
		"Q" ratio $\frac{A\ (Mod.\ Std.)}{A\ \ Sample}$	10.639	19.004
		σQ ±	1.167	3.467
		Age: 8035 ln ("Q" ratio)	19000 B.P.	23660 B.P.
		Age Statistics +	19840-19000 = 340	25010-23660 = 1350
		-	19000-18070 = 930	23660-22040 = 1620
		Sample Age (B.P.)	19000 ± 840/930	23660 ± 1350/1620

APPENDIX IV

Grain Size Distribution

Core	Sample Interval (centimetres)	Sand (%)	Silt (%)	Clay (%)
77-14-43	0-2	3	58	39
	10-12	2	53	45
	20-22	3	52	45
	29-31	3	53	44
	39-41	3	53	44
	50-51	3	52	45
	59-61	6	51	43
	69-71	0	54	46
	80-81	1	54	46
	90-91	0	52	48
	100-101	0	59	41
	109-111	2	58	40
	125-126	22	57	21
	129-131	0	57	43
	139-141	2	57	41
	149-151	1	58	41
	159-161	1	56	43
	170-171	1	58	41
77-14-45	0-2	0	55	45
	9-11	0	52	48
	19-21	0	55	45
	30-32	0	60	40
	39-41	1	54	45
	49-50	1	51	48
	59-61	0	64	36
	70-72	0	63	37
	80-82	0	62	38
	90-92	1	42	57
	100-102	0	42	58
	109-111	0	47	53
	119-121	0	45	55
	129-131	1	58	41
	139-141	0	53	47
	149-151	0	45	55
	159-160	1	42	57
77-14-47	0-2	1	33	66
	10-11	1	33	66
	20-21	1	33	66
	30-31	1	32	67
	40-41	0	35	65
	50-51	0	33	67
	60-61	1	35	64
	70-71	0	33	67
	80-81	1	31	68
	95-96	0	33	67
	105-106	1	43	56
	110-111	0	47	53

APPENDIX IV Grain Size Distribution continued.

Core	Sample Interval (centimetres)	Sand (%)	Silt (%)	Clay (%)
77-14-47 cont.	120-121	0	47	53
	130-131	0	50	50
	135-137	0	64	36
77-14-51	0-2	3	39	58
	15-17	3	39	58
	30-32	3	36	61
	45-47	3	38	59
	60-61	5	37	58
	75-77	2	37	61
	90-92	2	37	61
	105-107	1	48	51
	120-122	0	35	65
77-14-54	0-2	1	36	63
	13-15	1	32	67
	19-20	1	34	65
	24-26	0	35	65
	29-31	0	36	64
	35-36	1	37	62
	39-41	0	38	62
	45-46	1	38	61
	49-51	2	70	28
77-14-56	0-2	6	41	53
	10-12	7	65	28
	20-22	1	56	43
	30-32	0	61	39
	40-42	0	73	27
	50-52	2	59	39
	55-57	2	72	26
	65-67	0	69	31
77-14-61	0-2	1	34	65
	20-22	1	37	62
	30-32	0	36	64
	40-42	0	34	66
	50-52	0	41	59
	60-62	0	37	63
77-14-62	0-3	1	46	53
	15-17	1	42	57
	30-32	1	43	56
	44-46	0	47	53
	60-62	0	43	57
	75-77	0	43	57
	90-92	0	40	60
	105-107	0	41	59

APPENDIX IV Grain Size Distribution continued.

Core	Sample Interval (centimetres	Sand (%)	Silt (%)	Clay (%)
77-14-62 cont.	120-122	0	40	60
	148-150	0	42	58
	157-159	0	41	59
	166-168	1	43	56
77-14-63	0-2	0	36	64
	15-17	0	42	58
	30-32	0	33	67
	45-47	0	37	63
	60-62	0	38	62
	75-77	0	42	58
	90-92	0	40	60
	105-107	0	43	57
	120-122	2	51	47
	135-137	0	42	58
77-14-66	0-2	1	45	54
	10-12	11	46	43
	19-21	1	43	56
	29-31	1	45	54
	39-41	1	45	54
	44-46	0	46	54
77-14-67	0-2	1	38	61
	15-16	0	40	60
	45-46	1	39	60
	59-61	0	44	56
	75-76	0	41	59
	89-91	0	45	55
	105-106	0	47	53
	119-120	1	37	62
	135-136	0	44	56
	150-152	0	46	54

APPENDIX V

Philips X-ray Diffractometer Settings For Sediment Analysis

Radiation source	$CuK\alpha$
Filter	Ni
Scanning speed	2^{o} 2θ/min.
Scale expansion	4×10^{2}
Time constant	1
Voltage	40 kV
Current	20 mA
Baseline/Window	150/120
Divergence slit	1^{o}
Receiving slit	0.2^{o}
Scatter slit	1^{o}
Chart speed	20 mm/min.
2θ range	60^{o} to 4.5^{o}

APPENDIX VI

Relative Clay Mineral Proportions

Core	Sample Interval (centimetres)	Montmorillonite %	Montmorillonite Rel. Std. Dev.	Illite %	Illite Rel. Std. Dev.	Chlorite %	Chlorite Rel. Std.* Dev.
77-14-43	0-2	15	(12)	41	(5)	44	(3)
	50-52	18	(8)	36	(4)	46	(3)
	100-102	20	(7)	35	(4)	45	(1)
	150-152	21	(2)	34	(1)	45	(4)
	170-172	15	(3)	31	(4)	54	(4)
77-14-45	0-2	22	(6)	22	(13)	56	(3)
	49-51	13	(8)	56	(3)	31	(4)
	100-102	15	(5)	43	(8)	42	(1)
	149-151	15	(18)	40	(5)	45	(5)
77-14-47	0-2	33	(3)	45	(14)	22	(8)
	50-52	43	(2)	29	(18)	28	(5)
	105-107	24	(6)	46	(6)	30	(4)
	149-151	17	(1)	43	(1)	40	(2)
77-14-51	0-2	21	(6)	40	(13)	39	(1)
	44-46	26	(5)	47	(6)	27	(6)
	90-92	13	(6)	44	(2)	43	(2)
	105-107	6	(22)	64	(4)	30	(2)
	120-122	12	(6)	56	(7)	32	(4)
77-14-54	0-2	27	(4)	24	(7)	49	(2)
	49-51	15	(8)	48	(6)	37	(4)
77-14-56	0-2	32	(6)	38	(7)	30	(4)
	50-52	18	(10)	35	(17)	47	(5)
	65-67	10	(9)	50	(7)	40	(1)
77-14-61	0-2	46	(4)	30	(6)	24	(5)
	50-52	41	(2)	31	(4)	28	(2)
77-14-62	0-2	34	(6)	36	(5)	30	(1)
	44-46	34	(4)	35	(2)	31	(3)
	90-92	42	(7)	31	(6)	27	(3)
	120-122	45	(5)	28	(8)	27	(3)
	166-168	35	(4)	29	(8)	37	(2)
77-14-63	0-2	37	(3)	39	(4)	25	(2)
	45-47	47	(4)	28	(5)	25	(3)
	134-136	37	(2)	29	(2)	33	(1)
77-14-66	0-2	57	(1)	23	(7)	20	(1)
	44-46	42	(6)	30	(2)	28	(2)
77-14-67	0-2	39	(1)	33	(2)	28	(2)
	45-47	46	(5)	30	(3)	24	(6)
	89-91	39	(4)	23	(10)	38	(2)
	150-152	33	(3)	30	(2)	36	(3)

* - Relative Standard Deviation